NASA CR-
160213

(NASA-CR-160213) INVESTIGATIONS OF RESPIRATORY CONTROL SYSTEMS SIMULATION (Kansas State Univ.) 201 p HC A10/MF A01 CSCL 06P

N79-25726

Unclas
G3/52 22202

JUN 1979
RECEIVED
NASA STI FACILITY
ACCESS DEPT.

ASD
APOLLO SYSTEMS DEPARTMENT
GENERAL ELECTRIC

HOUSTON, TEXAS TECHNICAL INFORMATION RELEASE

TIR 741-MED-3047

FROM	TO
R. C. Croston, Ph.D.	J. A. Rummel, Ph.D./DB6

DATE	WORK ORDER REF:	WORK STATEMENT PARA:	REFERENCE:
9/7/73	MA-252T	NAS9-12932	Program Plan 1.3.8 & 1.3.9

SUBJECT

Research Report
Investigations of Respiratory Control Systems
by R. R. Gallagher, Ph.D.

This Research Report, prepared by Dr. R. R. Gallagher who provided consultation services in the area of respiratory system modeling, provides the results of a detailed evaluation of several respiratory control system models published in the open literature. The control models evaluated include Gray's, Loyd and Cunningham, Milhorn, and Grodins. Detailed comparisons of the operational utility of Grodins' and Milhorns' models are also provided based upon the requirements for such a model in this program.

R. C. Croston

R. C. Croston, Ph.D.

Attachment

/db

CONCURRENCES

Counterpart:

Medical Projects Unit Manager: C. W. Fulcher

Engrg. & Advanced Programs Subsection Mgr. W. J. Beittel

DISTRIBUTION NASA/JSC: Technical Library/JM6 (1979 distribution)

GE: Central Products File

ASD 4028

RESEARCH REPORT

INVESTIGATIONS OF RESPIRATORY CONTROL SYSTEMS SIMULATION

by

R. R. Gallagher, Ph.D.
DEPARTMENT OF ELECTRICAL ENGINEERING
KANSAS STATE UNIVERSITY
MANHATTAN, KANSAS

Supported by

GENERAL ELECTRIC COMPANY
CONTRACT NUMBER
036-E31001-M5906
and
ENGINEERING EXPERIMENT STATION
KANSAS STATE UNIVERSITY

INVESTIGATIONS OF RESPIRATORY CONTROL SYSTEM SIMULATIONS

TABLE OF CONTENTS

	PAGE
1. INTRODUCTION	1
1.1 Fundamental Philosophy of Physiological System Modelling	1
1.2 Various Respiratory System Models	2
1.3 Theoretical Aspects of Respiration and Exercise Interrelationships	5
1.4 Comments on Physiological Systems' Interactions	8
1.5 Acknowledgements	11
2. TERMINOLOGY	12
2.1 Terminology Associated with Grodins' Models	12
2.2 Terminology Associated with Milhorn's Models	16
3. EVALUATION OF GRODINS' RESPIRATORY CONTROL MODEL MODIFICATIONS	19
3.1 Statement of Objectives	19
3.2 Description of Grodins' Respiratory Control Model and Modifications	19
3.2.1 Controlled System	19
3.2.2 Controlling System	20
3.2.3 Exercise and Related Subroutines	21
3.3 Model Parameter Variations	48
3.3.1 Resting State and Sea Level Conditions	51
3.3.2 Exercise States at an Altered Environment	52
3.4 Evaluation of Exercise Feature	55
4. MILHORN'S RESPIRATORY CONTROL MODELS	60
4.1 Statement of Objectives	60
4.2 Models' Variations and Significant Features	60
5. CONCLUSIONS AND RECOMMENDATIONS	64
5.1 Grodins' Respiratory Control Model	64
5.2 Milhorn's Respiratory Control Models	68
6. APPENDICES	70
6.1 Study Report - Respiratory Control System Simulation	71
6.2 Study Report - Summarization of the Major Features of Milhorn's Respiratory System Models	160
6.3 Program Listing for the Modified Grodins' Respiratory Control System	192
7. BIBLIOGRAPHY	253

LIST OF FIGURES

		PAGE
FIGURE 1.	Time course of ventilation during exercise.	9
FIGURE 2.	Block diagram of respiration control model	10
FIGURE 3.	RC12's relationship to the other program subroutines	23
FIGURE 4.	Flow chart for RC12	24
FIGURE 5.	Classical relationship between steady-state oxygen uptake and workload	33
FIGURE 6.	Piecewise linear relationship of steady-state oxygen uptake and workload used in model	35
FIGURE 7.	Inverse time constant versus work	36
FIGURE 8.	Uptake of oxygen from resting conditions	37
FIGURE 9.	Uptake of oxygen for successive workloads	38
FIGURE 10.	Oxygen uptake for decreasing workloads	40
FIGURE 11.	Flow chart for controller subroutine	42
FIGURE 12.	Steady-state ventilation	44
FIGURE 13.	The relationship between oxygen uptake and RMLIN	46
FIGURE 14.	The relationship between oxygen uptake and RMLIN for 75 watts from 25 watts	47
FIGURE 15.	Relationship between important variables used in controller equation at 75 watts	49
FIGURE 16.	Simulation run number one for 0-50-100 watts	56
FIGURE 17.	Simulation run for 0-25-75-0 watts	58
FIGURE 18.	Simulation run number three for 25-70-100-0 watts	59
FIGURE 19.	Simulation run number five for 0-50-0 watts	66

LIST OF TABLES

		PAGE
Table 1.	Symbols and Terms Used in the Basic Grodins' Respiratory Control System Simulation	12
Table 2.	Symbols and Terms Associated With the Exercise Subroutines in the Modified Grodins' Respiratory Control System Simulation	15
Table 3.	Symbols and Terms Used in Milhorn's Respiratory System Models	16
Table 4.	Input Data Cards Specifying the Altered Environment	53
Table 5.	Input Data for Workload Schedule	53
Table 6.	Input Data Cards for Five Exercise Simulation Runs	55

1. INTRODUCTION

1.1 Fundamental Philosophy of Physiological System Modelling

The importance of physiological system modelling within the area of biomedical research is becoming more evident. In particular, the application of control theory which involves the mathematical description of element functionings and interrelationships between elements has made possible the simulation of very complex physiological feedback control systems. The mathematical relationships range from algebraic formulations and ordinary linear differential equations to nonlinear differential-difference equations and stochastic processes.

Generally, physiological systems are very complex and comprise many interrelated variables. In the initial phases of model formulation verbal descriptions are used to formulate the expressions that are based upon experimental physiological data or assumptions. This approach of verbally explaining the functioning of the physiological system becomes very unwieldy as the system's complexity increases. For this reason specific variables and symbols are defined and related to each other by mathematical expressions. Once the system is defined in logical mathematical terms the analysis process is then adapted to various computational devices, i.e. digital, analog, and hybrid computers. By altering parameter and functional relationships the model's responses are correlated with experimented data. At this stage in the model's development, the refinements made by the investigator determines how well the model faithfully describes the actual system.

According to Yamamoto and Raub (1) the best means of categorizing the present stage of development of respiratory control system models would be to describe them as being in a transition stage from verbal to mathematical statements. There are still many physiologically related respiratory functions that are not easily described mathematically. One necessary component of the overall plan to rectify this situation is the establishment of experimental efforts that provides quantitative measures instead of qualitative measures. From this point

of view perhaps the respiratory system and the related simulation efforts are even more firmly established than for other physiological systems. In particular, the control mechanism associated with respiration and its interaction with the mathematical description of the controlled component is defined by several sources (2-8).

Prior to deciding upon a particular physiological system model one should utilize the expertise found in the literature and correlate the features of the published models with the goals of the immediate project. This is precisely the approach that was established in this research effort involving the respiratory control systems.

1.2 Various Respiratory System Models

The system modelling effort that is discussed in the following report is one related to the respiratory control system. Several models have been developed for the respiratory control system emphasizing particular features which make them adaptable for specific experimental and simulated environmental conditions.

A few brief comments about some of the respiratory modelling efforts and their salient characteristics follow. Alveolar ventilation responses were of prime importance for the output responses of a model developed by Bellville et al. (9). Frequency, amplitude, and mean level of inhaled CO_2 were altered in a manner corresponding to sinusoidally varying CO_2 inhalation allowing a frequency response analysis of the respiratory system.

The phenomenon of pulmonary mechanics as related to various forms of inspired-expired flow systems has been researched by Fry (10). Here variables related to physiological and pathological features of the air passageways are better defined. Elastic behavior of the lungs, airway compliances, and resistances were considered by Mead (11) in a model possessing characteristics similar to those of Fry's model.

Saidel et al. (12) developed a lumped parameter simulation of the pulmonary gas transport system with the ultimate goal of analyzing parameter changes. The model included five variable-volume compartments approximating the airway and alveolar regions and a constant-volume compartment representing the capillary bed. Extensive efforts were taken to mathematically describe the mass balance of the gas compartments and blood compartments.

Breathing patterns related to CO_2 oscillatory exchanges are presented in a model developed by Yamamoto and Hori (13). A linear controller equation is used to describe, indirectly, the dependence of tidal volume and rate of breathing upon cerebral P_{CO_2}.

Exercise levels (workload) are very important inputs for the proposed research. Analysis of maximum ventilation related to chronic airway obstruction and exercise has been conducted by Pierce et al. (14). This particular research was not intended to be a respiratory control system model study; however, the results of the endeavor are very applicable to modelling of airway passages and to the investigation of the respiratory-exercise relationships.

A more detailed discussion of previous efforts involving exercise-respiratory phenomena is given in Section 1.3. Both humoral and neural control mechanisms are presented with supportive experimental work by several investigators (15-23).

Milhorn and Brown's steady-state human respiratory system (5) is very closely related to Grodins' respiratory control system (2). In this particular model by Milhorn, a controlling system and a controlled system form the basis from which mass balance equations are written describing the exchange mechanisms for CO_2 and O_2. The controlling equation of Milhorn's model is an important fundamental component and is similar to one of the forms in Grodins' model except for the void in exercise dependence and the monitoring of CO_2 and O_2 instead of compartmental H^+ concentrations.

Closely associated with Milhorn and Brown's model is a study of pulmonary capillary gas exchange by Milhorn and Pulley (24). This work portrays a more detailed version of the capillary gas exchange by introducing anatomical parameters into the model.

Assuming a second order representation for the mechanical portion of the respiratory system Hilberman et al. (25) has utilized the Fourier series analysis and phasor notation to determine the modulus of impedance, phase angle, compliance, and resistance of the respiratory system. In doing so this research has developed a technique for adjusting parameters associated with respiratory mechanics. Although this research effort is not directly related to the present research the evaluation of parameters for specific environmental conditions might be useful in extending the proposed model's capabilities.

As outlined in the following sections of this report, Grodins' respiratory control system model is the one to which modifications are proposed. Since the pH of each compartment of this proposed model is an important monitored variable the research by Hermansen et al. (26) relating exercise and blood pH could prove to be a valuable piece of supportive research in determining a level of maximal exercise for experimental subjects and in turn for the simulation efforts.

A comparison of several respiratory system models' characteristics and capabilities are presented by Yamamoto and Raub (1). This particular review emphasizes that all models possess unique features but are categorized into three groups (a) Models related to those of Gordins, (b) Models related to Horgan's efforts, and (c) Models related to Milhorn's research. Also this review cites several other models giving their comparisons to the above three groups.

1.3 Theoretical Aspects of Respiration and Exercise Interrelationships

It is a well established fact that exercise plays a very important role in the control of respiration. As stated by Strippoli (27) three significant variables that must be considered in determining the degree of respiratory system dependency upon exercise are:

(A) Intensity of exercise,

(B) Type of exercise, and

(C) Environmental conditions

The following material which explains the theories of respiratory control involving chemical, neural, and neural-chemical interactions was reported by Strippoli (27). The first approach utilized in explaining exercise-respiratory control interactions involved a simple explanation of decreasing arterial O_2 and increasing arterial CO_2. The chemical reaction is defined as

$$CO_2 + H_2O \rightleftarrows H_2CO_3 \rightleftarrows H^+ + HCO_3^-. \qquad (1-1)$$

At this point uncertainty prevailed as to whether the response was caused by CO_2 itself or the H^+ concentration released by the hydrated form of CO_2, carbonic acid (H_2CO_3). However, experimental evidence indicated that neither CO_2, anoxia, or the combination of high CO_2 and low O_2 levels would produce the magnitude of the ventilation response observed during exercise. This fact stimulated research efforts to justify yet another form of stimuli during exercise. The humoral, neurogenic, and neurohumoral theories are discussed in the following paragraphs.

(A). Humoral Theories

Three chemical substances are known which are related to exercise hyperpnea. These are the arterial gas tensions of CO_2, O_2, and the H^+ concentration. There is also a possibility

of a release of chemical substances formed in the muscles which affect the respiratory response, but these are not well documented. A brief discussion of the effects of the three forenamed chemical substances are included here.

1. Carbon dioxide tension, P_{CO_2}

The CO_2 production is increased during muscular exercise. This increase should lead to an increased concentration of CO_2 in the arterial system sufficient to stimulate the respiratory center so that the response (hyperventilation) would lead to a decreased blood CO_2 level. This regulation of respiration process would be similar to the operation of a feedback system. However, the blood CO_2 level increases very little during exercise, certainly not of sufficient magnitude to explain the observed change in ventilation.

2. Oxygen tension, P_{O_2}

One would expect to see a slight decrease in blood P_{O_2} during exercise. However, this decrease would not amount to more than a few mm Hg, since the saturation of arterial blood with O_2 is not greatly affected by exercise. Oxygen tension of approximately 60 mm Hg would be required to produce a realizable stimulus from the chemoreceptors in the aortic arch and carotid bodies (15).

3. H^+ concentration

An increase in H^+ concentration of the arterial blood due to CO_2 accumulation has never been observed in mild exercise. Only during severe exercise does the H^+ concentration of the arterial blood significantly increase. This increase is caused by large amounts of lactic acid produced by the exercising muscles during severe exercise when anaerobic metabolism accounts for the majority of energy.

Even if all of the humoral mechanisms described above were functioning simultaneously the increase in ventilation (l/min) observed during exercise could not be justified. Within the limits of aerobic metabolism, even if there are no appreciable alterations in blood chemistry, there is a linear relationship between steady-state ventilation and oxygen uptake.

(B). Neurogenic Theories

Krogh and Lindhard (16) were the first to interpret the sudden increase of ventilation at the beginning of exercise on a neural basis. They postulated that impulses from the motor cortex of the brain were sent to the respiratory center to effect a change in ventilation. In a different study, experimentation illustrated that the passive movements of the limbs elicited a ventilatory response (1). It was then thought that impulses from mechanoreceptors in the muscles, tendons and joints transmitted to the respiratory center were the cause of the response. Comroe and Schmidt (17) found that the mechanoreceptors involved were limited only to the joints.

While performing cross circulation experiments on dogs, Kao (18) showed that the hyperventilation accompanying muscular activity is limited to the exercising neural dog. The humoral dog whose head was perfused by blood coming from the active limbs of the neural dog showed no change in ventilation. Thus, the increased ventilation of the neural dog was not due to the chemical stimulus of the respiratory center, since there were no changes in the blood of the humoral dog.

From these experiments and the research of Jensen et al. (19) it is established that at the onset of exercise, pulmonary ventilation increases abruptly in a much shorter time period than the circulation time; that is, before chemical substances formed by the exercising muscles can reach the respiratory center.

Neurogenic controls alone are inadequate to maintain the delicate chemical balance of the blood during exercise at the same level as when the body is at rest. Therefore, both humoral and neurogenic mechanisms are involved for the most effective control of respiration during muscular exercise.

(C). Neurohumoral Theory

Dejours (20) recorded ventilation and arterial CO_2 tension, P_{aCO_2}, on a single breath basis to detect the very fast changes in ventilation at the initial and terminal phases of exercise. The ventilation increases abruptly at the beginning of exercise, causing a fall in P_{aCO_2}. The ventilation then increases more slowly and reaches a steady-state level in a few minutes. Simultaneously, the P_{aCO_2} increases and returns to the pre-exercise level. Corresponding changes take place at the end of exercise. A sudden decrease in ventilation causes an increase in P_{aCO_2} followed by a slow decrease in P_{aCO_2} to the resting value.

Since the neurohumoral theory seems to be adequately justified by experimental results, it has been utilized in the description of exercise hyperpnea. A representation of ventilation using the neurohumoral approach is shown in Figure 1.

The modification of Grodins' model which simulates the exercise phenomenon utilizes a form of both neural and humoral control (28) with Figure 2 illustrating the stimuli paths. However, there are still some uncertainties as to the degree of neural control in the on- and off-transient responses in ventilation (21).

1.4 Comments on Physiological Systems' Interactions

As the project progresses there must be a concerted effort in establishing the criteria for the interaction between the four physiological systems; respiratory, cardiovascular, thermal, and the renal/endocrine/body fluid systems. Research such as that of Albergoni

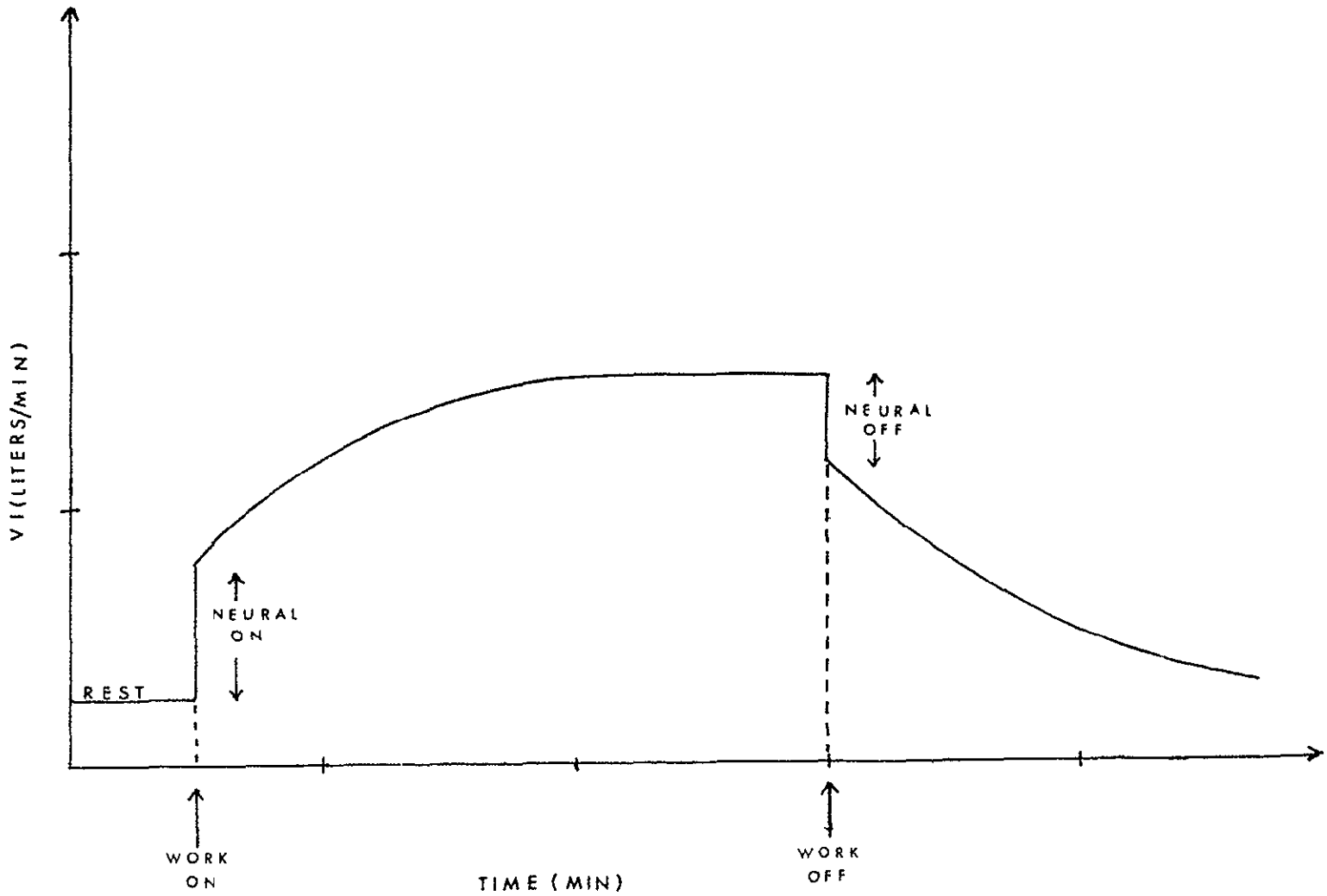

FIGURE 1. Time course of ventilation during exercise

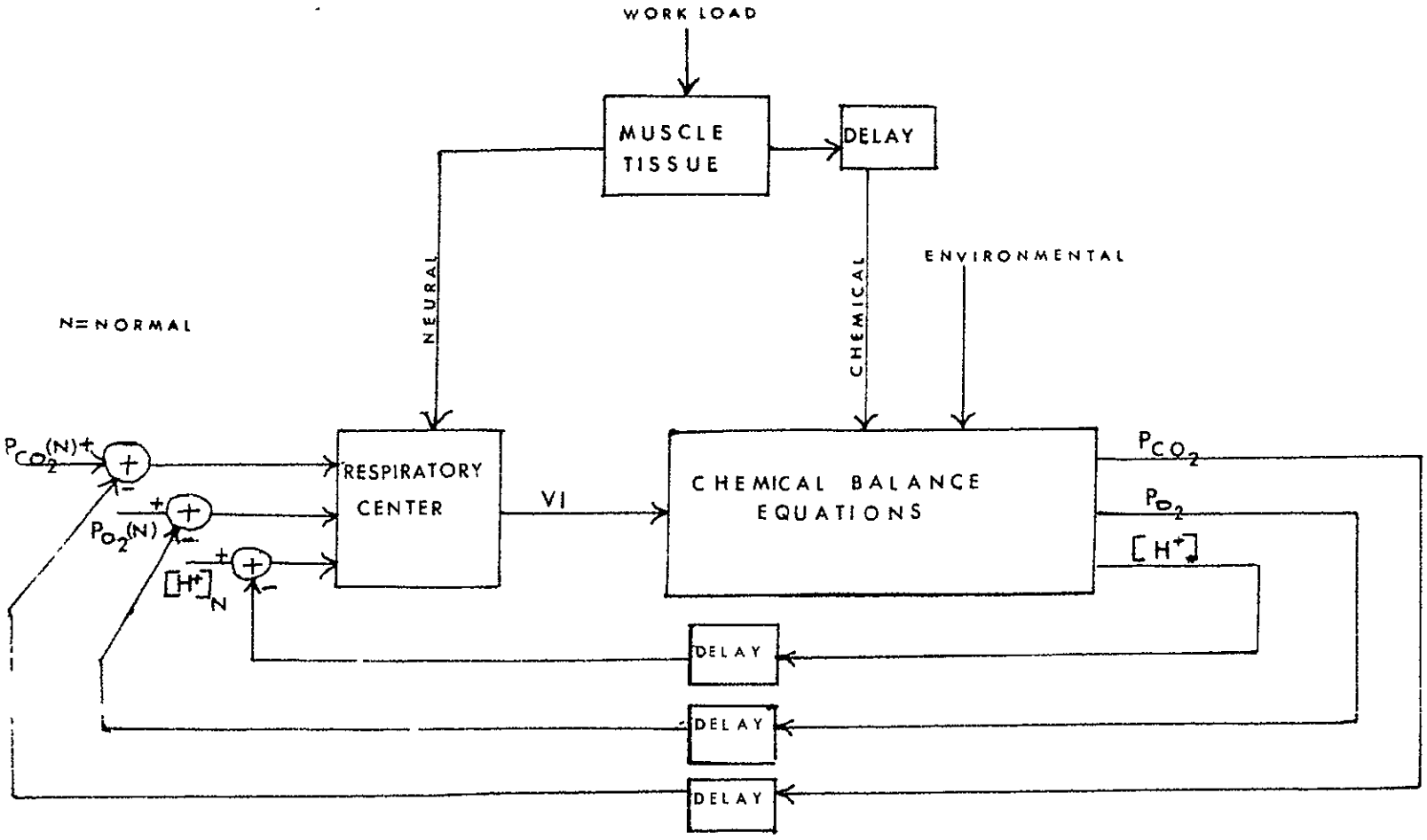

FIGURE 2. Block diagram of respiration control model

et al. (29) which attempts to define the significant variables used in the interfacing model of the circulatory and respiratory systems and the recently published research effort of Guyton et al. (30) will help in the formulation of these criteria. Guyton's research may prove most valuable since it attempts to integrate some of the dynamical interactions of various physiological subsystems; i.e. circulatory dynamics, pulmonary dynamics, regional blood flow control and its relationship to P_{O_2}, tissue fluids and pressures, heart rate, and stroke volume.

To fully appreciate the transition between model choices or the potential capabilities of a model an understanding of the preceding references is mandatory. This is certainly not an exhaustive listing, but several references have excellent bibliographies which makes it an adequate state-of-the-art listing for this research.

1.5 Acknowledgements

It is appropriate to acknowledge the NASA-ASEE Summer Faculty Research Program for its support in the initial phases of the study. A continuation of the research was supported in part by the General Electric Company (Contract Number 036-E31001-M5906) and the Kansas State University Engineering Experiment Station. Personal gratitude is extended to Dr. John A. Rummel, Environmental Physiology Branch, Biomedical Research Division, Life Sciences Directorate, NASA-JSC; and Dr. Clay W. G. Fulcher, General Electric Company. Also, system programming and evaluation support by Mr. Victor Marks, General Electric Company and Mr. Carlo Strippoli, Kansas State University was appreciated.

2. TERMINOLOGY

There are many terms and symbols used in the respiratory control system simulations of Grodins and Milhorn which are common to both. The terms involved with these simulations are related to each other and in turn compared to other simulations in a summary by Yamamoto and Raub (1). However, there are some specialized terms which have particular meanings when used only with their respective models.

Throughout the following report, including the study reports (See Appendices 6.1 and 6.2), new terms are defined when they are used. A listing of the more common terms are presented in Tables 1-3 of this section.

2.1 Terminology Associated with Grodins' Models

Terms associated with the basic Grodins' respiratory control system are presented in Table 1 (2).

Table 1. Symbols and Terms Used in the Basic Grodins' Respiratory Control System Simulation

Symbol *	Description	Units
α_j	Solubility coefficient for gas ($j = CO_2$, O_2, N_2) in blood	liters/liter blood/atm, 37C
α_{ij}	Solubility coefficient for gas ($j = CO_2$, O_2, N_2) in brain ($i = B$), tissue ($i = T$), cerebrospinal fluid ($i = CSF$).	liters/liter blood/atm, 37C
B	Barometric pressure	mm Hg
$(BHCO3)_i$	Bicarbonate content of blood ($i = b$), tissue ($i = T$), cerebrospinal fluid ($i = CSF$), brain ($i = B$).	liters CO_2/ liter i, 37C

*Note: The symbol A_{ij} is defined as follows. A designates variable class. i designates model location of the variable. j designates the chemical species of the variable.

Symbol	Description	Units
C_{ij}	Concentration of j (gas, HbO_2, H^+) in blood at lung exit (i = a), in blood at brain entrance (i = aB), in blood at tissue entrance (i = aT), in brain (i = B), in cerebrospinal fluid (i = CSF), in tissue (i = T), in blood at lung entrance (i = v), in blood at carotid body (i = ao), in blood at brain exit (i = vB), in blood at tissue exit (i = vT).	1. liters x/liter y where x = gas or O_2 for HbO_2 and y = blood, brain, CSF, or tissue. 2. nanomoles/liter y for H^+ ion and y defined as above
D_j	Diffusion coefficient of j (CO_2, O_2, N_2) across blood-brain barrier	liters/min per mm Hg
F_{ij}	Volumetric fraction of j (CO_2, O_2, N_2) in dry alveolar gas (i = A), in dry expired gas (i = E), in dry inspired gas (i = I).	dimensionless
(Hb)	Blood oxygen capacity	liters/liter blood
k	conversion factor	atm/mm Hg
K^1	Dissociation constant for carbonic acid	nanomoles/liter
K_i	Volume of brain (i = B), cerebrospinal fluid (i = CSF), tissue (i = T), alveoli (i = L)	liters
MR_{ij}	Metabolic rate of carbon dioxide production (j = CO_2), oxygen consumption (j = O_2) by brain (i = B), tissue (i = T)	liters/min
P_{ij}	Partial pressure of j (CO_2, O_2, N_2) in alveoli (i = A), in blood at lung exit (i = a), in brain (i = B), in cerebrospinal fluid (i = CSF), in inspired air (i = I).	mm Hg

Symbol	Description	Units
pH_i	pH of blood at lung exit ($i = a$), of blood at brain exit ($i = vB$), of blood at tissue exit ($i = vT$), of cerebrospinal fluid ($i = CSF$)	---
Q	Cardiac output	liters/min
Q_i	Cerebral blood flow ($i = B$) Normal resting blood flow ($i = N$)	liters/min
ΔQ	Change in cardiac output	liters/min
ΔQ_i	Change in cerebral blood flow ($i = B$)	liters/min
ΔQ_j	Change in cardiac output due to CO_2 ($j = CO_2$), due to O_2 ($j = O_2$).	liters/min
r_i	Time constant associated with first order differential equation for cardiac output response ($i = 1$), for cerebral blood flow response ($i = 2$).	minutes
t	Time	minutes
τ_{ij}	Blood transport delay from lung to brain ($i = aB$) from lung to tissue ($i = aT$) from brain to lung ($i = vB$) from tissue to lung ($i = vT$) from lung to carotid body ($i = ao$) for specified path segment ($j = (1)$)	minutes
V_i	Expiratory gas flow rate ($i = E$) Inspiratory gas flow rate ($i = I$)	liters/min

One of the major modifications of the basic Grodins' model involves the addition of the exercise (workload) simulations. Table 2 gives a description of some of the terms used in the modification's subroutines.

Table 2. Symbols and Terms Associated With the Exercise Subroutines in the Modified Grodins' Respiratory Control System Simulation.

Symbol	Description	Units
CXT	Term set equal to simulation time	minutes
DEADVT	Dead space ventilation	liters
DURAT	Workload duration	minutes
FREQ	Respiratory frequency	$minute^{-1}$
HRATE	Heart rate	$minute^{-1}$
RMLIN	Linear function of O_2 consumption as used in subroutine RC12	liters/min
RMTB	Function of steady-state O_2 consumption at specific workload.	liters/min
RMTB(2)	Term set equal to RMT(2) in subroutine RC12.	liters/min
RMTM	Term set equal to RMT(2) in subroutine RC 12.	liters/min
RMT(1)	Metabolic rate of CO_2 in tissues	liters/min
RMT(2)	Metabolic rate of O_2 in tissues	liters/min
SSO2W(WORK)	Steady-state O_2 requirement for specific workload	liters/min
SSVENT	Steady-state ventilation for the workload of interest	liters/min
SVNT	Parameter used to signify start of linear change in ventilation to steady-state value	liters/min
SVNT2	Difference in ventilation between VI chemical and the steady-state VI for a particular workload	liters/min

Symbol	Description	Units
TCT	Inverse of time constant associated with exponential components in exercise subroutine calculations	dimensionless
TIMEON	Time when workload is initiated. It is set equal to CXT after workload is read.	minutes
TVNT	Minute Volume	liters/min
WORK	Workload	watts
WORK2	Workload (new)	watts

2.2 Terminology Associated with Milhorn's Models

Generally speaking, many variables appearing in Grodins' basic model also appear in Milhorn's models with different symbol notations. Table 3 gives a listing of most of the variables that are incorporated into the discussions of Milhorn's models as presented in Section 4 and Appendix 6.2.

Table 3. Symbols and Terms Used in Milhorn's Respiratory System Models

Symbol	Description	Units
A	Effective diffusing area of pulmonary membrane	mm^2
A_o	Normal effective diffusing area of pulmonary membrane	mm^2
A, B, C, D	Empirical constants used in Lloyd and Cunningham's controller equation	A, B, C (mm Hg) D (liters/min mm Hg)
$C_{A_{CO_2}}$	Alveolar CO_2 concentration	vol fraction
$C_{A_{O_2}}$	Alveolar O_2 concentration	vol fraction
$C_{A_{\beta O_2}}$	Carotid bodies' site O_2 concentration	vol fraction

Symbol	Description	Units
$C_{B_{CO_2}}$	Brain tissue CO_2 concentration	vol fraction
$C_{B_{H^+}}$	H^+ concentration at central receptor on blood side of blood-brain barrier	nanomoles/liter
$C_{B_{O_2}}$	Brain tissue O_2 concentration	vol fraction
$C_{CSF_{H^+}}$	H^+ concentration at central receptor on cerebrospinal fluid side of blood-brain barrier.	nanomoles/liter
$C_{PS_{H^+}}$	H^+ concentration at peripheral sensors	nanomoles/liter
$C_{T_{CO_2}}$	Body tissue CO_2 concentration	vol fraction
$C_{T_{O_2}}$	Body tissue O_2 concentration	vol fraction
D	Brain tissue CO_2 diffusion coefficient	liters/min/mm Hg
f	Blood flow through a single capillary	liters/min
fV_D	Minute dead space	liters/min
k_i ; i=1,...,8	Constants used in cerebral circulatory controller equation	---
k_2	Constant determined from CO_2-O_2 dissociation curve	dimensionless
k_5	Ratio of normal arterial P_{O_2} to normal alveolar P_{O_2}	dimensionless
n	Constant used in a controller equation	dimensionless
$P_{a_{CO_2}}$	CO_2 arterial tension	mm Hg
$P_{a_{O_2}}$	O_2 arterial tension	mm Hg
$P_{B_{CO_2}}$	Deep brain tissue CO_2 tension	mm Hg
$P_{CSF_{CO_2}}$	Cerebrospinal fluid CO_2 tension	mm Hg

Symbol	Description	Units
P_{H_2O}	Water vapor pressure	mm Hg
P_{ICO_2}	Inspired carbon dioxide partial pressure	mm Hg
P_{IO_2}	Inspired oxygen partial pressure	mm Hg
$\dot{Q}_B$	Cerebral blood flow	liters/min
$\dot{Q}_C$	Total blood flow through pulmonary capillaries	liters/min
$\dot{Q}_{C_o}$	Normal blood flow through pulmonary capillaries	liters/min
$\dot{Q}_{CS}$	Average blood flow at effective sensor site	liters/min
$\dot{Q}_S$	Pulmonary shunt flow	liters/min
R	Respiratory quotient	dimensionless
S	CO_2 dissociation curve's slope	mm Hg^{-1}
$\dot{V}$	Minute pulmonary ventilation	liters/min
$\dot{V}_A$	Alveolar ventilation	liters/min
$\dot{V}_{CO_2}$	Rate of change in volume due to CO_2 production	liters/min
V_D	Dead space	liters
V_L	Lung volume	liters
V_{L_o}	Normal lung volume	liters
$\dot{V}_{O_2}$	Rate of change in volume due to O_2 consumption	liters/min
V_T	Tidal volume	liters
X	Effective depth of sensor below medulla's surface	mm

3. EVALUATION OF GRODINS' RESPIRATORY CONTROL MODEL MODIFICATIONS

3.1 Statement of Objectives

One phase of the research effort was the evaluation of Grodins' respiratory control model as it simulated the effects of altered environments; in particular, the simulation of various exercise levels in an altered environment. Part of this research is described in a Study Report (See Appendix 6.1). Additional investigation involving the interactions of exercise and respiratory control is included in this section.

The objectives of this component of the research was to evaluate Grodins' program and to recommend modifications to increase the program's fidelity. This included the establishment of an evaluation procedure, comparison of program responses to published data, identify problem areas, and indicate modifications to rectify or alter known simulation shortcomings.

3.2 Description of Grodins' Respiratory Control Model and Modifications

The approach used to present the material in this section will be in the form of a summary of the Study Report (Appendix 6.1). The portions of the Study Report that were expanded after it was written, i.e. further investigations involving the exercise subroutines, will be presented in more detail here. The system can be envisioned as a feedback control system comprised of a "plant" (the controlled system) and the "regulatory component" (controlling system).

3.2.1 Controlled System

The controlled system as represented in Appendix 6.1 is partitioned into three compartments corresponding to the lungs, brain, and tissue with a fluid interconnecting path representing the blood. A set of differential-difference equations describing a gas transport and exchange system between the lungs, blood, brain, and tissue compartments constitutes the framework for the model. Equilibria formulations involving acid-base buffering and metabolism for the

alveolar-arterial, venous blood-brain, and venous blood-tissue interfaces are qualitatively and quantitatively described. As indicated these formulations are the most complex of any of the model segments.

Reference should be made to Appendix 6.1 for a condensed listing of the assumptions and features of the model's compartments. It is important to note these assumptions since an evaluation of the system's performance would be irrelevant without them.

An important aspect of the simulation is related to the blood transport time delays. As with any physically dynamic system involving flow dynamics or transfer of information, there are time delays in signal transmission. The time delay, τ, is associated with the blood flow from the lung to the brain compartment, from the lung to the tissue compartment, from the tissue to the lung compartment, from the brain to the lung compartment, and from the lung compartment to the carotid body receptors. These are very necessary terms and their incorporation in the system equations enhances the confidence placed upon the dynamics of the simulation. To further define these time delays, they are not considered to be predetermined constants but are continuously recalculated. They are time dependent in that they are functions of cardiac output, brain blood flow, and vascular segment volumes. This reasoning is very sound since the blood flow dynamics obviously affect relative site gas concentrations. It should also be mentioned that the inclusion of these variable time delays necessarily increases the time for the calculation routines. Therefore, the sophistication that they provide might be offset by the cost of the simulation process.

3.2.2 Controlling System

To provide the closed loop (feedback control) phenomenon a controlling system is utilized. Ignoring the exercise influence, three of the controlled system's outputs are

monitored as inputs for the controlling system. A controller equation describing the inspired ventilation as a weighted function of the H^+ concentration in the cerebrospinal fluid $\left(C_{CSF(H^+)}\right)$, the H^+ concentration in the arterial system $\left(C_{a(H^+)}(t-\tau_{ao})\right)$, the H^+ concentration in the venous blood of the brain $\left(C_{a(H^+)}(t-\tau_{aB})\right)$, and the oxygen contribution at the carotid chemoreceptor sites $(F_{A(O_2)})$ provides this feedback mechanism. Using the terminology as defined in Appendix 6.1 the controller equation is written as

$$V_I = 1.1380\left[C(16)C_{a(H^+)}(t-\tau_{aB}) + (1.0 - C(16))\,C_{CSF(H^+)}\right] + 1.1540C_{a(H^+)}(t-\tau_{a0}) + \text{TERM} - \text{VI (N)} \qquad (3-1)$$

where

$$\text{TERM} = 23.6(10)^{-9}\left[104 - (B-47)F_{A(O_2)}(t-\tau_{a0})\right]^{4.9}$$

$$\text{for } (B-47)F_{A(O_2)}(t-\tau_{ao}) < 104 \qquad (3-2)$$

$$\text{TERM} = 0 \text{ for } (B-47)F_{A(O_2)}(t-\tau_{ao}) \geq 104. \qquad (3-3)$$

The study has indicated that the controller equation is the most flexible component of the entire simulation and also the component which provides the most uncertainties. This fact is even more evident when variations in exercise levels are being simulated. Equation 3-1 takes on a different form when exercise levels are being simulated. Several other forms of controller equations are presented in both Apprendices 6.1 and 6.2. The idea that the controller equation needs continued evaluation is amplified in the conclusions and recommendations.

3.2.3 Exercise and Related Subroutines

In Appendix 6.1 several simulation runs were made in order to establish the significance of the exercise subroutine modification that Weissman (28) had added to Grodins' program. The ventilation responses for varying exercise levels at an altered environment (Skylab conditions) did not appear to be completely satisfactory. First of all, the neural component

response in the off-transient was not evident. Also, after a change in the exercise level was initiated the transient response to a steady-state value of ventilation seemed to be longer than would be desirable. To better understand the exercise subroutines a more detailed investigation of the computer program was performed (27). The following material is a portion of that investigation. The existing computer program (Appendix 6.3) has a limited number of comment statements. Fortunately, the entire program is partitioned into subroutines. The exercise modification is contained in subroutine RC12. The block diagram in Figure 3 shows subroutine RC12's relationship to the other subroutines in the program. RC12 is embedded in a loop that establishes and solves the controlled and controlling system equations. Therefore, the controller subroutine, RC17, is also a part of the loop. The controller subroutine is called before the system equations are calculated in RC11 since inspiratory ventilation rate (VI) and expiratory ventilation rate (VE) are both needed in the calculation of the system equations. RC17 will be considered later.

A flow chart shown in Figure 4 was formed in order to get an insight into the functioning of the exercise subroutine. In this subroutine the tissue metabolic rates of oxygen (RMT(2)) and carbon dioxide (RMT(1)) are calculated along with heart rate (HRATE), respiratory frequency (FREQ), minute volume (TVNT), and dead space (DEADVT). The above mentioned metabolic rates are the variables that interface this subroutine with the remainder of the program. Both metabolic rates are used in the system equations.

The subroutine reads in a workload (WORK2) and duration (DURAT) from the input data cards. See Appendices 6.1 and 6.3 for a description of input data cards. A decision is then made concerning the workload which depends upon the workload's absolute magnitude and its magnitude relative to the previous workload (WORK). This decision is needed since there

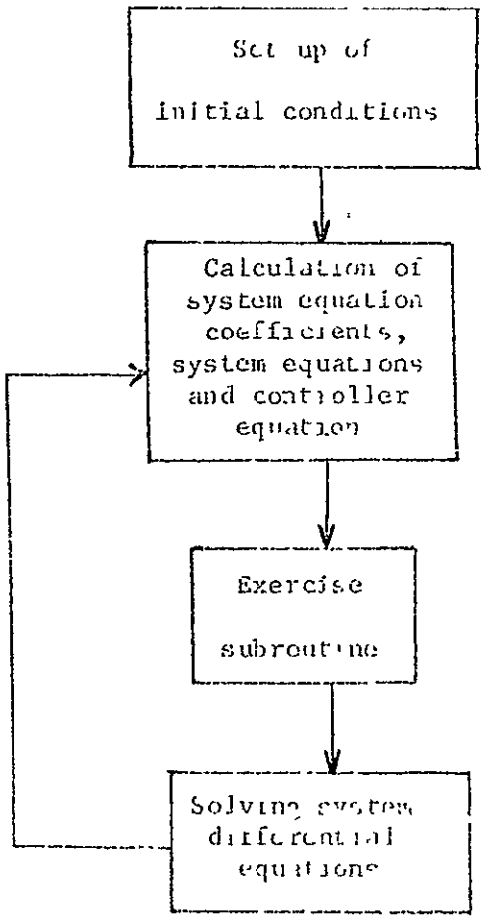

ORIGINAL PAGE IS
OF POOR QUALITY

FIGURE 3 KCT2's relationship to the other program subroutines

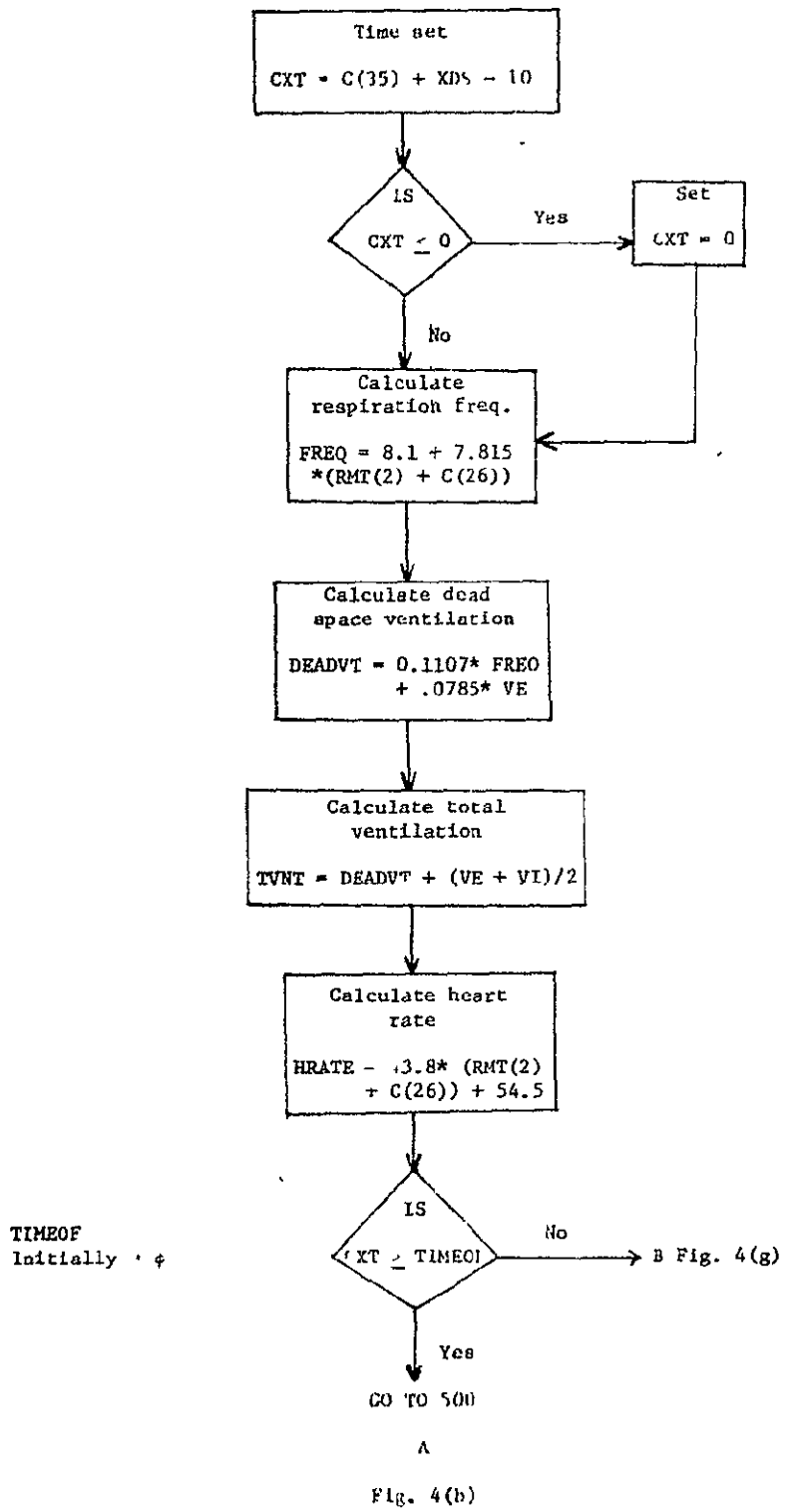

FIGURE 4. Flow chart for RC12.

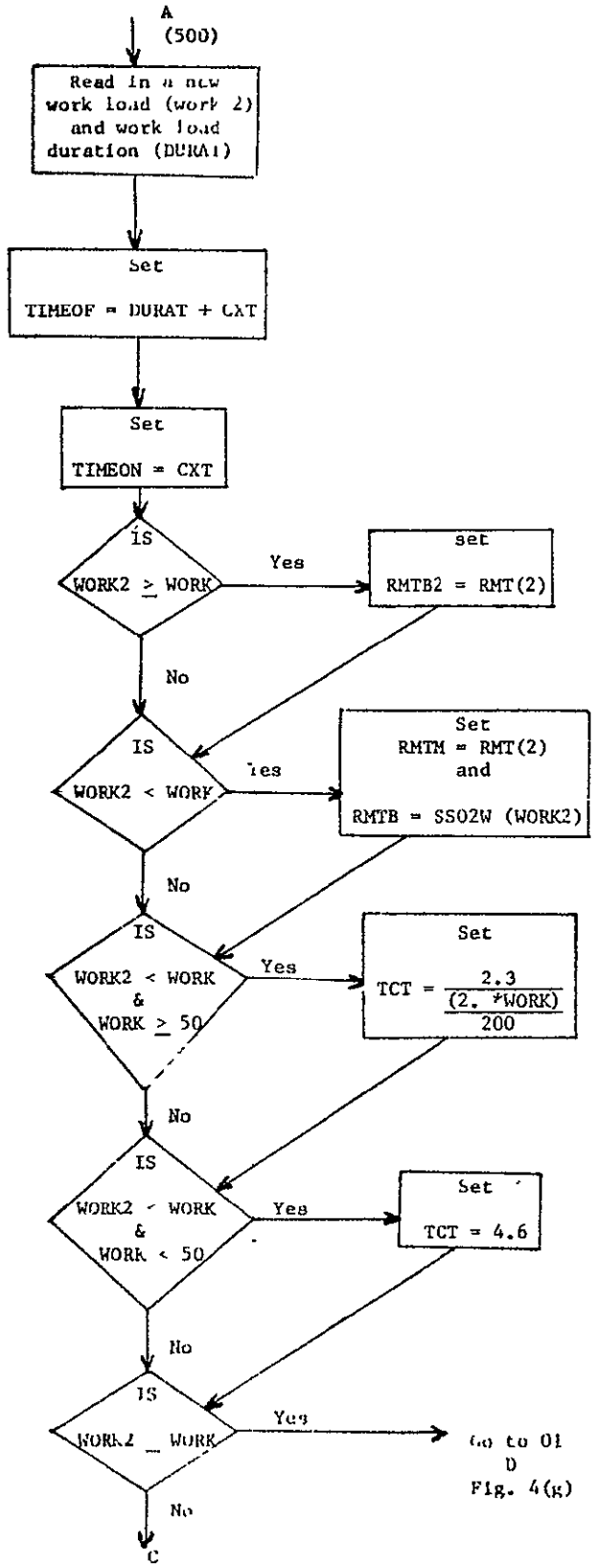

Fig. 4(c)

FIGURE 4(b). Continuation of flow chart for RC12.

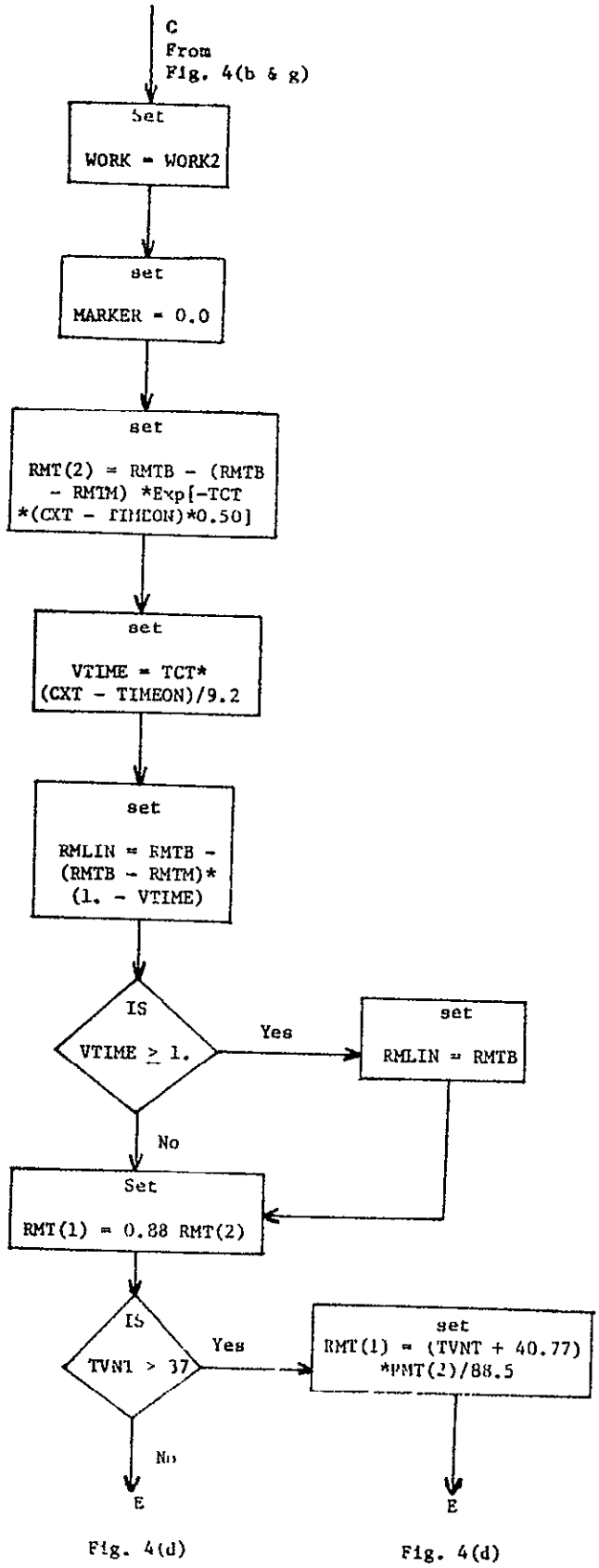

FIGURE 4(c). Continuation of flow chart for RC12.

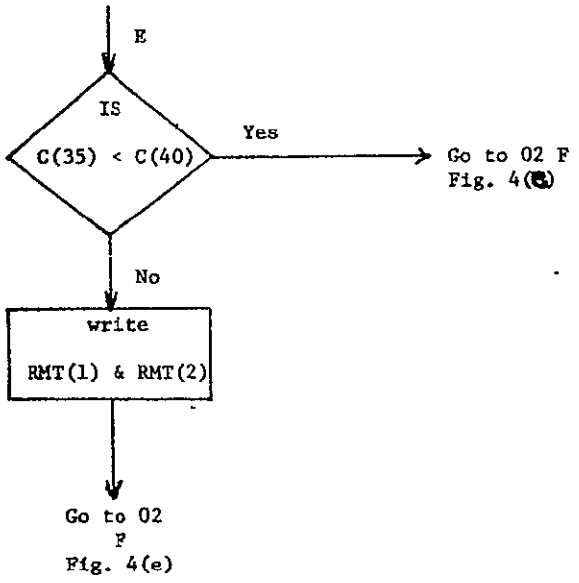

FIGURE 4(d). Continuation of flow chart for RC12.

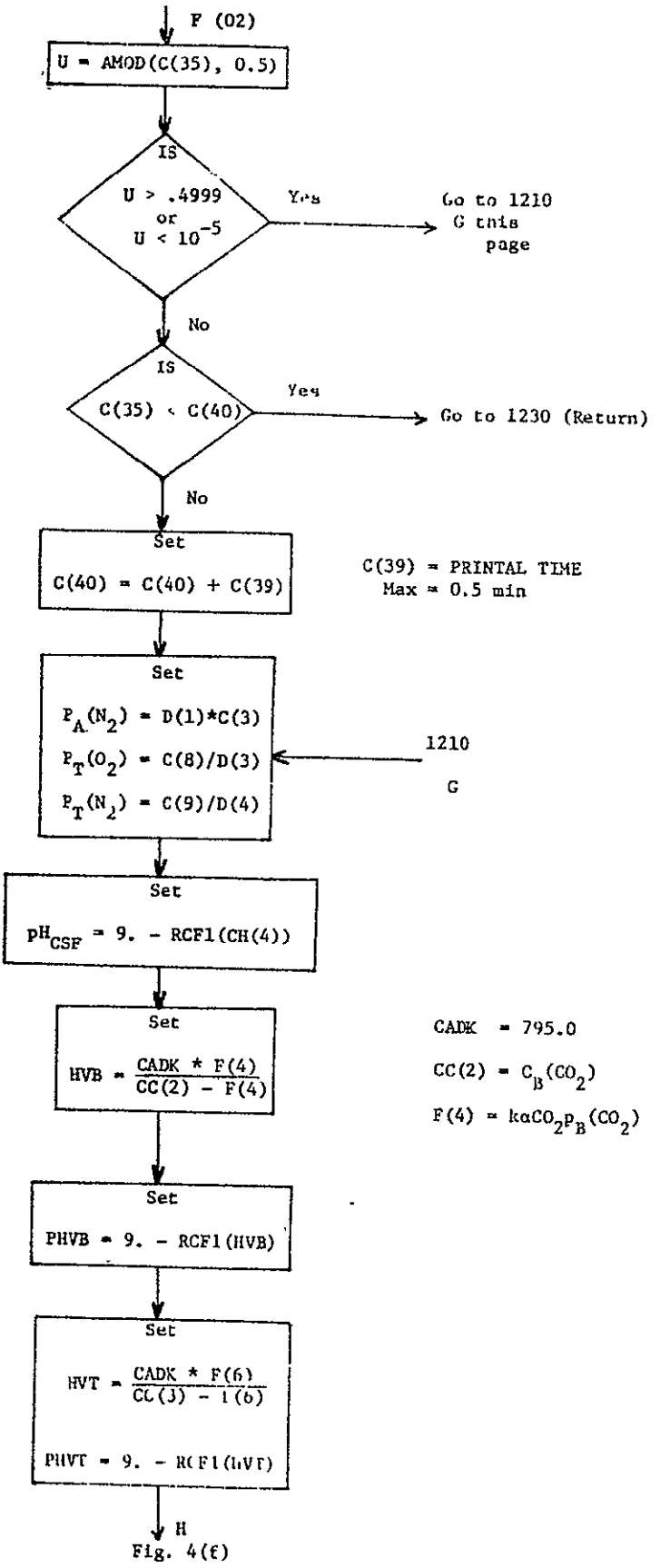

FIGURE 4(e). Continuation of flow chart for RC12.

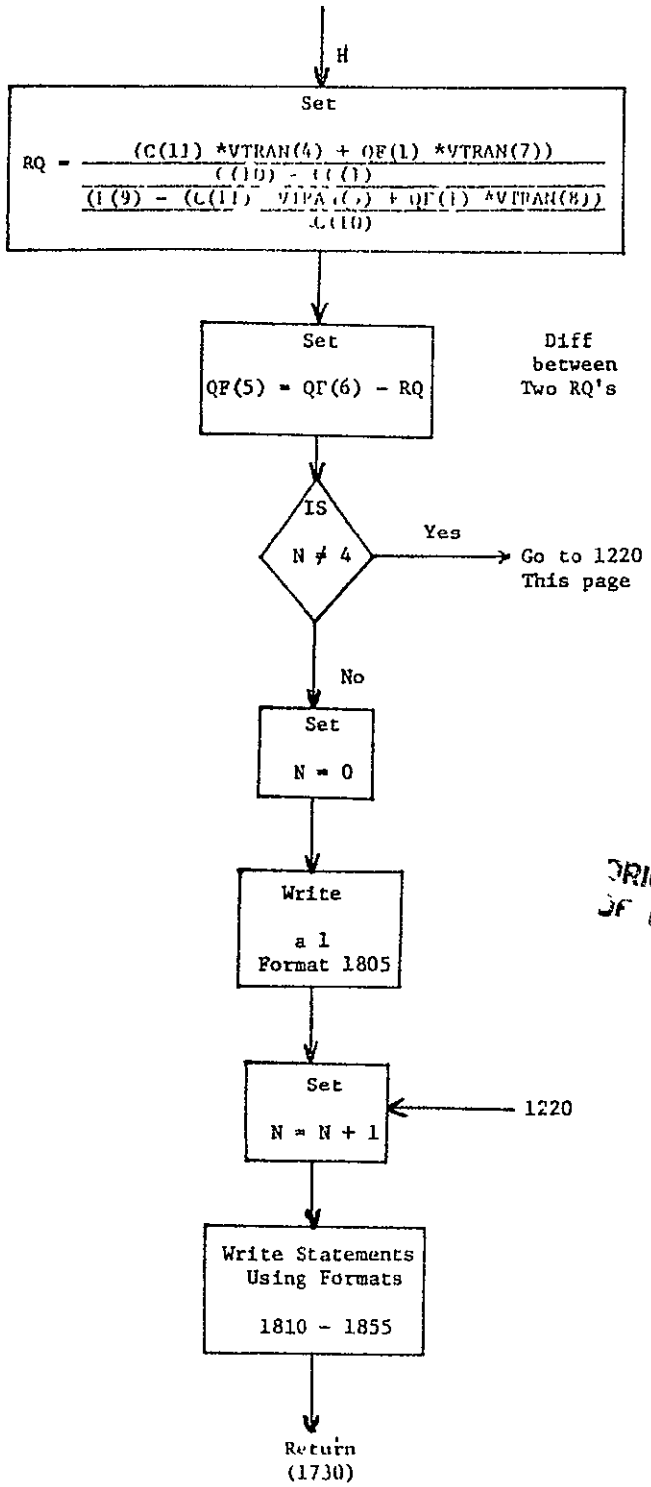

ORIGINAL PAGE IS OF POOR QUALITY

FIGURE 4(f). Continuation of flow chart for RC12.

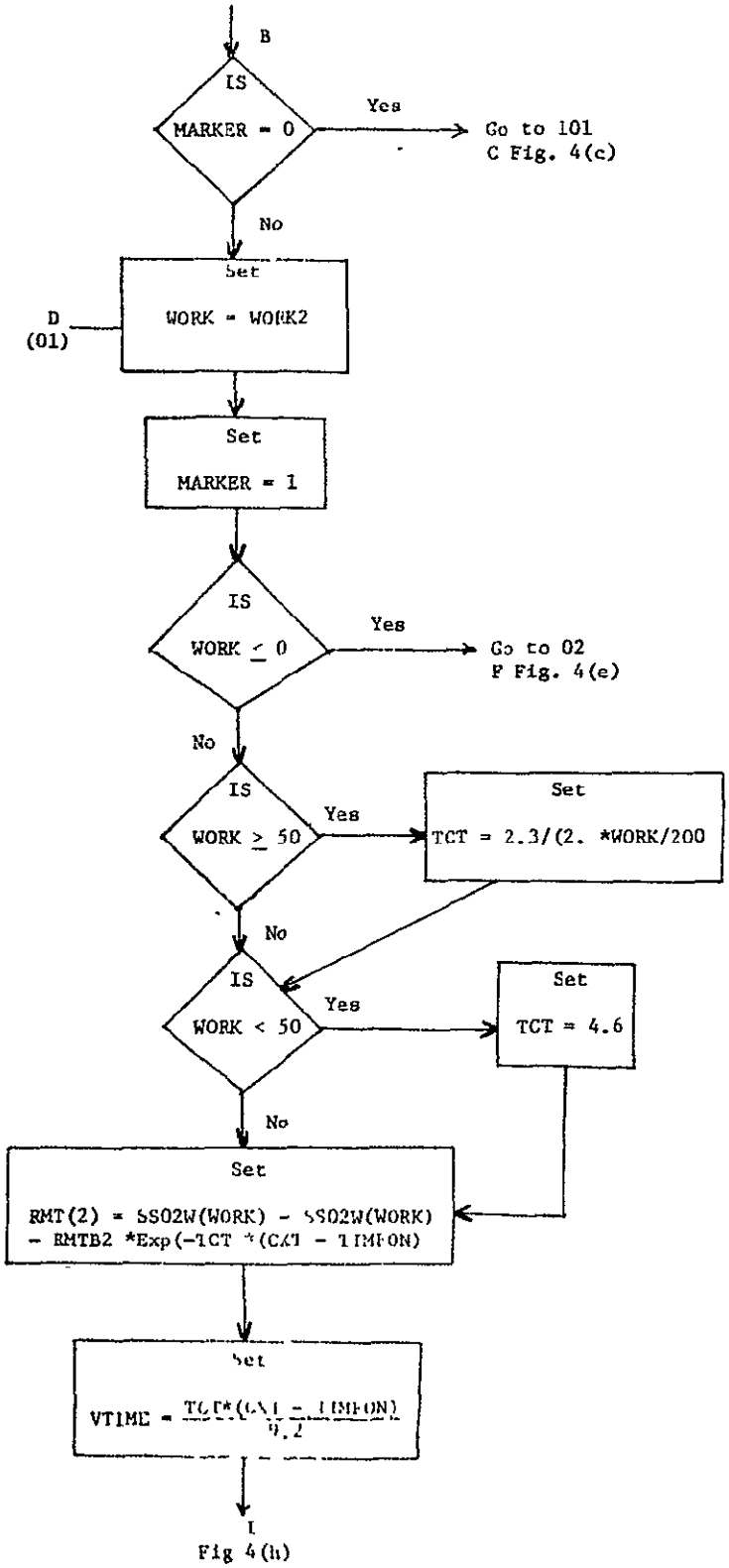

FIGURE 4(g). Continuation of flow chart for RC12.

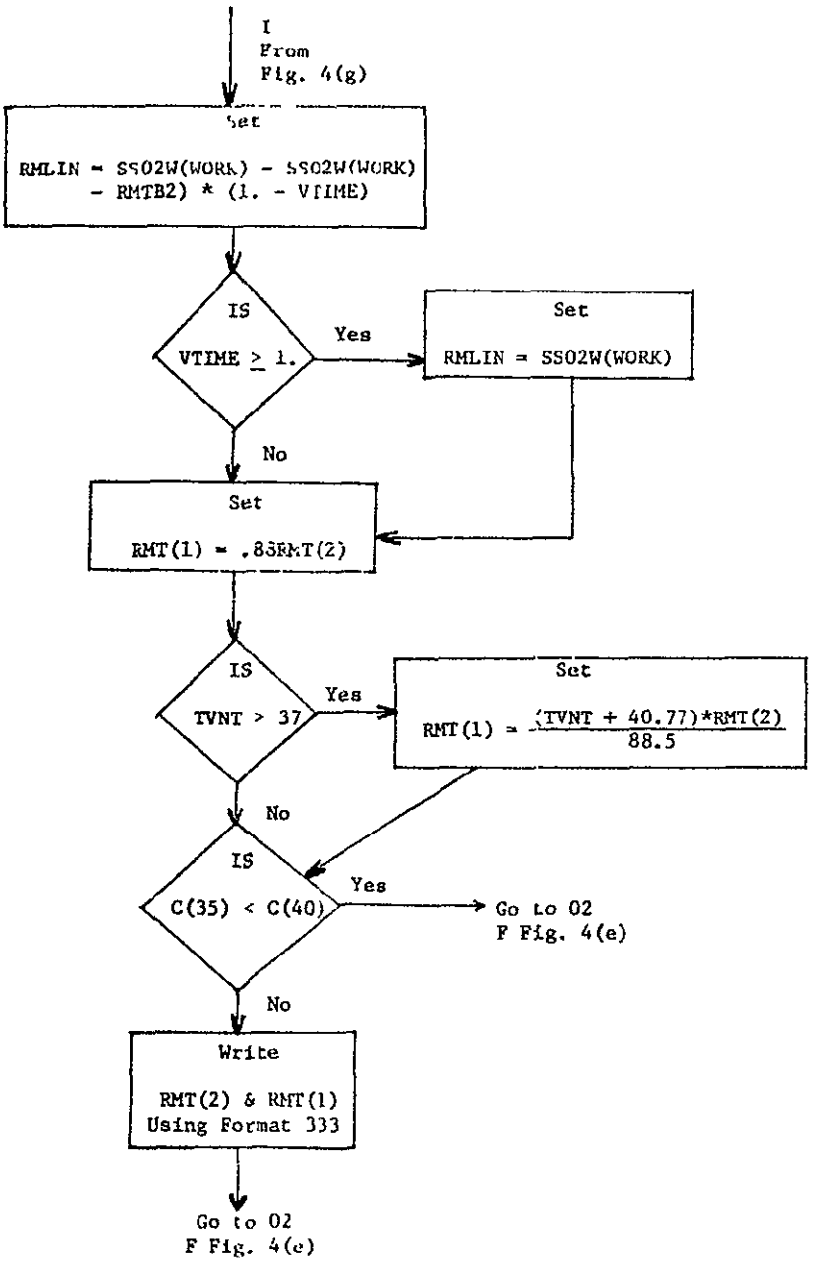

FIGURE 4(h). Continuation of flow chart for RC12.

are two different equations that calculate the metabolic rate of oxygen. One is for WORK2 less than WORK, and one is for WORK2 greater than equal to WORK. To make sure that the program knows where it is at all times, a flag is set depending on the relative magnitude of the new workload. If WORK2 is less than WORK, MARKER is set equal to zero (MARKER = 0). If it is greater than or equal to WORK, MARKER is set equal to one (MARKER = 1). This flag is necessary because the program is continually calling RC12. The flag makes it possible for the program to return to the same set of equations until a new workload is read in. This will occur whenever the simulation time, C(35), is greater than TIMEOF. TIMEOF is set equal to the duration time plus the simulation time, CXT, when the workload is read in:

$$\text{TIMEOF} = \text{CXT} + \text{DURAT} \qquad (3-4)$$

Physiological studies show that oxygen uptake is a good indicator for the amount of work that is being performed (31). For this reason many other physiological parameters are always related to oxygen uptake. As mentioned before, the modification under discussion for this program is based mainly on two expressions for oxygen uptake; one for when the workloads are increasing, and one for when the workloads are decreasing. These two expressions are discussed in the following material.

(A). Increasing Workloads

For this case subroutine RC12 utilizes the expression

$$\text{RMT(2)} = \text{SS02W(WORK)} - (\text{SS02W(WORK)} - \text{RMTB2})^{*} \text{EXP}(-\text{TCT}(\text{CXT} - \text{TIMEON})) \qquad (3-5)$$

where:

SS02W(WORK) is the tissue steady-state oxygen consumption for a particular workload. Oxygen consumption varies linearly with workload as shown in Figure 5. However, the

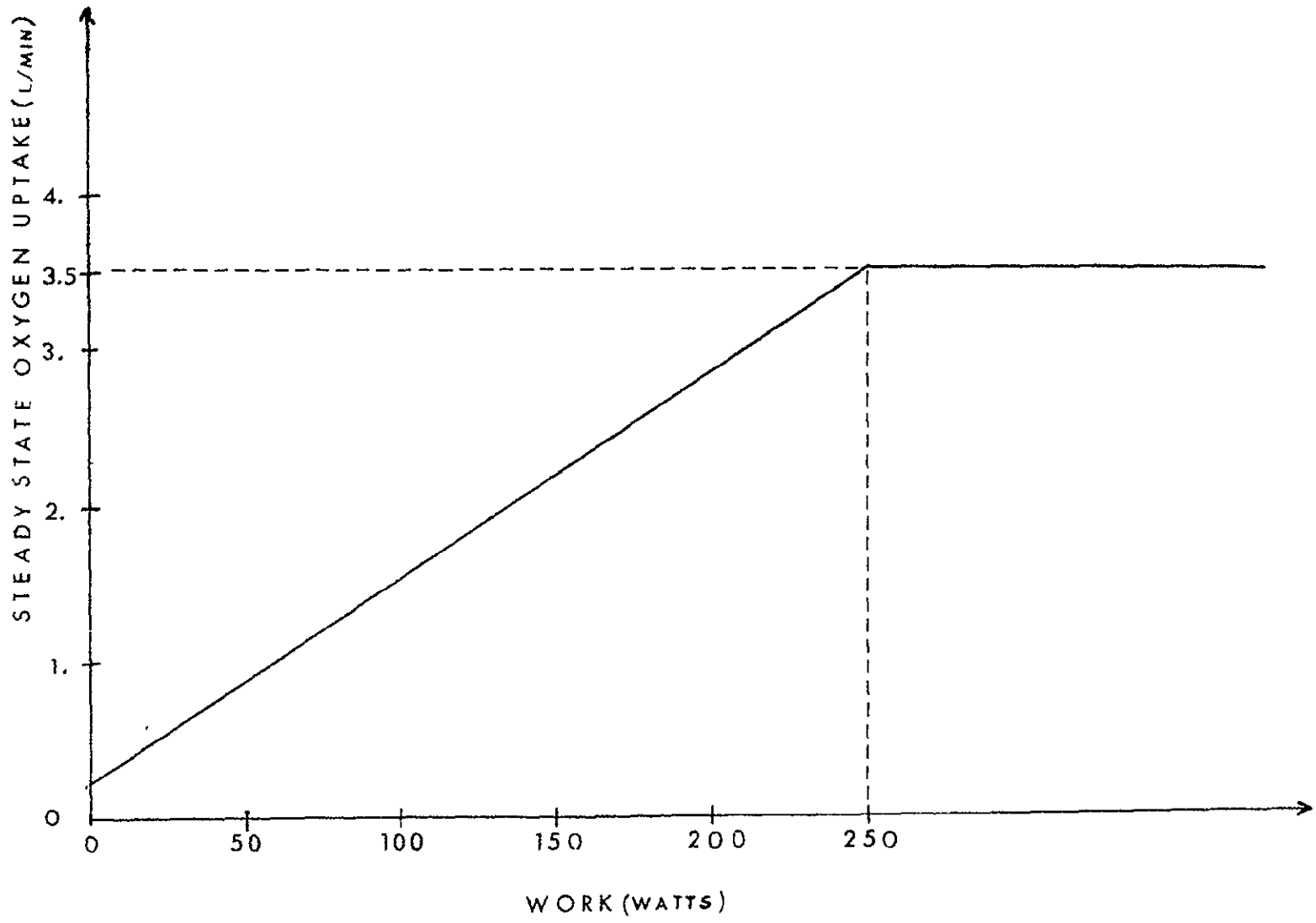

FIGURE 5. Classical relationship between steady-state oxygen uptake and work load

relationship between oxygen consumption and workload in this program is a piecewise linear relationship, as illustrated by Figure 6. Figures 5 and 6 illustrate a maximum value (3.5 liters/min) for the oxygen consumption. At this point there is no additional increase in oxygen consumption for a further increase in workload. This value is known as the maximum oxygen uptake (MAX O_2). It is a measure of one's physical fitness. In the average male the MAX O_2 is about 3.5 liters per minute at a workload of 250 watts. MAX O_2 is higher in the more physically fit individual. The dotted line in Figure 6 is a suggested change that would eliminate the discontinuity at 250 watts.

RMTB2 is the oxygen consumption at the time the workload is initiated. If the workload is started from rest, this value is 0.215 liters per minute.

TCT is the inverse of the time constant. It determines the rise time of the exponential components. TCT is related to the workload by the following expressions:

$$TCT = \begin{cases} 4.6 & \text{for work} \leq 50 \text{ watts} \\ 2.3/2*WORK/200 & \text{for work} > 50 \text{ watts} \end{cases} \qquad (3 - 6)$$

The term TCT as a function of workload is plotted in Figure 7. From this plot it is seen that, as the workload is increased, TCT becomes smaller. This means that as the workload increases, more time is required to reach steady-state.

CXT is equal to the simulation time C(35).

TIMEON is the time when the workload is started. After the workload is read in, the subroutine sets TIMEON = CXT. Thus CXT - TIMEON is elapsed time of the workload at any time C(35).

To gain a better insight into the functional relationship of RMT(2) as workloads are varied, Figures 8 and 9 illustrate the times required for the steady-state oxygen uptakes

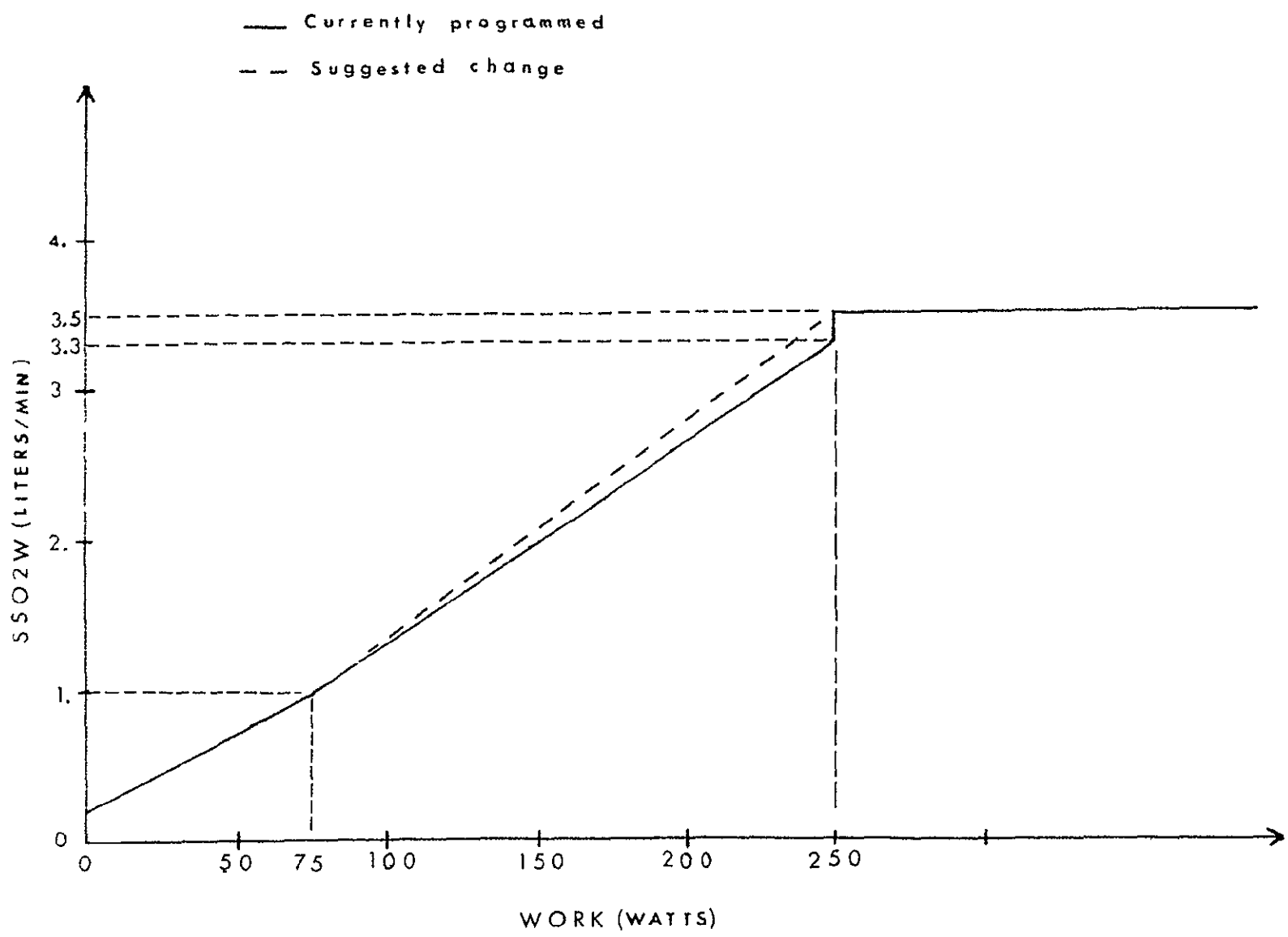

FIGURE 6. Piecewise linear relationship of steady-state oxygen uptake and work load used in model

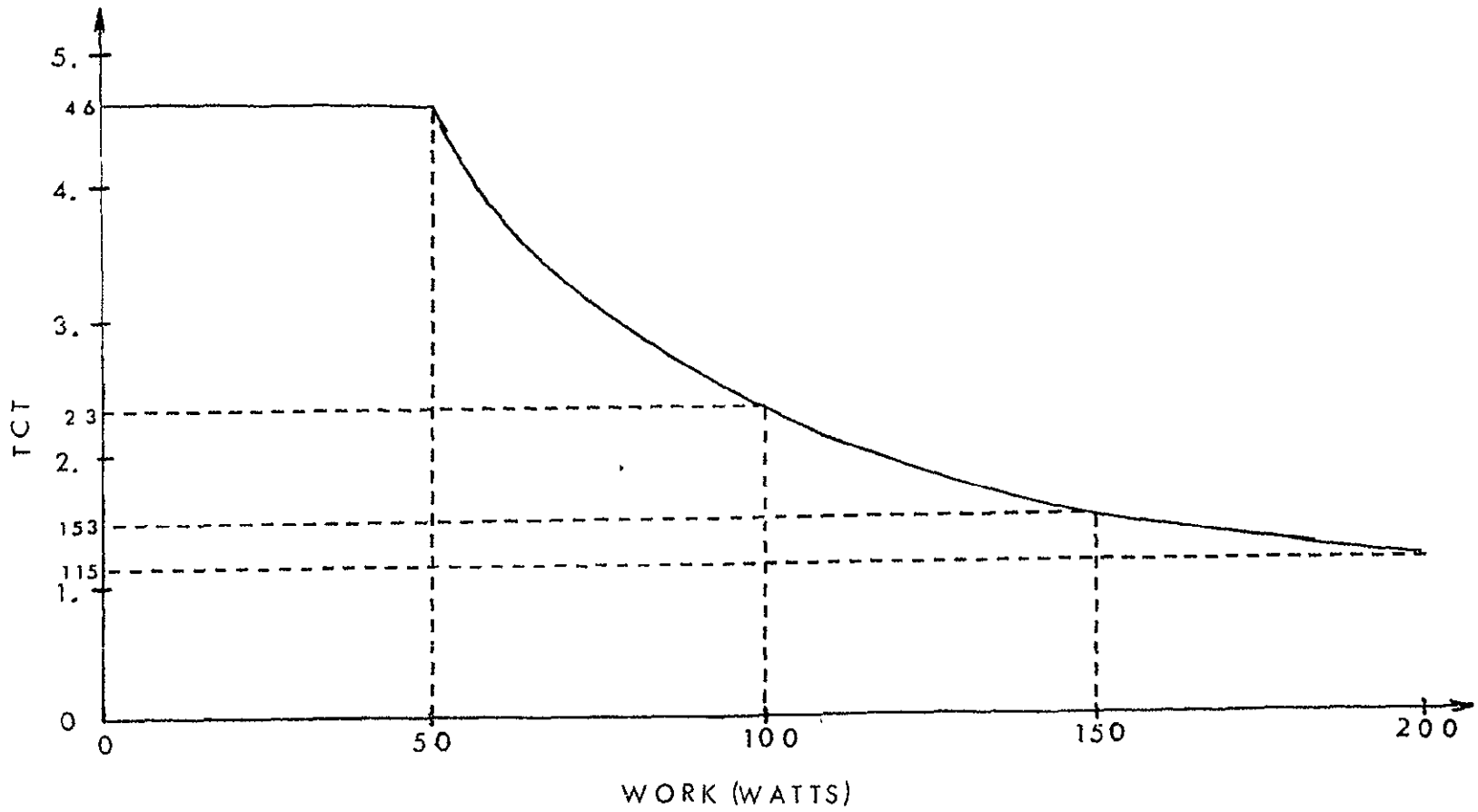

FIGURE 7. Inverse time constant versus work

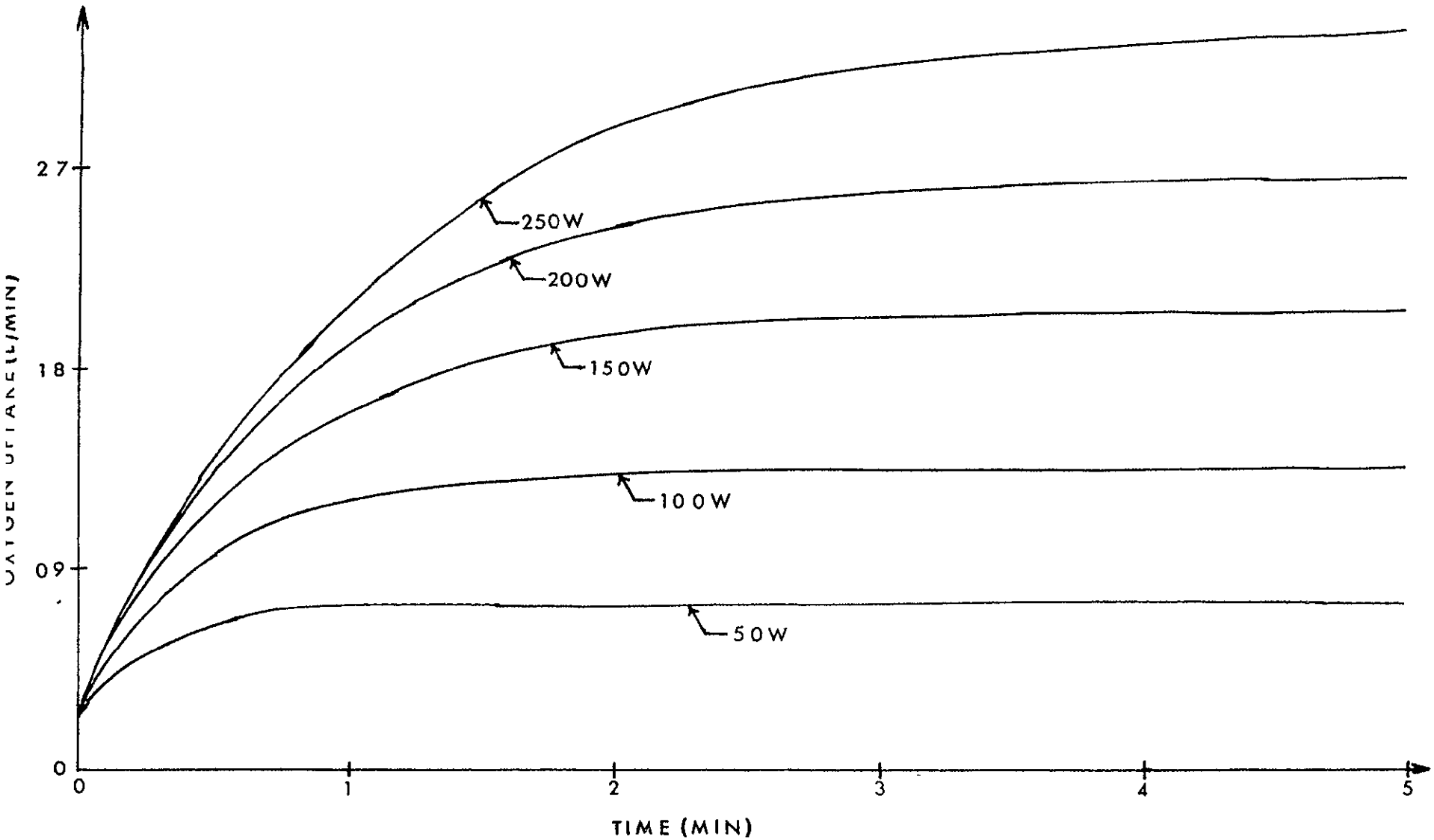

FIGURE 8. Uptake of oxygen from resting conditions

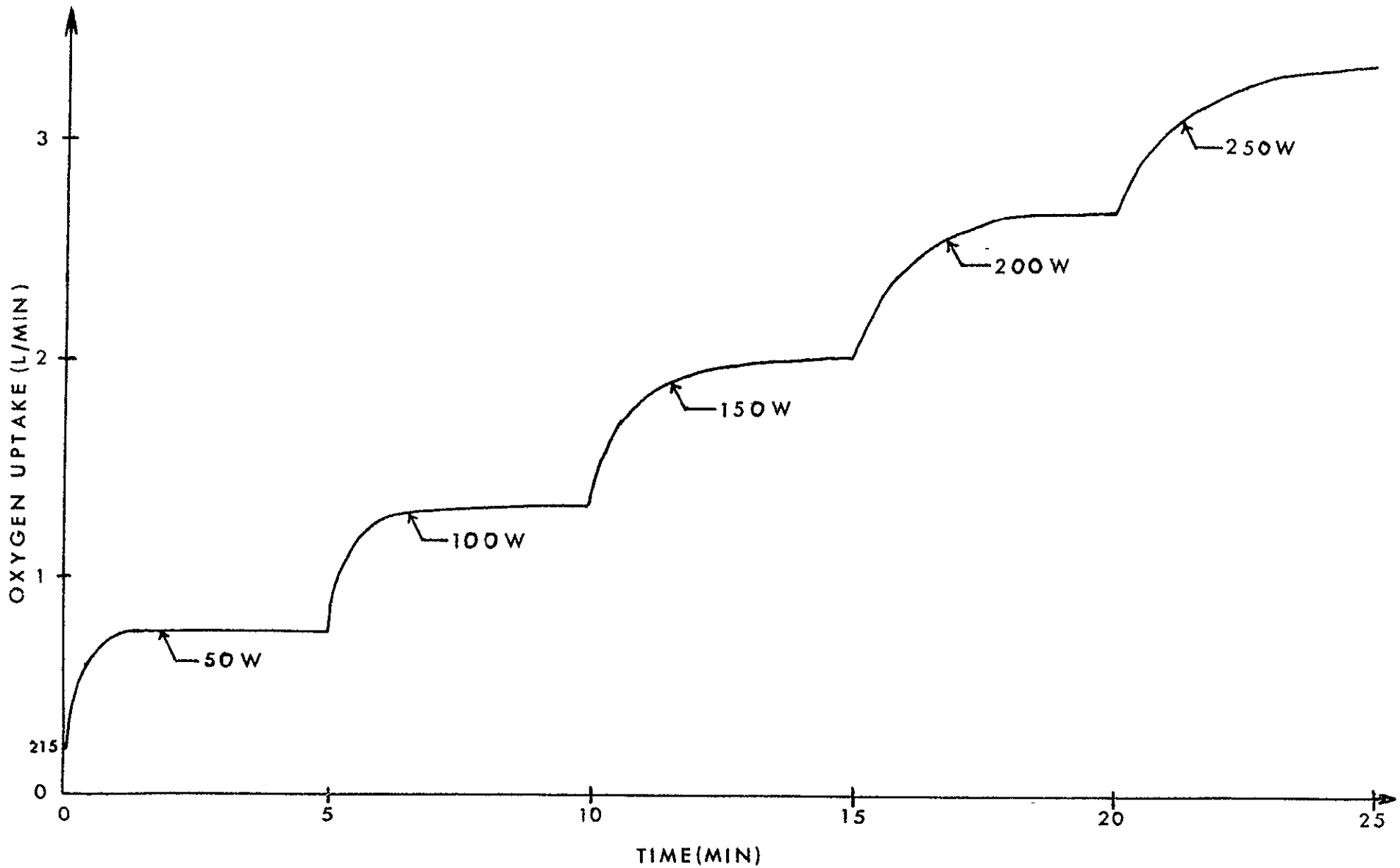

FIGURE 9. Uptake of oxygen for successive work loads

to be achieved when exercise transition is from rest or from other exercise levels. In both figures it is readily seen that the transient response is longer for greater workloads, the transition being either from rest or another workload.

(B). Decreasing Workloads

For decreasing workloads RC12 utilizes an oxygen consumption expression that is a decaying exponential. It has a time constant that is twice as long as the time constant used in the expression for increasing workloads. The expression is written as

$$RMT(2) = RMTB - (RMTB-RMTM) * EXP(-TCT*(CXT-TIMEON) + 0.5) \qquad (3 - 6)$$

where:

RMTB is the steady-state oxygen consumption at the new, lower workload.

CXT, TCT, and TIMEON are defined as with increasing workloads. However, it is important to notice that TCT is determined not by the new workload but by the previous workload. This is physiologically justified because the swiftness by which the body returns to the resting state is dependent upon the prior exercise level. The greater the prior exercise level the longer it takes to replace the oxygen and high energy stores of the body.

Figure 10 is a plot of RMT(2) for transitions from various exercise levels to rest, for five different workloads.

No changes are made for the metabolic production of CO_2 during increasing and decreasing workloads. For both increasing and decreasing workloads the metabolic production of carbon dioxide, RMT(1), is calculated by the same equations:

$$RMT(1) = (TVNT + 40.77)*RMT(2)/88.5 \qquad (3 - 7)$$

for TVNT less than or equal to 37.

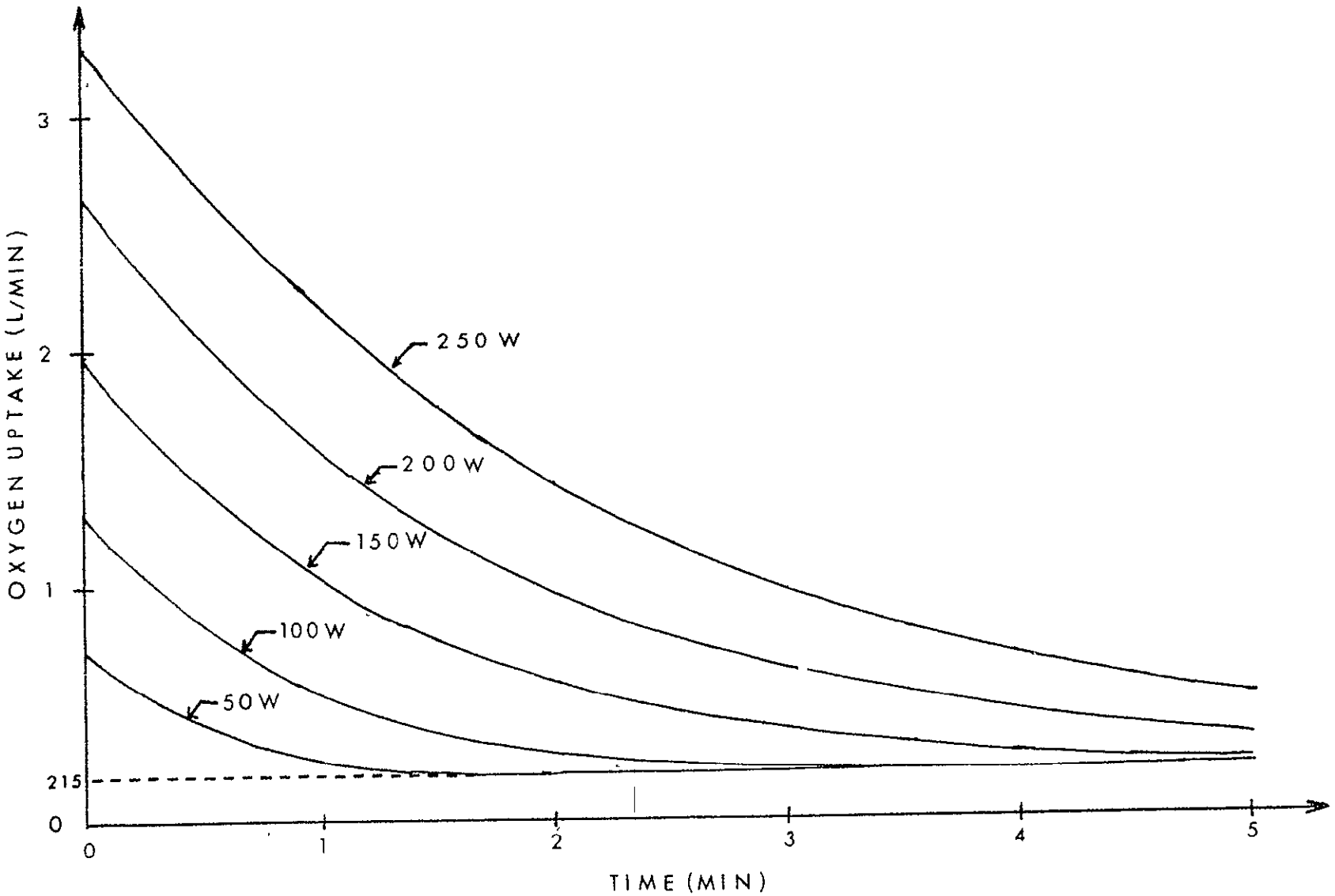

FIGURE 10. Oxygen uptake for decreasing work loads

For TVNT greater than 37

$$RMT(1) = 0.88RMT(2) \qquad (3-8)$$

where TVNT is the minute volume.

(C). System Controller Equation

Up to this point, only the alteration of the controlled system's equations during exercise has been discussed. It is still necessary to determine how the controller equation subroutine, RC17, is modified to take exercise into account.

As before, a flow chart can be obtained for RC17 as shown in Figure 11. From the flow chart it is still difficult to determine the interaction of the steps and how the various individual elements of the routine interact. A print routine which prints out the important variables is added to this subroutine. See Appendix 6.3 (RC17) . When the program is run at different workloads, knowledge of the subroutine functioning is obtained by utilizing these printouts.

Verification that the modification of the controller equation is based on the neurohumoral theory as discussed in Section 1.3 is possible. That is, it consists of a fast neural component and a slower humoral component. Referring to Appendix 6.3, which is the subroutine listing, the first calculation made is that of the ventilation as given by Grodins' controller equation, (VI). This value is then subtracted from the steady-state ventilation for the workload of interest, (SSVENT(SS02W(WORK))). This steady-state ventilation is calculated using the relationship given by the plot in Figure 12. This plot effectively illustrates that steady-state ventilation is linearly related to steady-state oxygen consumption. However, oxygen consumption is dependent upon the workload as previously discussed. The difference, if less than or equal to 15 liters per minute, between this steady-state value and the value

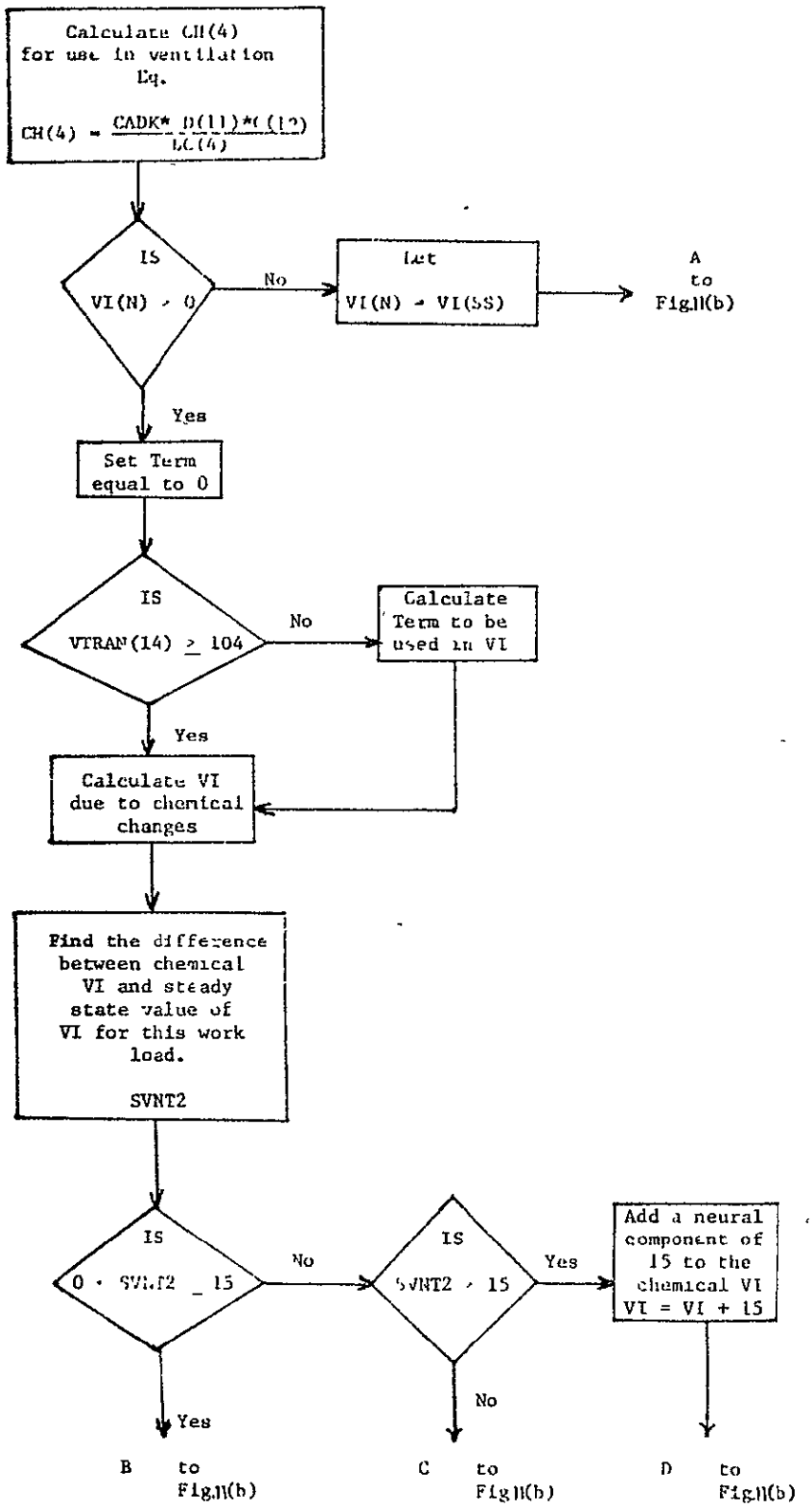

FIGURE 11. Flow chart for controller subroutine

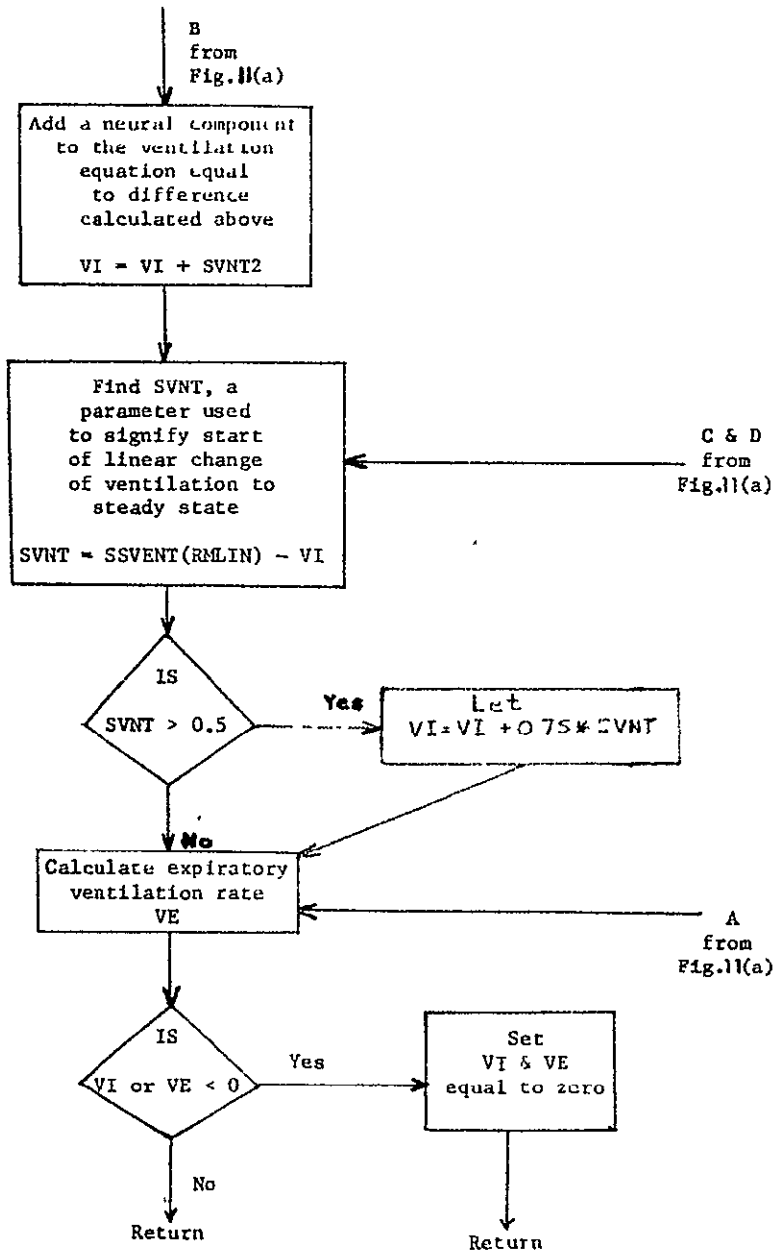

FIGURE 11(b). Continuation of flow chart for controller subroutine

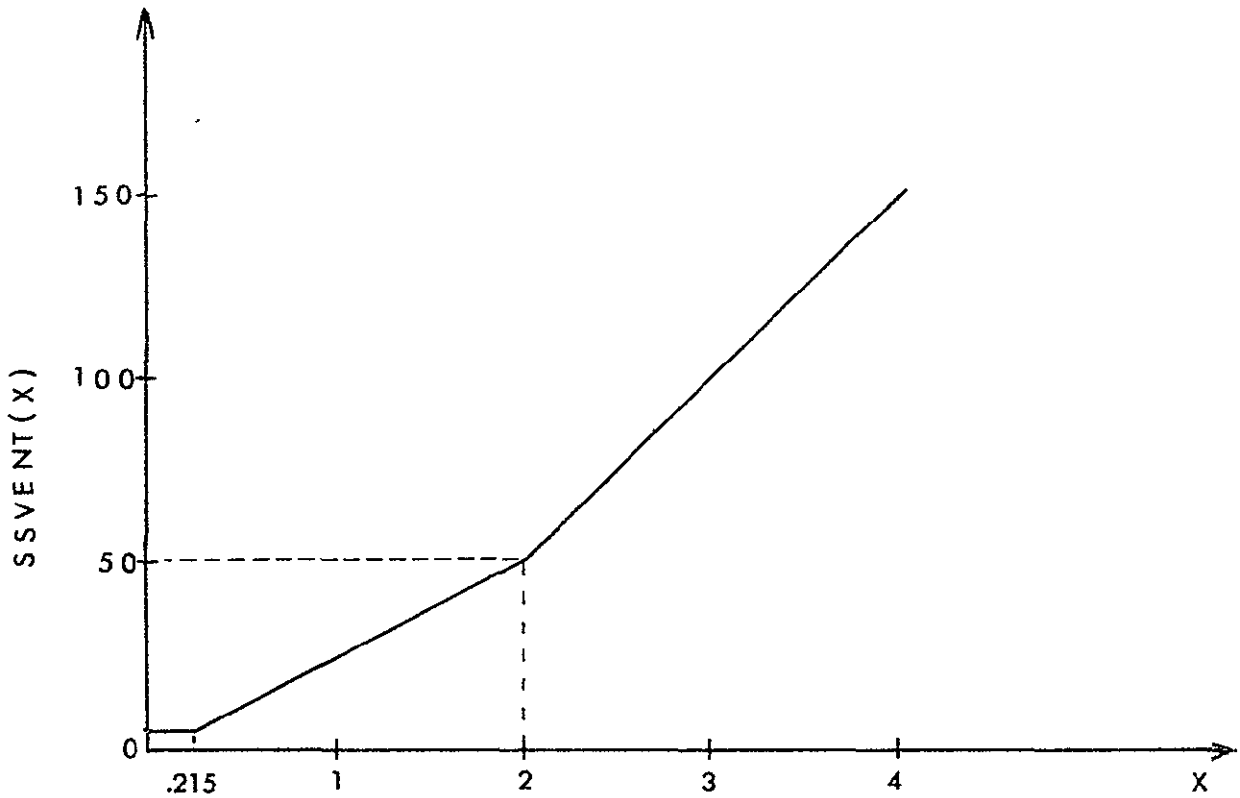

When X=SSO2 W(WORK) this plot illustrates a linear relationship between steady state ventilation and steady state oxygen uptake

FIGURE 12. Steady-state ventilation

obtained by Grodins' controller equation is the neural component. If the difference is greater than 15 liters per minute, the neural component is set equal to 15. The difference is given the variable name SVNT2. This neural component is added to the value of ventilation that is calculated by Grodins' controller equation and a new value for VI is obtained. Thus VI is defined as

$$VI = VI + SVNT2 \quad \text{for } 0 < SVNT2 \leq 15 \qquad (3-8)$$

or

$$VI = VI + 15 \quad \text{for } SVNT2 > 15 \qquad (3-9)$$

At this point, another variable is calculated, SVNT. SVNT is the difference between another steady-state value for ventilation defined by the term SSVENT(RMLIN) and the value of ventilation which is calculated in Equation 3-8 or 3-9. The variable SVNT is formulated as

$$SVNT = SSVENT(RMLIN) - VI \; . \qquad (3-10)$$

The argument RMLIN used to determine the steady-state ventilation term is calculated in RC12. RMLIN is a slowed down, linearlized version of RMT(2). It is given by

$$RMLIN = SS02W(WORK) - (SS02W(WORK) - RMTB2)(1.VTIME) \qquad (3-11)$$

where SS02W(WORK) and RMTB2 are as previously discussed. VTIME is the function that slows down RMLIN in relationship to RMT(2). It is given by

$$VTIME = TCT(CXT - TIMEON)/9.2 \quad \text{for } VTIME < 1 \qquad (3-12)$$

The value 9.2 makes RMLIN approach its steady-state value at a rate four times slower than RMT(2) when the workload is 100 watts. For workloads less than 100 watts, the response of RMT(2) is less than four times as fast. For workloads greater than 100 watts, the response of RMT(2) is greater than four times as fast Figures 13 and 14 show the relationship between RMLIN and RMT(2) for two different workloads (25 watts and 75 watts). Figure 13 represents a transition from rest to 25 watts while Figure 14 represents a transition from 25 watts to 75 watts.

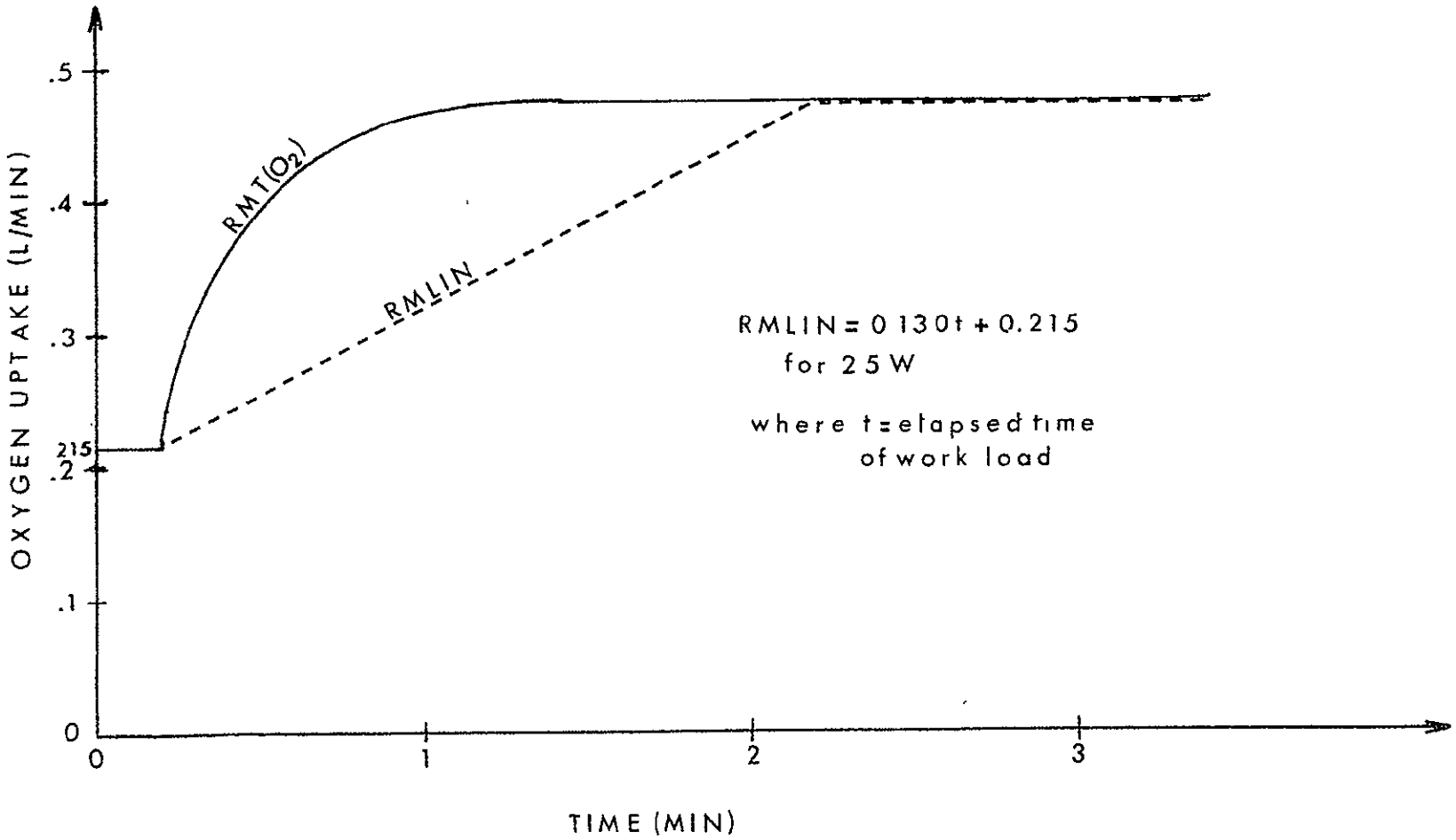

FIGURE 13. The relationship between oxygen uptake and RMLIN

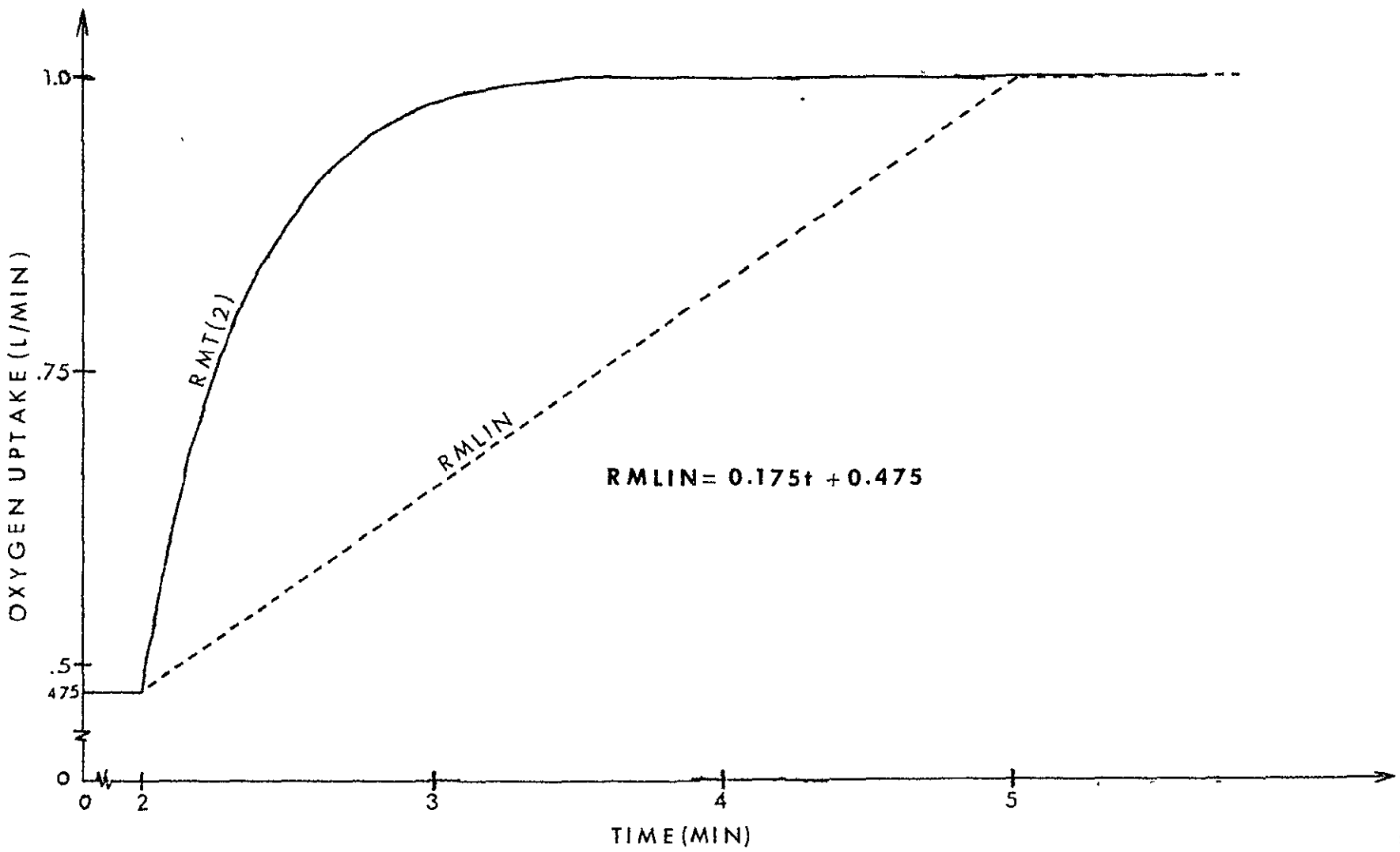

FIGURE 14. The relationship between oxygen uptake and RMLIN for 75 watts from 25 watts

When VTIME reaches the value of 1, RMLIN has reached steady-state and is given by:

$$RMLIN = SS02W(WORK). \qquad (3 - 13)$$

Returning to the discussion of the controller equation, if SVNT is greater than 0.5, ventilation will linearly approach its steady-state value. This is done by adding 75% of SVNT to the value of VI calculated above. The relationship used is:

$$VI = VI + 0.75SVNT \qquad (3 - 14)$$

After inspiratory ventilation has been calculated, expiratory ventilation is calculated, again using a relationship given by Grodins (2).

Figure 15 illustrates plots of the various variables discussed above for a workload of 75 watts. From these plots it is easily shown that the sum of VO and SVNT2 equals SSVENT (SS02W(WORK)) for SSVENT(RMLIN$<$0.5 + VI. VI is equal to the sum of VO and the neural component. When SSVENT(RMLIN) becomes greater than the sum of 0.5 + VI, VI starts a linear increase to its steady-state value for that particular workload by using Equation 3-14.

The controller equation modification has no physiological significance. This is justified by the detailed investigation of the appropriate subroutines. As indicated by Strippoli with further justification presented in Section 3.4 it does permit a reasonable simulation for specific workloads (27). The fast on- and off-transient responses can be associated with neural components. However, the functional expressions which simulate this component do not actually describe the physiology involved. This particular physiology has not been well documented.

3.3 Model Parameter Variations

One of the goals of the investigation was to evaluate Grodins' modified program with regard to sensitivities for reasonable variations in parameter values. Grodins' modified

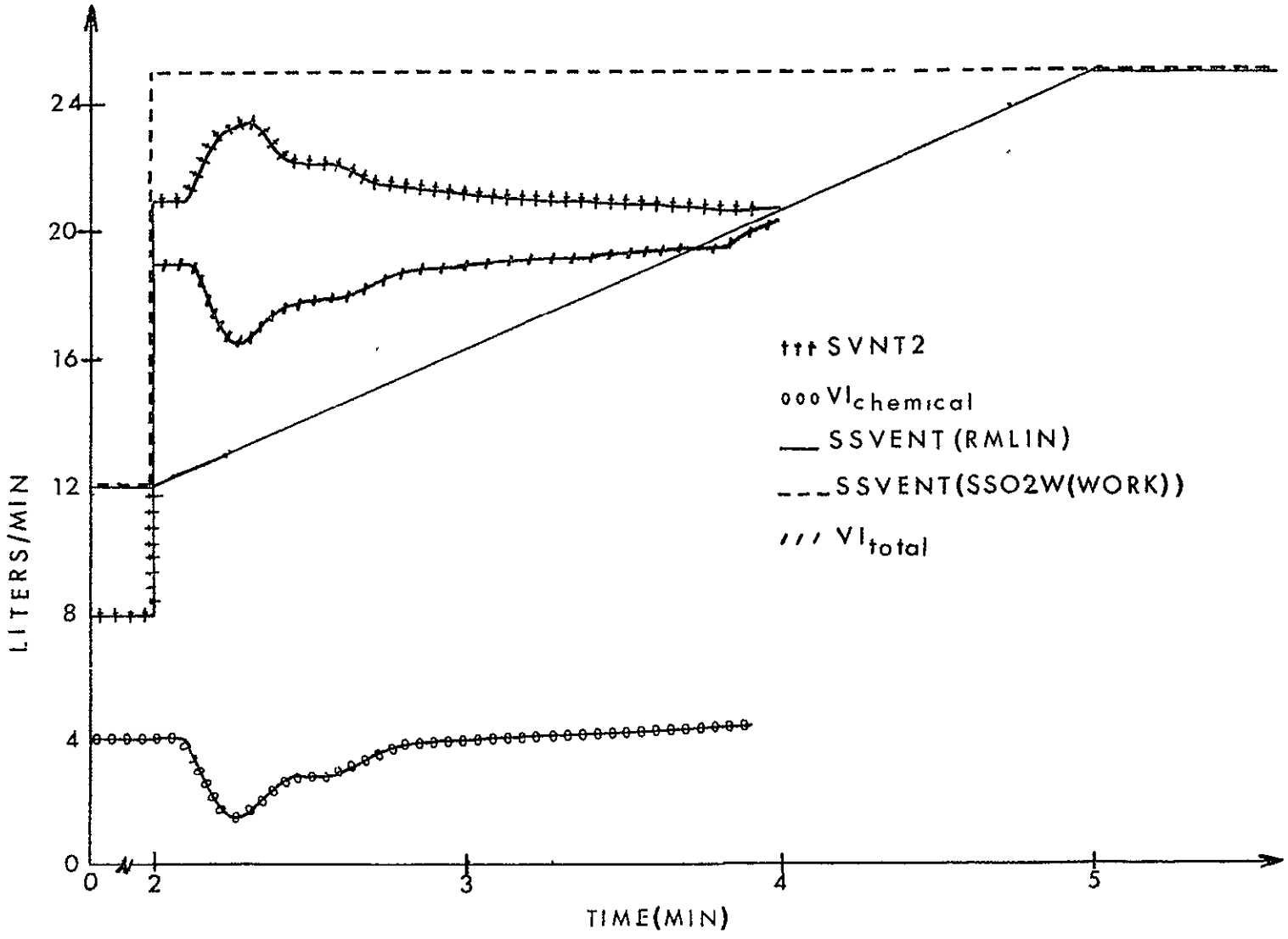

FIGURE 15. Relationship between important variables used in controller equation at 75 watts

program provides for various parameter variations by the use of input data cards. There are many standard conditions for inspired volumetric fractions of gases from which to base a sensitivity analysis. The decision was made to use the following data from which all simulations of variations in parameters are compared

$$
\begin{aligned}
B &= 760 \text{ mm Hg} \\
FI(CO2) &= 0.1000 \\
FI(O2) &= 0.1100 \\
FI(N2) &= 0.7900
\end{aligned}
$$

See Appendix 6.1 for the type of responses obtained and the table of input data cards used for the base run.

It is believed that these base conditions were adequate for the sensitivity analyses performed. However, one should use extreme caution in projecting, in a direct fashion, the sensitivity of any parameter to other base conditions. Only one parameter or group of common parameters was altered at one time. This is really the first step in what should be a continuing effort in analyzing combinations of parameter variations and weightings.

The format followed in the Study Report (Appendix 6.1) is one which hopefully conveys the model's capabilities and limitations in a concise and informative manner. There is a tremendous amount of data which is not discussed or presented in graphical form. Only the variables which present significant changes are addressed. This is not meant to deemphasize the other variables' importance. General Electric Company's Technical Information Release 741-MED-3008 and 741-MED-3009 illustrate the output data format and the possible relationships between variables that can be generated (32,33).

With regard to inspired gaseous concentrations only the on-transient and related steady-state conditions are analyzed. The off-transient as related to the transition from an exercise to the resting state is presented later in Section 3.3.2.

3.3.1 Resting State and Sea Level Conditions

The computer program is a modified version of Grodins' program similar to that used by Weissman (28). Although it has a subroutine which involves a work-exercise phenomenon, the case of the resting subject is considered first. A table in Appendix 6.1 presents the input data format giving card number, symbol, normal initial value, and a brief description of each parameter.

Since a detailed discussion and evaluation of the parameter sensitivity analyses are presented in Appendix 6.1 only a few comments are included here.

The controlled system parameters that were varied include

(1) The time constants R1 and R2 of the first order differential equations describing cardiac output and brain blood flow,

(2) the standard bicarbonate content BHCO3 BRAIN and BHCO3 TISSUE of the brain and tissue compartments, and

(3) the diffusion coefficients D(CO2) and D(O2) of CO_2 and O_2 across the blood-cerebrospinal fluid barrier.

Briefly, the simulation proved to be insensitive to variations in R1 and R2 after an initial transient disturbance of about 1 minute duration. The simulation was found to be much more sensitive to changes in the bicarbonate content of the tissues than of the brain which is thought to be related to relative volume sizes of the two compartments in addition to the buffering and metabolism relationships. Results of the simulations with varying diffusion coefficients supported the known physiology (blood-cerebrospinal fluid barrier highly permeable to CO_2) involved in that the system was sensitive to D(CO2) variations and insensitive to D(O2) variations (34).

The controlling system parameter weightings that were varied for the resting subject include

(1) the weighting of the H^+ concentration in the CSF compartment, CNT SENS COF,

(2) the weighting of the H^+ concentration at the carotid bodies' site, CRTD BDY SCF,

(3) the weighting of the relative influence of the H^+ concentration in the CSF and brain compartments, CENT SENS PT, and

(4) combinations of (1) and (2).

No significant variations were observed in any compartmental H^+ concentration, $P_{a(O_2)}$, Q, or $P_{a(CO_2)}$ for variations in CNT SENS COF. However, VI was shown to be directly dependent upon CNT SENS COF although not responding rapidly in the initial transient. Considering all of the variables monitored there was a greater degree of sensitivity toward variations in CRTD BDY SCF than CNT SENS COF. Thus, there is an indication that the system responds more rapidly to chemical changes at the carotid bodies' site than in the CSF compartment. This feature was further emphasized when combinations of CNT SENS COF and CRTD BDY SCF variations were used. Simulation runs illustrated that the brain compartment H^+ concentration detector mechanism responds faster than the CSF H^+ concentration detector system. All of the variables illustrated a faster response as CENT SENS PT was increased.

3.3.2 Exercise States at an Altered Environment

The usefulness of such a model must be evident for conditions which approximates those of actual experiments. Thus, this model must perform quality simulations under environmental

conditions such as those of Skylab. From the simulations run for sea level conditions, barometric pressure =760 mm Hg, it was concluded that the most sensitive component of the system was the controlling equation. Thus, the simulation efforts related to an altered environment were concentrated on the controlling equation and its variable weightings both for the resting state and various exercise levels.

Initial variable values were obtained by allowing the simulation to reach steady-state conditions when subjected to the altered environment. This first simulation effort involved a change of only the barometric pressure and inspired gaseous concentrations. Thus, these specific input data cards were altered as shown in Table 4 with the CO_2 concentration corresponding to 5 torr.

Table 4. Input Data Cards Specifying the Altered Environment

Card No.	Symbol	Revised Initial Values
C(30)	B	260.0000
C(31)	FI(CO2)	.0192
C(32)	FI(02)	.7000
C(33)	FI(N2)	.2808

The use of the steady-state values obtained from this run compensated for the preconditioning period. See Table 2 of Appendix 6.1. Exercise levels of 5-minute intervals were utilized as shown in Table 5 for the following set of time intervals.

Table 5. Input Data for Workload Schedule

Time Interval	Workload *
$0 \leq t <$ 5 min	0 watts
5 min $\leq t <$ 10 min	50 watts
10 min $\leq t <$ 15 min	100 watts
15 min $\leq t <$ 20 min	150 watts
20 min $\leq t <$ 30 min	0 watts

*See Appendix 6.3 for Workload Input Data Format.

Since the simulations discussed in Section 3.3.1 indicated that the most influential component of the system was the controller equation simulations of exercise at Skylab conditions concentrated on further evaluations of the controller equation.

The controlling system parameter weightings that were varied during the transition from one exercise level to another include

(1) the weighting of the relative influence of the H^+ concentration in the CSF and brain compartments, CENT SENS PT,

(2) the weighting of the H^+ concentration in the CSF compartment, CNT SENS COF, and

(3) the weighting of the H^+ concentration at the carotid bodies' site, CRTD BDY SCF.

All exercise levels produce a slightly lower steady-state response for V_I when CENT SENS PT is increased while the decrease in exercise level is not significantly altered by variations in CENT SENS PT. The greater the weighting of the H^+ concentration sensing in the venous blood of the brain, the higher the relative arterial CO_2 tension is for any instant of time. As expected the level of the H^+ concentration in the CSF compartment is greater when CENT SENS PT is increased.

Since $C_{CSF(H^+)}$ does not deviate from the base run for variations in CNT SENS COF other variables are not altered significantly either. As observed in Section 3.3.1 the simulation is more sensitive to alterations in CRTD BDY SCF than CNT SENS COF. This fact is also evident under exercise conditions.

Appendix 6.1 also includes plots of $P_{a(O_2)}$ versus Q for the complete exercise cycle (rest-exercise levels-rest). One interpretation of these plots is that a depletion and recovery of arterial oxygen is evident for the exercise transitions that do not initiate from a resting state. Other conclusive statements should not be made without further investigation.

3.4 Evaluation of Exercise Feature

For further supportive evidence of the role that exercise plays in the control of respiration, other exercise levels and level transitions were simulated (27). In particular, the justification of both neural and humoral components was considered with an expansion of the investigation of the exercise subroutines discussed in Section 3.2.3. The values for the input data cards are shown in the following listing. All other input data cards have values indicated in Appendix 6.1.

Table 6. Input Data Cards for Five Exercise Simulation Runs

Input Data Cards	Run #1	Run #2	Run #3	Run #4	Run #5
C(1)	0.1783	↑	0.1674	0.1746	↑
C(2)	0.5336		0.5419	0.5231	
C(3)	0.2881		0.2907	0.3123	
C(4)	0.6413		0.6345	0.6359	
C(5)	0.0012		0.0011	0.0011	
C(6)	0.0011		0.0011	0.0011	
C(7)	0.6153	Same	0.6164	0.6390	Same
C(8)	0.0015	as	0.0011	0.0007	as
C(9)	0.0012	Run #1	0.0012	0.0011	Run #1
C(10)	6.0000		7.3800	11.5717	
C(11)	0.7496		0.6839	0.7260	
C(12)	48.1202		47.9542	47.3567	
C(13)	36.6316		36.0486	35.3290	
C(14)	70.6804		68.5268	66.2437	
RMT(1)	0.1820		0.1820	1.1699	
RMT(2)	0.2150	↓	0.2150	1.3294	↓
WORK2	0.0/0.2 *	0.0/0.2 *	25/0.2 *	100/2.5 *	0.0/0.2 *
WORK2	50/1.8 *	25/1.8 *	70/2.0 *	0.0/30 *	50/2.5 *
WORK2	100/2.0 *	75/2.0 *	100/2.0 *	------	0.0/2.0 *

*Watts/Min

Gallagher (22) showed that at workloads of 50, 100, and 150 watts no neural component was simulated for the transitions to 100 and 150 watts when the transition was made during steady-state. The absence of the neural response was also shown by some of the above simulation runs. Figure 16 is a plot of VI for Run #1.

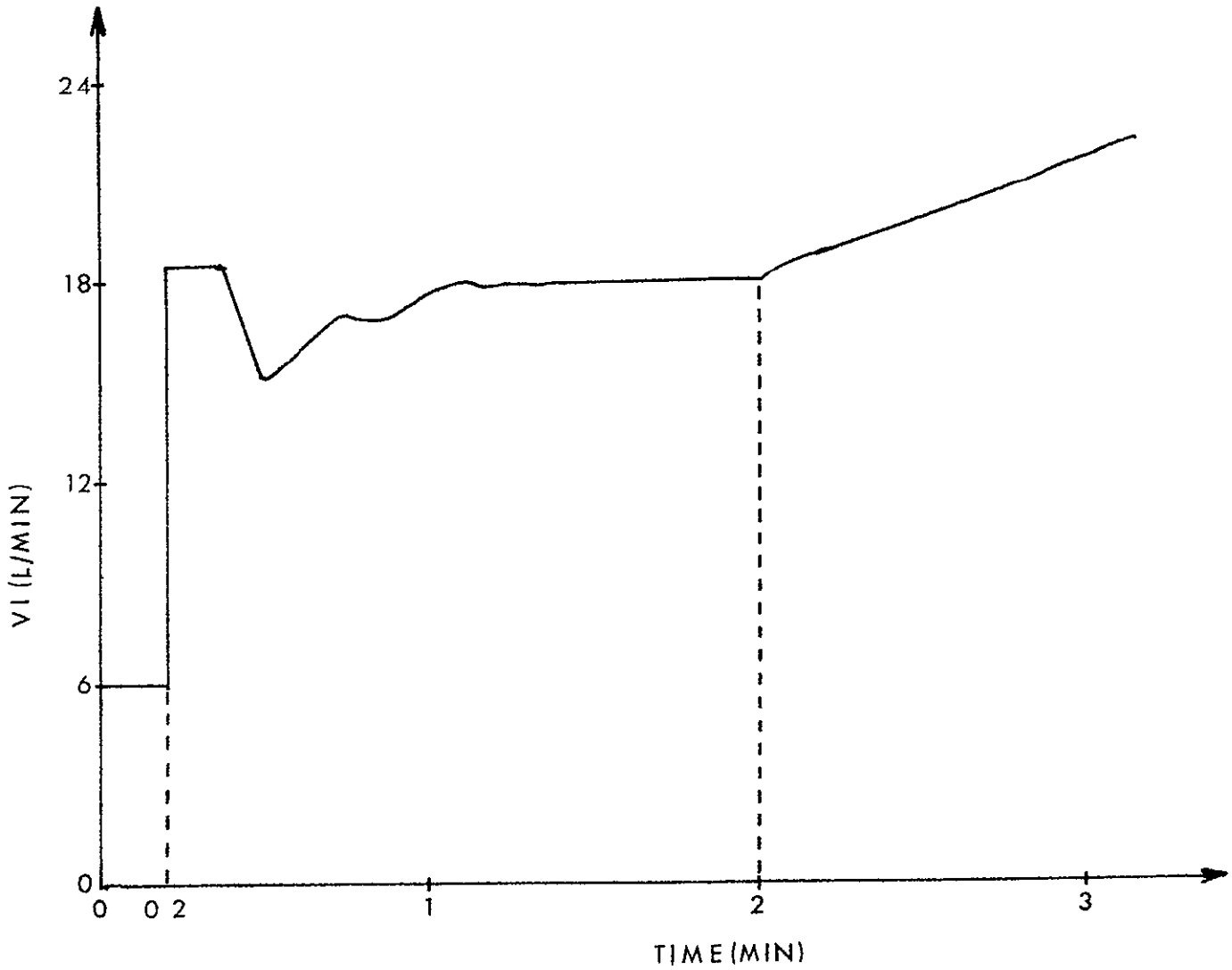

FIGURE 16. Simulation run number one for 0–50–100 watts

For a simulation run of 0, 25, and 75 watts (Run #2) neural components were observed for both exercise transitions. Figure 17 illustrates the VI response for this run. It is also observed that the neural response accounted for the entire response in the 0 to 25 watt transition. This type of response was also justified by D'Angelo et al. (23) when they reported that ventilation during low levels of exercise was predominately associated with a neural response.

Run #3, having exercise transitions of 25 to 70 watts and 70 to 100 watts, simulated neural components at both transitions as shown by Figure 18. Although no quantitative experimental data is available for comparison it appears that the neural component is sensitive to the level and increment of exercise levels. Also, the problem discussed later in this paragraph, that of system initialization, prevailed in the initial transient response; however, the initial deviation in the system's variables are not as severe for 25 watts. Run #4, with exercise levels of 100 and 0 watts, was used to determine the type of response that would be obtained in the off-transient of exercise. The off-transient response obtained was not justifiable. Further investigation of the exercise subroutines revealed that at the first calculation of the controller equation, which occurs before RC12 is implemented, the initial work level is considered to be 0 watts instead of the desired 100 watts. Thus, the transient responses are invalid. Further modification of the program is required if simulations are to be initialized with other than 0 workload (or small workloads).

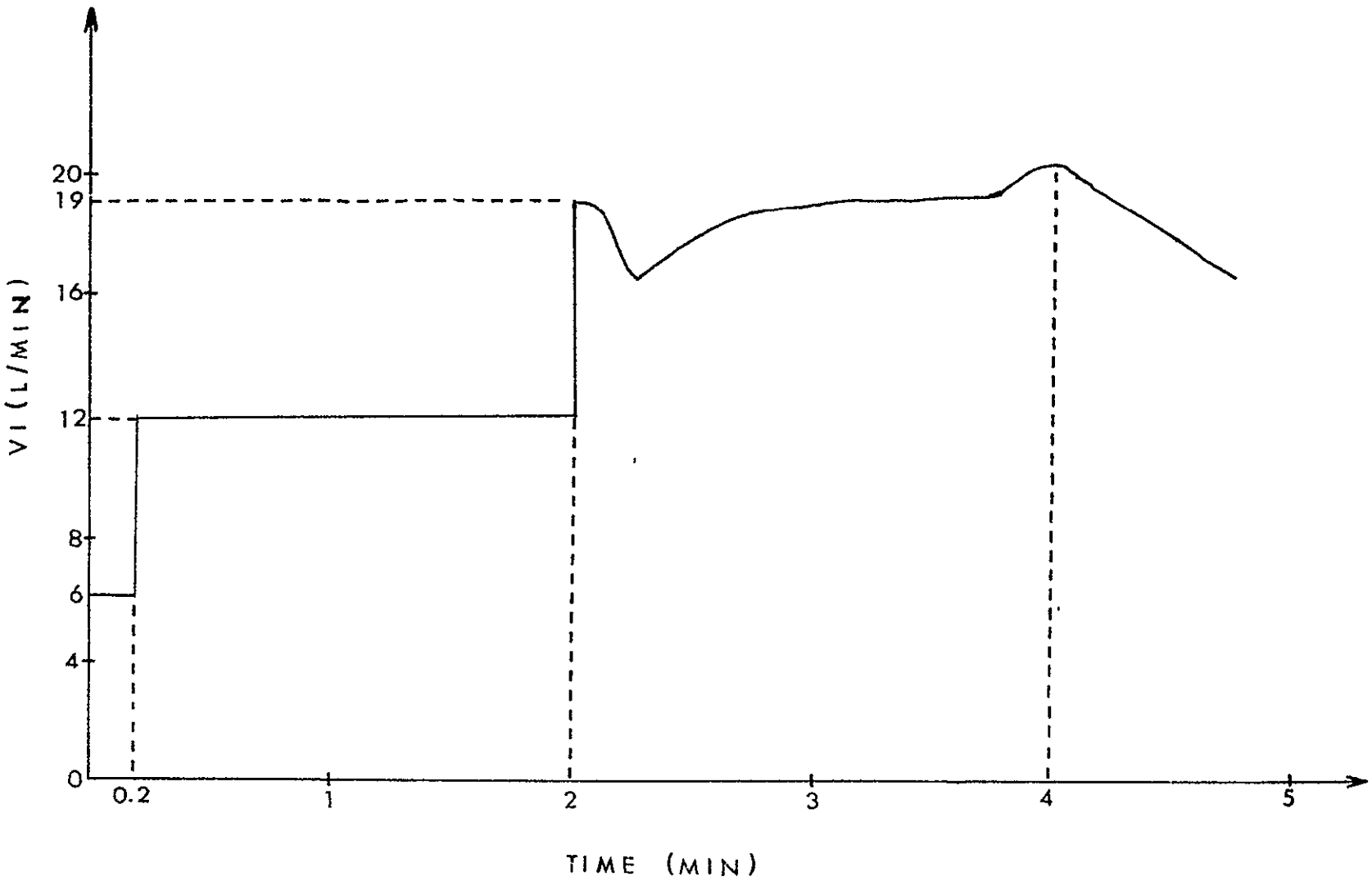

FIGURE 17. Simulation run for 0-25-75-0 watts

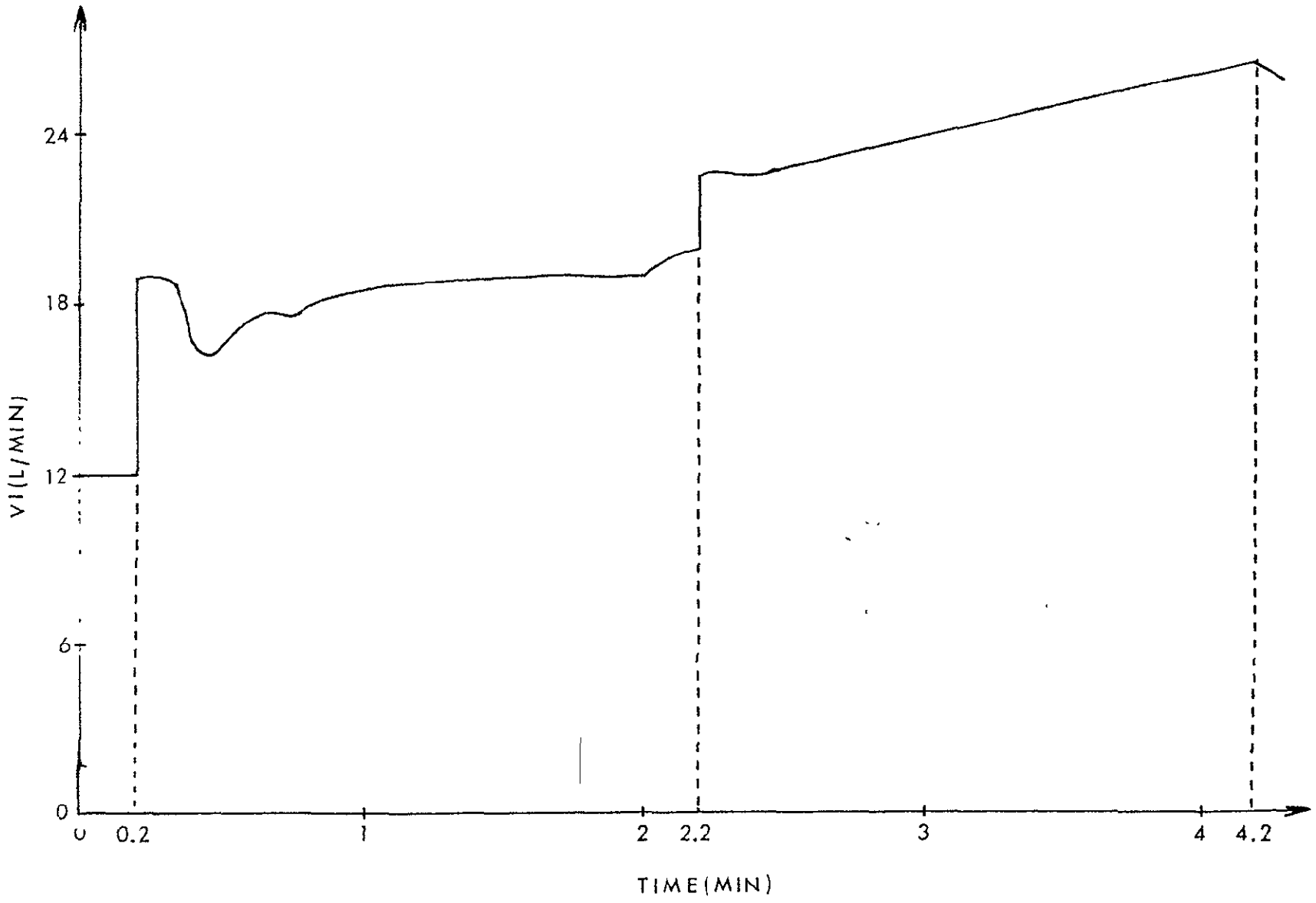

FIGURE 18. *Simulation run number three for 25–70–100–0 watts*

4. MILHORN'S RESPIRATORY CONTROL MODELS

4.1 Statement of Objectives

The other phase of the research effort was the study and analysis of Milhorn's respiratory control models. The major thrust of this effort was in the summarization of the theory and assumptions of existing models which are associated with Milhorn's research (4, 5, 7, 8, 24, 35). One aspect of the objectives was to analyze published program results and describe potential applications of Milhorn's work to improve Grodins' program. These potential modifications could then be implemented in Grodins' program and evaluated at a future date if the continuation of the modelling effort should include such implementation.

4.2 Models' Variations and Significant Features

The detailed evaluation of Milhorn's models leading to the fulfillment of the above objectives is presented in Appendix 6.2. Most of Milhorn's models, although developed under different experimental conditions and for varying motivations, contain features that are similar to Grodins' work. Therefore, to complete an investigation of two of the major groups of respiratory control models it seemed appropriate to discuss the salient features of Milhorn's models and suggest special modifications which might enhance Grodins' model.

With Appendix 6.2 (Study Report) available it is not necessary to go into any depth in the summary of the Study Report. Only a brief statement concerning the various models that were presented in the Study Report is contained in this section.

One of Milhorn's first models was a compartmental respiratory model with the basic assumption being that the control of alveolar ventilation was due to CO_2 and O_2 levels (7). The effects of the H^+ stimulus was related to P_{CO_2} by a linear relationship. The model contained a controlled system and a controlling system; thus, having an overall similarity

to that of Grodins' model. Upon the establishment of variable and functional interrelationships a set of eight variables and eight differential equations was used to describe the system. The ventilatory controller equation provided the feedback mechanism. An evaluation of some of the simulation responses is contained in Appendix 6.2.

Another model which illustrated the static, dynamic, mechanical, and cyclic phenomena emphasized a restructuring of the ventilatory controller equation (8). Special weightings of the H^+ contribution from the peripheral sensors, a central receptor in the brain, and a central receptor in the cerebrospinal fluid were given for the controller equation. No exercise phenomena were presented. The interrelationships between the cardiovascular and respiratory systems were experimentally investigated with the goal being to expand the range of Lloyd and Cunningham's controller equation range for $P_{A_{CO_2}}$.

The concept of venous admixture and a detailed description of the capillary shunts form the basis for another model (24). Features of this model would be of value to the present research if a modification of Grodins' model included a description of the gas exchange mechanism associated with the lung compartment. The most important advantage in the use of this model would be the component of the simulation associated with the admixture phenomenon as the fractional gaseous concentrations of the environment were altered.

For a complete understanding of the transient ventilatory response, the receptor sites, number of sites, and the general nature of the responses at these sites should be better defined. Consequently, the system presented by Milhorn and Brown (5) was formulated in such a manner as to more fully utilize the information from the steady-state responses in order to improve the transient simulations. Alveolar O_2 and CO_2 tensions are described in

terms of inspired O_2, O_2 consumption, alveolar ventilation, respiratory quotient, water vapor pressure, and barometric pressure. Since all of these terms are accessible in Grodins' model these equations could be made compatible with such a model. Interdependence of these forenamed variables are discussed in detail in Appendix 6.2. A comparison of Gray's controller equation and Lloyd and Cunningham's controller equation was made using the model framework as described above. Three-dimensional plots with inspired O_2 and CO_2 tensions and either alveolar ventilation, tidal volume, or respiratory frequency were presented. Also three-dimensional plots with alveolar O_2 and CO_2 tensions and either alveolar ventilation, tidal volume, or respiratory frequency were given. With an expansion of this system to include exercise it appears to contain features which would be appropriate for suggested modifications to Grodins' program. Further discussion of this modification is presented in Section 5.

Stimuli of 3, 5, 6, and 7% CO_2 - air mixtures were used in a model developed by Reynolds et al. (35). The basic purpose of the experiment was to correlate the strength of the stimuli and the magnitude of the responses. Minute ventilation, tidal volume, respiratory frequency, alveolar oxygen tension, and alveolar carbon dioxide tensions were recorded in order to better define the transient responses of the variables. Summary discussions concerning the transient half-times in addition to the responses of the forenamed variables for the various stimuli are presented in Appendix 6.2. This type of experimentation will help to chart subject responses for rapid changes in the gaseous mixtures of the air.

The H^+ concentration is a variable that is well established as a contributor to the control of ventilation. The precise H^+ concentration detector sites are not established. It is

conceivable that two detector sites, one corresponding to the CSF compartment and one corresponding to the venous blood of the brain, might be appropriate for respiratory control monitoring of the H^+ concentration. A model has been formulated which attempts to establish a satisfactory transient response in ventilation which would apply if the CO_2 detection site (or H^+ concentration) was assumed to be on either side of the control receptors (4). With this model ventilation is assumed to be controlled by the peripheral sensor H^+ concentration and the central sensor H^+ concentration. Pulmonary ventilation is the sum of two signals. These two signals have a weighted functional dependence upon the peripheral and central sensors. This special weighting allows for the establishment of a single sensor depth. Utilizing a CO_2 tension gradient this depth was found to correspond to a position which is 77% of the distance between cerebrospinal fluid P_{CO_2} and deep brain tissue P_{CO_2}. Three different controller equations were evaluated using this single sensor site depth.

This section has contained a summary of a review of control system models developed by Milhorn and his associates. Chronologically speaking, the models encompass those developments associated with the steady-state models published in the mid-1960's to the more recent investigations involving CFS perfusion studies. These recent developments also attempt to simulate transient responses as well as steady-state responses.

5. CONCLUSIONS AND RECOMMENDATIONS

5.1 Grodins' Respiratory Control Model

After an evaluation of the parameter sensitivity analyses, the simulation runs at an altered environment, and the exercise subroutines it appears that Grodins' Respiratory Control Model can be made adaptable to the research efforts of the Environmental Physiology Branch, Biomedical Research Division, Life Sciences' Directorate, NASA-JSC. Several alterations to the program which could improve the physiological soundness of the variable responses are included in this section. Here specific considerations are directed toward the exercise phenomenon while Section 5.2 contains suggested modifications for Grodins' program which evolve from Milhorn's work.

With regard to the formulation of Grodins' basic program the parameter sensitivity analyses should be extended to include combinations of parameter variations especially in the off-transient environmental conditions. Considering the assumptions used in developing the model a tolerable range of environmental CO_2 levels should be established. Since levels of inspired CO_2 are physiologically correlated with ventilation rates, coma, anesthetized states, and death, the model should perform in a similar manner. If it doesn't perform as required CO_2 limits must be specified.

At present, the model includes no general description of the control of cardiac output and regional blood flow. Certainly the regional blood flow feature will be important when the interfacing of the cardiovascular, thermal, renal/endocrine/body fluid, and respiratory systems are considered. This would pertain to both the resting and exercising subject.

In the investigation of the interrelationships of parameters that comprise the exercise subroutines of Grodins' modified program it was observed that the metabolic rate of oxygen

consumption was the basis for the modification. The system controller equation which incorporates the exercise phenomenon is based upon the neurohumoral theory. Inspired ventilation (V_I) is simulated by a fast neural component and a slow linear component when transition in exercise levels occurs. The slow linear component is related to oxygen consumption via a linear version of RMT(2) called RMLIN. See Section 3.2.3 and Appendix 6.3 for the details of this modification.

Based upon the investigations thus far, there are several suggested modifications for the existing program that would improve the simulation with regard to exercise. According to published experimental data, a transition in exercise levels produces a faster transient response for ventilation. With a modification of the expression for VTIME (Subroutine RC12) from

$$\text{VTIME} = \text{TCT}(\text{CXT}-\text{TIMEON})/9.2 \qquad (5-1)$$

to

$$\text{VTIME} = \text{TCT}(\text{CXT}-\text{TIMEON})/4.6 \qquad (5-2)$$

the variable responses to exercise will be more acceptable.

A punched card output is available for the first fourteen input data cards. If, in addition to these output data cards, the workload, time, metabolic rate of oxygen (RMT(2)), and the metabolic rate of carbon dioxide (RMT(1)) were included as punched output data it would permit the responses corresponding to one workload to be used as the initial conditions for a succeeding workload. To complete this change, the initialization of time and workload should be removed. Although not completely justified, these changes might also require a renaming of variables in the exercise portion of the controller equation since WORK is used for both resting and exercising conditions.

The off-transient response for exercise is not extremely satisfying from a physiological point of view. The output response VI for simulation Run #5 (See the listing in Section 3.4.) is shown in Figure 19. The initial off-transient contains an instantaneous decrease in VI

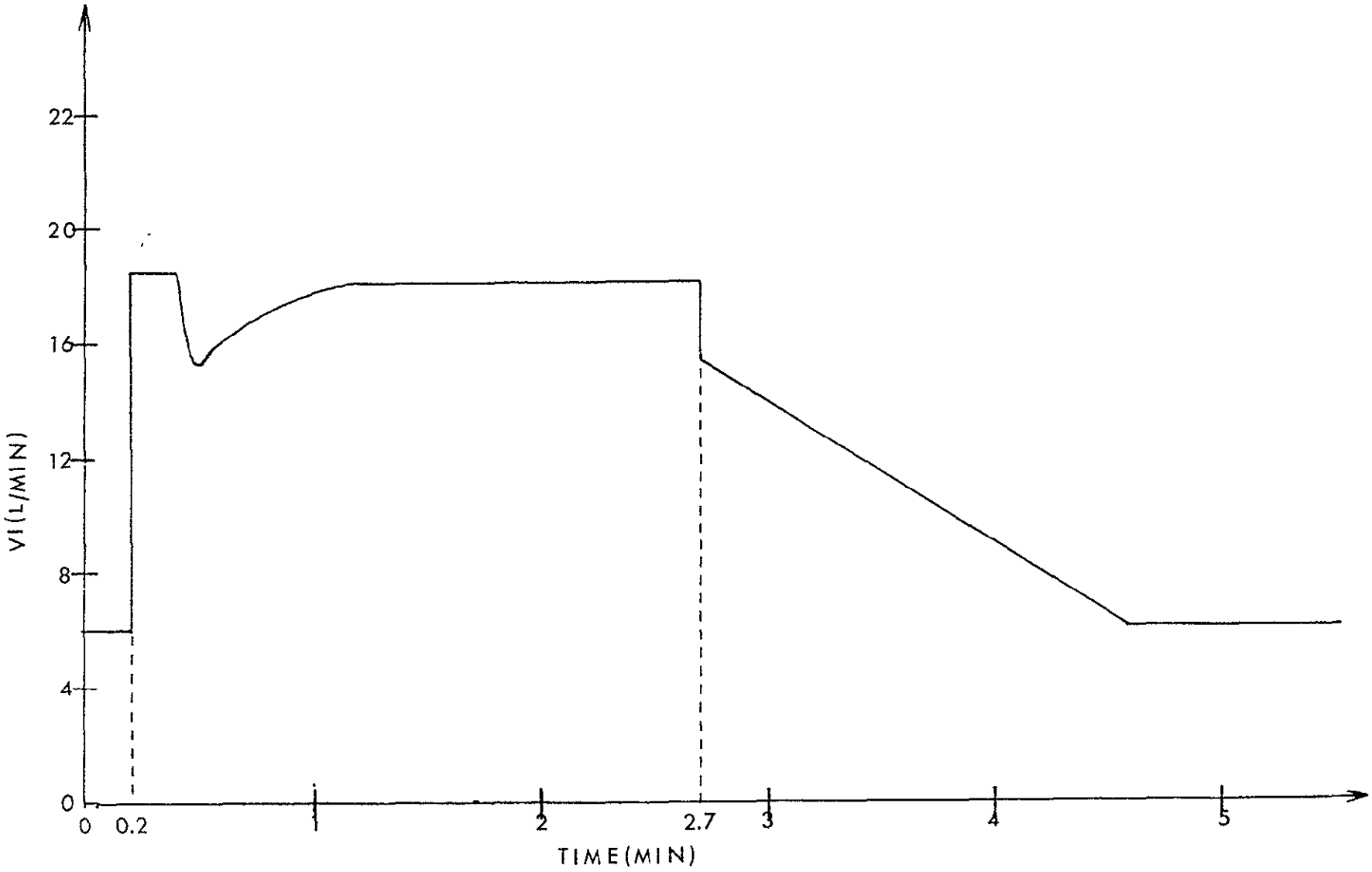

FIGURE 19. Simulation run number five for 0–50–0 watts

followed by a linear decrease to the resting level. This instantaneous decrease which one associates with the neural response is of smaller magnitude than the corresponding instantaneous increase in the on-transient for 50 watts. Whether the implication that a neural component functions after exercise has ceased is physiologically sound or not is uncertain.

It was observed that when an off-transient in exercise was initiated before steady-state conditions were reached for the previous exercise level there was no instantaneous decrease in the VI response. In fact, under these conditions, it was possible to generate an increase in the initial off-transient for VI. This particular response is caused by the fact that the routine for the off-transient is dependent upon the inspired ventilation reaching steady-state.

In subroutine RC12, calculations are made for respiratory frequency (FREQ) and heart rate (HRATE). These two functions are not utilized in any other portion of the program. They are given as functions of the O_2 metabolic rates of the tissue (RMBT(2)) and brain (RMB(O2)) compartments.

$$FREQ = 8.1 + 7.815\ (RMT(2) + RMB(O2)) \qquad (5 - 3)$$

$$HRATE = 43.8\ (RMT(2) + RMB(O2)) + 54.5 \qquad (5 - 4)$$

These two expressions do not simulate in a faithful manner the respiratory frequency and heart rate for exercise transitions. For example, heart rate increases instantaneously in the initial transient of exercise and usually overshoots the steady-state value for any particular exercise level (31). But, since RMT(2) does not change in this rapid manner, neither will HRATE. It is postulated that the immediate increase in heart rate corresponds to a neurological phenomenon.

A fairly linear relationship has been established between steady-state heart rate and work load. Starting at approximately 65-70 BPM for the resting state the heart rate increases to about 200 BPM for maximal exercise of a normal individual. Data related

to these steady-state values in addition to data corresponding to an exercise dependent neurological component would form the basis for an improved HRATE expression.

A similar postulation can be made for the respiratory frequency. In comparing the two formulations for FREQ and HRATE, FREQ has probably the more stable response of the two since the overshoot, if there is any, is not as pronounced as for HRATE.

5.2 Milhorn's Respiratory Control Models

Several of Milhorn's models and their corresponding experimental justifications are presented in Appendix 6.2. The models that were summarized included those which concentrated on steady-state responses and also some of the more recent ones which simulate transient responses. The prime objective in the evaluation of these models was to establish some of their features as possible modifications for Grodins' model. As with Grodins' work several of Milhorn's models were involved in evaluation or establishment of controller equations. The suggested modifications involving the controller equation do not include any dependencies upon exercise. Thus, any controller equation alteration or substitution must be made compatible with the existing exercise controller functions of Grodins' model.

The two most promising modifications of Grodins' program involve Equations 22 and 23 of Appendix 6.2. They are repeated here for convenience.

$$\dot{V} = 2\left(P_{A_{CO_2}} - 37.24\right)\left(1 + 13.6/(P_{A_{O_2}} - 25)\right) \geqslant 0 \qquad (5-5)$$

$$P_{CS_{CO_2}} = P_{B_{CO_2}} + \left(P_{CSF_{CO_2}} - P_{B_{CO_2}}\right) \exp\left[-x\sqrt{\frac{\dot{Q}_{cs}\ S}{D/760}}\right] \qquad (5-6)$$

Equation 5-5 allows for the additive and multiplicative effects of O_2 and CO_2 instead of monitoring the compartmental H^+ concentrations. Since Equation 5-5 is only valid for $P_{A_{CO_2}} \geqslant 37.24$ mm Hg a new range is required so that simulations under the environmental

conditions of 5 torr CO_2 at 260 mm Hg can be run. Both variables involved here are accessible in Grodins' model.

The modification involving the lone sensor site for the detection of CO_2 tension is more complex. This modification relates to Equation 5-6. The components of Grodins' controller equation which rely upon the H^+ concentration of the venous blood of the brain and the CSF subsystem would be replaced by a form of Equation 5-6. The essence of this modification is that it combines the sensing mechanisms of the brain and CSF compartments. Another technique involving the utilization of Equation 5-6 but still allowing the control of V_I to be H^+ concentration oriented would be to convert $P_{CS_{CO_2}}$ into a corresponding H^+ concentration. This particular H^+ concentration would be a weighted value corresponding to the effective sensor site.

It is felt that these modifications would be the most beneficial to pursue in that they add missing detail and flexibility to the present modified version of Grodins' model.

6. APPENDICES

The Appendices include two Study Reports and the program listing for the modified Grodins' Respiratory Control System. The Study Reports are essentially complete documents in that they each contain a table of contents, data with related discussions, conclusions, recommendations, and their own bibliographies. Both Study Reports and the program listing are included as Appendices in this research report to add continuity and completeness.

6.1 Study Report - Respiratory Control System Simulation

General Electric Company TIR-741-MED-3021

6.2 Study Report - Summarization of the Major Features of Milhorn's Respiratory System Models

General Electric Company TIR-741-MED-3030

6.3 Program Listing for the Modified Grodins' Respiratory Control System

Minor modifications are indicated in the right hand margins of subroutines RC13 and RC17. The addition to RC13 is to prevent the simulation from getting into a loop which was found to occur under certain conditions. The RC17 modification provides additional print routines as mentioned in the text.

General Electric Company TIR-741-MED-3008

ASD
APOLLO SYSTEMS DEPARTMENT
GENERAL ELECTRIC

HOUSTON, TEXAS TECHNICAL INFORMATION RELEASE

TIR 741-MED-3021

FROM	TO
R. C. Croston, Ph. D.	J. A. Rummel, Ph. D.

DATE	WORK ORDER REF:	WORK STATEMENT PARA:	REFERENCE:
3/15/73	MA-252T	NAS9-12932	

SUBJECT

Study Report of a Respiratory Control System Simulation

The attached study report was submitted to G. E. by Dr. R. R. Gallagher in partial fulfillment of his subcontract.

R. C. Croston

R. C. Croston, Ph. D.

Attachment
/db

CONCURRENCES

Counterpart:

Medical Projects Unit Manager: C. W. Fulcher

Engr'g. & Advanced Programs Subsection Mgr. W. J. Beittel

DISTRIBUTION GE/AGS: Central Product File

ASD 4028

PROGRESS REPORT

GENERAL ELECTRIC COMPANY
CONTRACT NUMBER
036-E31001-M5906

RESPIRATORY CONTROL SYSTEM SIMULATION

by

R.R. GALLAGHER, Ph.D.
DEPARTMENT OF ELECTRICAL ENGINEERING
KANSAS STATE UNIVERSITY
MANHATTAN, KANSAS

RESPIRATORY CONTROL SYSTEM SIMULATION

TABLE OF CONTENTS

I. INTRODUCTION 1

A. Overview of Physiological System Modelling 1
B. Model Variations 1

II. DESCRIPTION OF GRODINS' RESPIRATORY CONTROL MODEL 6

A. General Model Description 6
B. Comparison of Various Controlling Functions 11
1. Gray's Controller Equation 12
2. Lloyd and Cunningham's Controller Equation 12
3. Milhorn's Controller Equation 13
4. Grodins' Controller Equation 14

C. Research Goals for the Study Report 16

III. VARIATIONS IN MODEL PARAMETERS 18

A. General Considerations and Philosophy 18
B. Controlled System Parameter Variations - Barometric Pressure = 760 mmHg 25
C. Controlling System Parameter Weightings - Barometric Pressure = 760 mmHg 33
D. Comments on Simulated Skylab Conditions 44
E. Controlling System Parameter Weightings - Barometric Pressure = 260 mmHg 47

IV. CONCLUSIONS AND RECOMMENDATIONS 66

V. APPENDIX 69

VI. BIBLIOGRAPHY 85

I. INTRODUCTION

A. Overview of Physiological System Modelling

The importance of biological system modelling within the area of biomedical research is becoming more evident. In particular, the application of control theory which involves the mathematical description of element functionings and interrelationships between elements has made possible the simulation of very complex physiological feedback control systems. The mathematical relationships range from algebraic formulations and ordinary linear differential equations to nonlinear differential-difference equations and stochastic processes.

Prior to deciding upon a particular physiological system model it is instructive to utilize the expertise found in the literature and optimally meet the demands of the project with combinations or variations of existing research efforts. This is precisely the procedure established in this research involving the respiratory system.

B. Model Variations

The system modelling effort that is discussed in the following report is one related to the respiratory control system. Several models have been developed for the respiratory control system emphasizing particular features which make them adaptable for specific experimental and simulated environmental conditions.

A few brief comments about some of the respiratory modelling efforts and their salient characteristics follow. Alveolar ventilation responses were of prime importance for the output responses of a model developed by Bellville et al. (1). Frequency, amplitude, and mean level of inhaled CO_2 were altered in a manner corresponding to sinusoidally varying CO_2 inhalation allowing a frequency response analysis of the respiratory system.

The phenomenon of pulmonary mechanics as related to various forms of inspired-expired flow systems has been researched by Fry (2). Here variables related to physiological and pathological features of the air passageways are better defined. Elastic behavior of the lungs, airway compliances, and resistances were considered by Mead (3) in a model possessing characteristics similar to those of Fry's model.

Saidel et al. (4) developed a lumped parameter simulation of the pulmonary gas transport system with the ultimate goal of analyzing parameter changes. The model included five variable-volume compartments approximating the airway and alveolar regions and a constant-volume compartment representing the capillary bed. Extensive efforts were taken to mathematically describe the mass balance of the gas compartments and blood compartments.

Breathing patterns related to CO_2 oscillatory exchanges are presented in a model developed by Yamamoto and Hori (5). A linear controller equation is used to describe, indirectly, the dependence of tidal volume and rate of breathing upon cerebral P_{CO_2}.

ORIGINAL PAGE IS
OF POOR QUALITY

Exercise and/or work load is a very important input for the proposed research. Analysis of maximum ventilation related to chronic airway obstruction and exercise has been conducted by Pierce et al. (6). This particular research was not intended to be a respiratory control system model study; however, the results of the endeavor are very applicable to modelling of airway passages and to the investigation of the respiratory-exercise relationships.

Milhorn and Brown's steady-state human respiratory system (7) is very closely related to Grodins' respiratory control system (8). In Milhorn's model, a controlling system and a controlled system form the basis from which mass balance equations are written describing the exchange mechanisms for CO_2 and O_2. The controlling equation of Milhorn's model is an important fundamental component which should be critically evaluated and compared to a similar component of Grodins' model.

Closely associated with Milhorn and Brown's model is a study of pulmonary capillary gas exchange by Milhorn and Pulley (9). This work portrays a more detailed version of the capillary gas exchange by introducing anatomical parameters in the model.

Assuming a second order representation for the mechanical portion of the respiratory system Hilberman et al. (10) has utilized the Fourier series analysis and phasor notation to determine the modulus of impedance, phase angle, compliance,

ORIGINAL PAGE IS
OF POOR QUALITY

and resistance of the respiratory system. In doing so this research has developed a technique for adjusting parameters associated with respiratory mechanics. Although this research effort is not directly related to the present research the evaluation of parameters for specific environmental conditions might be useful in extending the proposed model's capabilities.

Since the pH of each compartment of the proposed model is an important monitored variable the research by Hermansen et al. (11) relating exercise and blood pH will prove to be a valuable piece of supportive research in determining a level of maximal exercise for the experimental subjects and in turn for the simulation efforts.

A comparison of several respiratory system models' characteristics and capabilities are presented by Yamamoto and Raub (12). This review emphasizes that all models possess unique features but are categorized into three groups: (a) Models related to those of Grodins, (b) Models related to Horgan's efforts, and (c) Models related to Milhorn's research. Also this review cites several other models giving their comparisions to the above three groups.

As the project progresses there must be a concerted effort in establishing the criteria for the interaction between the four physiological systems; respiratory, cardiovascular, thermal, and the renal-body fluid systems. Research such as that of Albergoni et al. (13) which attempts to define the significant variables used in the interfacing model of the circulatory and respiratory systems and the recently published research

effort of Guyton et al. (14) will help in the formulation of these criteria. Guyton's research may prove most valuable since it attempts to integrate some of the dynamical interactions of various physiological subsystems; i.e. circulatory dynamics, pulmonary dynamics, regional blood flow control and its relationship to P_{O_2}, tissue fluids and pressures, heart rate, and stroke volume.

To fully appreciate the transition between model choices or the potential capabilities of a model an understanding of the preceding references is mandatory. This is certainly not an exhaustive listing but several references have excellent bibliographies which makes it an adequate state-of-art listing for this research.

II. DESCRIPTION OF GRODINS' RESPIRATORY CONTROL MODEL

The material presented in this section is a condensed summary of the model's description. Basically, this is the version of the model that was used for the simulations involving the parameter sensitivity analyses with various exercise levels and environmental conditions. These simulations will be explained in a later section. A more complete description of Grodins' model is included in the Appendix.

Also, included in this section are comparisons of several controlling functions and a brief statement of the immediate research goals as described in the following Study Report.

A. General Model Description

The model can be envisioned as a feedback control system comprised of a "plant" (the controlled system) and the regulatory component (controlling system). The controlled system is partitioned into three compartments corresponding to the lungs, brain, and tissue with a fluid interconnecting path representing the blood. A set of differential-difference equations describing a gas transport and exchange system between the lungs, blood, brain, and tissue compartments constitutes the framework for the models. A controller equation describing the inspired ventilation as a weighted function of the H^+ concentration in the cerebrospinal fluid ($C_{CSF(H^+)}$), the H^+ concentration in the arterial system ($C_{a(H^+)}(t - \tau_{ao})$), the H^+ concentration in the venous blood

of the brain ($C_{a(H^+)}(t - \tau_{aB})$), and the oxygen partial pressure at the carotid chemoreceptor sites ($F_{A(O_2)}$) provides the feedback mechanism. A good qualitative explanation of the alveolar-arterial, venous blood-brain, and venous blood-tissue equilibria formulations involving acid-base buffering, metabolism, and empirical relationships is given by Grodins (8). These particular relationships which are used in the development of the differential-difference equations are probably the most complex, both mathematically and physiologically speaking, of any of the model segments. The respiratory feedback system is represented by the block diagram in Figure 1.

With reference to the following description of the compartmentalization and notation used, a list of symbols is given in the Appendix of Grodins' paper (8). The same terminology is adhered to here and in the following discussions. The basic assumptions and features of the model's compartments that are characteristic of Grodins' program are enumerated below.

Lung Compartment:

1. Void of respiratory cyclic phenomena.
2. Constant volume and uniform content.
3. Flow rate of uniform gas stream is dependent upon the variations of RQ from unity.
4. $P_{a(CO_2)}$, $P_{a(O_2)}$, and $P_{a(N_2)}$ of expired air and lung exit arterial blood are equal.

Tissue Compartment:

1. Uniform partial pressures equal to venous blood partial pressures.

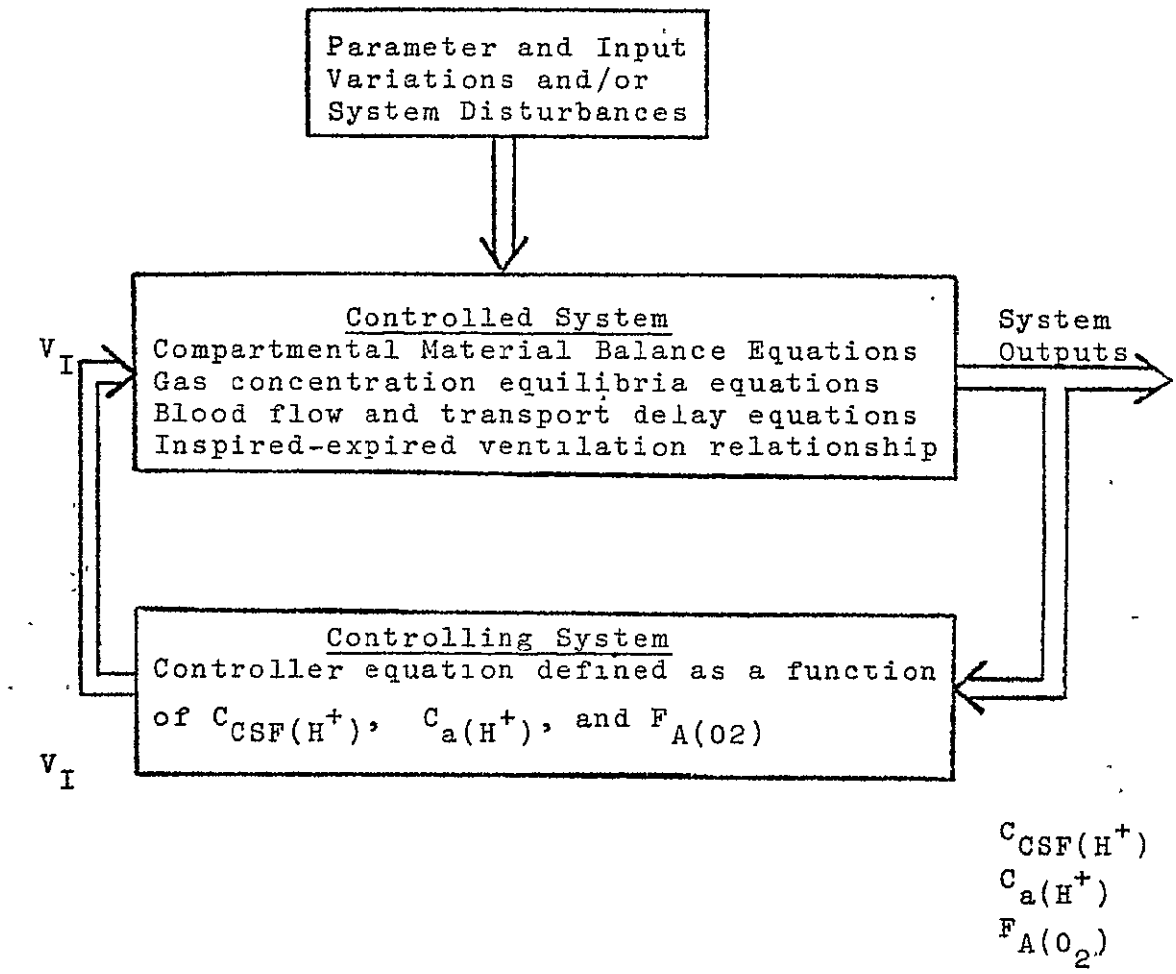

Figure 1. Respiratory Feedback Control System

2. Removal of CO_2 and supplying of O_2 at a constant rate are functions of metabolism.
3. Only physically dissolved O_2 and N_2 are considered.
4. $C_{T(CO_2)}$ is a function of $(BHCO_3)_T$ and appropriate buffer relations.
5. Bicarbonate concentration $\neq H^+$ concentration.

Brain Compartment:

1. Uniform partial pressures equal to venous blood partial pressures.
2. Removing of CO_2 and supplying of O_2 at a constant rate are functions of metabolism.
3. Only physically dissolved O_2 and N_2 are considered.
4. $C_{B(CO_2)}$ is a function of $(BHCO_3)_B$ and appropriate buffer relations.
5. Bicarbonate concentration $\neq H^+$ concentration.
6. Brain/CSF membrane is permeable only to respiratory gases.
7. Partial pressure gradient occurs only across membrane.
8. No buffering of carbonic acid in CSF. Bicarbonate content is constant for $P_{CSF(CO_2)} > 10$ mmHg.

Blood Interconnecting Pathways:

1. $C_{a(O_2)}$ is a function of $P_{a(O_2)}$, arterial pH, and the Bohr effect (effect of $P_{a(CO_2)}$).
2. $C_{a(CO_2)}$ is a function of $P_{a(CO_2)}$, $(BHCO_3)_b$, Hb, HbO_2, plasma protein content, and the Haldane effect (effect of $P_{a(O_2)}$).

3. Arterial blood pH is a function of $P_{a(CO_2)}$ and bicarbonate content evolving from the Henderson-Hasselbalch equation.
4. Only physically dissolved nitrogen is considered.
5. Transport delays are a function of volume and flow rates.
6. Q and Q_B are functions of $P_{a(CO_2)}$ and $P_{a(O_2)}$ with assumed time constants.
7. Recombination of venous tissue and venous brain blood enter the lungs after a variable transport delay.

Controlling System:

1. Not explicitly described in terms of receptor and sensor, locations, afferent nerves, central nervous system, motor nerves, and respiratory muscles.
2. No dynamically described elements in neurological aspects of the system--no time delays.
3. Direct input (chemical concentrations)--output (ventilation) relationships.

An important aspect of the simulation is related to the blood transport time delays. As with any physically dynamic system involving flow dynamics or transfer of information, there are time delays in signal transmission. The time delay, τ, is associated with the blood flow from the lung to the brain compartment, from the lung to the tissue compartment, from the tissue to the lung compartment, from the brain to the lung compartment, and from the lung compartment to the carotid

ORIGINAL PAGE IS
OF POOR QUALITY

body receptor. These are very necessary terms and their incorporation in the system equations enhances the confidence placed upon the dynamics of the simulation. To further refine these time delays, they are not considered to be predetermined constants but are continuously recalculated. They are time dependent in that they are functions of cardiac output, brain blood flow, and vascular segment volumes. This reasoning is very sound since the blood flow dynamics obviously affect relative site gas concentrations. However, consultation with Dr. Grodins has led to the questioning of the improvement in the simulation's fidelity with these time delay formulations in comparison to a more simplified version with a correspondingly simpler computer algorithm.

A modification of Grodins' program involves the determination of respiratory frequency and heart rate. (15) At present the simulation is using the following expressions. Respiratory frequency is defined as

$$FREQ = 8.1 + 7.815\ (RMT(O2) + RMB(O2))$$

and heart rate is defined as

$$HRATE = 43.8\ (RMT(O2) + RMB(O2)) + 54.5$$

where RMT(O2) and RMB(O2) refer to the O_2 metabolic rates of the tissue and brain compartments respectively.

B. <u>Comparison of Various Controlling Functions</u>

The controlling function is a very important link in the total feedback system. This is one component of the study that has not been evaluated in depth other than variations of the parameter weightings in the existing equation as is further

described in the parameter sensitivity analyses section. Other forms for the controller equation should be incorporated in Grodins' model for a more complete evaluation.

Since all controller functions simulate the actual system in a more realistic physiological manner over specific variable ranges, it seems instructive to compare some of the more established ones.

1. Gray's Controller Equation

Gray's controller equation (7) describes alveolar ventilation as a function of alveolar CO_2, P_{ACO_2}, and alveolar oxygen, P_{AO_2}, as

$$\overset{o}{V}_A = aP_{ACO_2} - b + c(d - P_{AO_2})^n \geq 0 \qquad (1)$$

with empirical constants, a, b, c, d, and n. $\overset{o}{V}_A$ is really a function of two expressions, one describing the dependency upon P_{ACO_2}, $(aP_{ACO_2} - b)$, and the other related to P_{AO_2}, $(c(d - P_{AO_2})^N)$. Consideration of only additive effects of CO_2 and O_2 has been proven invalid, but the inclusion of this equation illustrates one of the first stages of development of a controller equation.

2. Lloyd and Cunningham's Controller Equation

Lloyd and Cunningham's controller equation was developed under the basic assumptions that the product as well as the additive form of CO_2 and O_2 effects be included, that experimental data be used to empirically develop the equation for P_{ACO_2} & normal values, and that it would describe minute

ventilation, $\dot{V}$. It is given in the reference by Milhorn et al. (7) as

$$\dot{V} = D(P_{ACO_2} - B)\,[1 + {}^{A}/(P_{AO_2} - C)] \geq 0. \qquad (2)$$

The product of the two terms, D and the bracketed expression, describe a hyperbolic expression with P_{AO_2} as the dependent variable.

Here, $P_{ACO_2} \geq B = 37.24$ mmHg and $P_{AO_2} \geq C = 25$ mmHg.

In comparison to Gray's equation alveolar ventilation is given as

$$\dot{V}_A = \dot{V} - (\dot{V}/V_T)\,V_D \qquad (3)$$

with empirical expressions describing V_T and V_D as

$$V_T = M_1\,\dot{V}^{b_1} = \text{Tidal Volume}$$

and $$V_D = M_2\,V_T + b_2 = \text{Dead Space.}$$

All values for the empirical constants are given by Milhorn (7). A brief discussion describing the salient features of Lloyd and Cunningham's equation and Gray's equation is also given by Milhorn (7).

3. Milhorn's Controller Equation

Although the controlling equation utilized in some of Milhorn's more recent research appears to be of the form of Lloyd and Cunningham's equation, the reader is also encouraged to follow a more descriptive discussion of an earlier development in Milhorn's text (16). The alveolar ventilation, $\dot{V}_A$, is described as a function of the aortic-carotid bodies arterial O_2 concentration ($C_{A\beta O_2}$) and the brain tissue CO_2 concentration ($C_{B_{CO_2}}$). It is given as

$$\overset{\circ}{V}_A = a(C_{B_{CO_2}})^{1/\kappa_2} - b + d(m - \kappa_5 P_B C_{A\beta O_2})^n \geq 0. \qquad (4)$$

The term $(C_{B_{CO2}})^{1/\kappa_2}$ comes from an empirical CO_2 dissociation curve. Also it is assumed that the relationship between arterial P_{O_2} and alveolar P_{O_2} is

$$P_{aO_2} = \kappa_5 \, P_{A_{O_2}}. \qquad (5)$$

Then with

$$\kappa_5 P_{A_{O_2}} = \kappa_5 P_B C_{A\beta O_2} \qquad (6)$$

we have the form of the last term in Equation 4. Other constants in Equation 4 are described as follows. First of all, it should be noted that some of the constants will assume different values for the excitatory and inhibitory phases.

a = 810.0 (Excitatory)

a = 99.0 (Inhibitory)

b = 194.5 (Excitatory)

b = 19.6 (Inhibitory)

k_2 = 0.415 (Obtained from CO_2 dissociation curve)

k_5 = 0.92 (Normal arterial P_{O_2}/Normal alveolar P_{O_2})

d = 8.0 $(10)^{-4}$ } Determined under inhibitory conditions

n = 3.0

m = 98.0 (Normal arterial P_{O_2})

4. Grodins' Controller Equation

The controller equation that is used in Grodins' program is given here with the same terminology as previously used and which is used in the Appendix.

$$V_I = 1.1380[C(16)C_{a(H^+)}(t - \tau_{aB}) + (1.0 - C(16))C_{CSF(H^+)}]$$
$$+1.1540C_{a(H^+)}(t - \tau_{aO}) + TERM - VI(N) \qquad (7)$$

where

$$TERM = 23.6(10)^{-9}[104 - (B-47)F_{A(O_2)}(\tau - \tau_{aO})]^{4.9}$$
$$\text{for } (B - 47)F_{A(O_2)}(t - \tau_{ao}) < 104 \qquad (8)$$
$$TERM = 0 \text{ for } (B - 47)F_{A(O_2)}(t - \tau_{ao}) \geq 104. \qquad (9)$$

The obvious question that needs to be answered is whether an expression like Equation 7 is more physiologically representative than one like Equation 3. A summary of such a comparison yields the following list:

1. Grodins' modified program defines minute ventilation as TVNT = DEADVT + (VE + VI)/2.

   TVNT = (.1107)(FREQ) + (.0785)(VE) + (VE + VI)/2.(10)

   Milhorn's use of Lloyd and Cunningham's minute ventilation equation (Equation 2) should be compared to Equation 10.

2. Grodins' inspired ventilation, V_I, corresponds to the alveolar ventilation expression used by Milhorn which is Equation 3.

3. One major difference between Grodins' controller equation and Lloyd and Cunningham's controller equation is that with the former there is no product effect of CO_2 and O_2.

4. Grodins' system has the capability of distinguishing between the sensing mechanisms of the CSF compartment and the venous blood in the brain.

5. Grodins' model reflects the metabolism and acid-base buffering by utilizing a weighting of the H^+ concentration in the CSF compartment and at the carotid bodies site.

6. Appropriate time delays are utilized for lung-to-brain and lung-to-carotid bodies in Grodins' model. This feature simulates a more representative system in the dynamical sense.

It is very difficult to justify the use of some of the weighting factors in both systems. For a more complete comparison, a form of Milhorn's controller equation should be incorporated in Grodins' program. Then the benefits of H^+ concentration sensing and/or blood gas tension sensing can be discussed in better perspective. This particular research will be elaborated upon in a future Study Report.

C. Research Goals for the Study Report

As described in the contract's Statement of Work the underlying goal of this Study Report is to critically compare Grodins' respiratory program responses to Environmental Physiology Branch and published data and recommend and implement approved program changes to increase program fidelity. In order to fulfill this goal a description of the mathematical development of Grodins' model is presented. See Appendix. To evaluate and analyze the program responses a parameter sensitivity evaluation was performed using normal environmental conditions at a resting state and also environmental conditions

approximating those of Skylab with various levels of exercise.

Since the controller equation was shown to be a very influential component of the system a special sensitivity analysis for the weightings of the H^+ concentration in the cerebrospinal fluid and blood compartments was formulated. These results are shown in the following report. When the exercise data from the Environmental Physiology Branch is received a more quantitative evaluation of the program's capabilities will be made. As it now appears the program responds with logical transient and steady-state trends for exercise levels.

III. VARIATIONS IN MODEL PARAMETERS

A. General Considerations and Philosophy

Before discussing specific parameter variations, a few general comments are appropriate. The primary overall goal of this investigation is to evaluate the model sensitivities for reasonable variations in parameter values. Grodins' modified program provides for various parameter variations by the use of input data cards. There are many standard conditions for inspired volumetric fractions of gases from which to base a sensitivity analysis. The decision was made to use the following data from which all simulations of variations in parameters are compared.

$$B = 760 \text{ mmHg}$$
$$FI(CO2) = 0.1000$$
$$FI(O2) = 0.1100$$
$$FI(N2) = 0.7900$$

The time responses for V_I, Q, and $P_{a(CO_2)}$ are shown in Figures 2-4 respectively.

It is believed that these base conditions are adequate for the sensitivity analyses performed. However, one should use extreme caution in projecting, in a direct fashion, the sensitivity of any parameter to other base conditions. Only one parameter or group of common parameters was altered at one time. This is really the first step in what should be a continuing effort in analyzing combinations of parameter variations and weightings.

The format followed in the ensuing discussion is one which hopefully conveys the model's capabilities and limitations in a

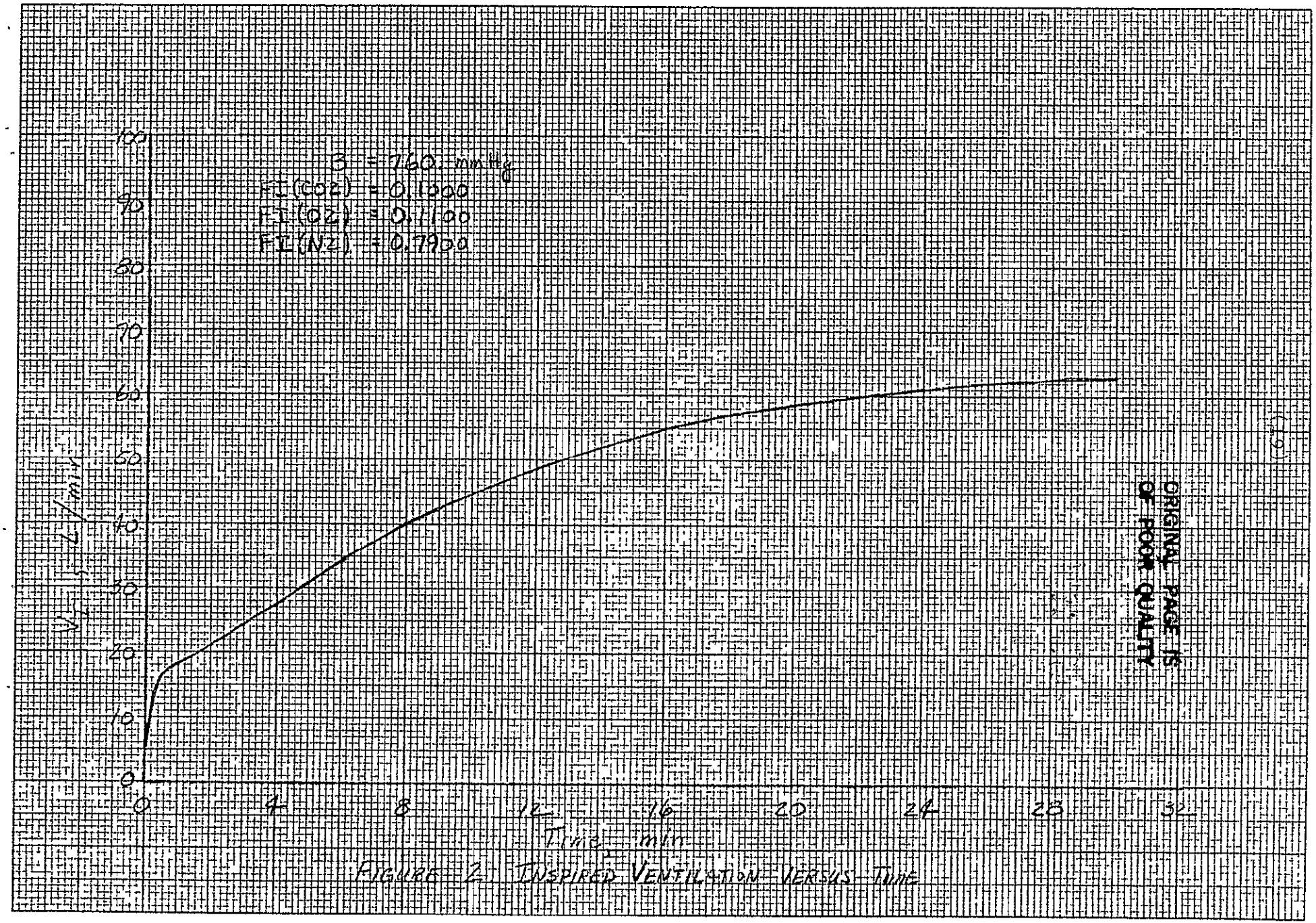

FIGURE 2. INSPIRED VENTILATION VERSUS TIME

ORIGINAL PAGE IS
OF POOR QUALITY

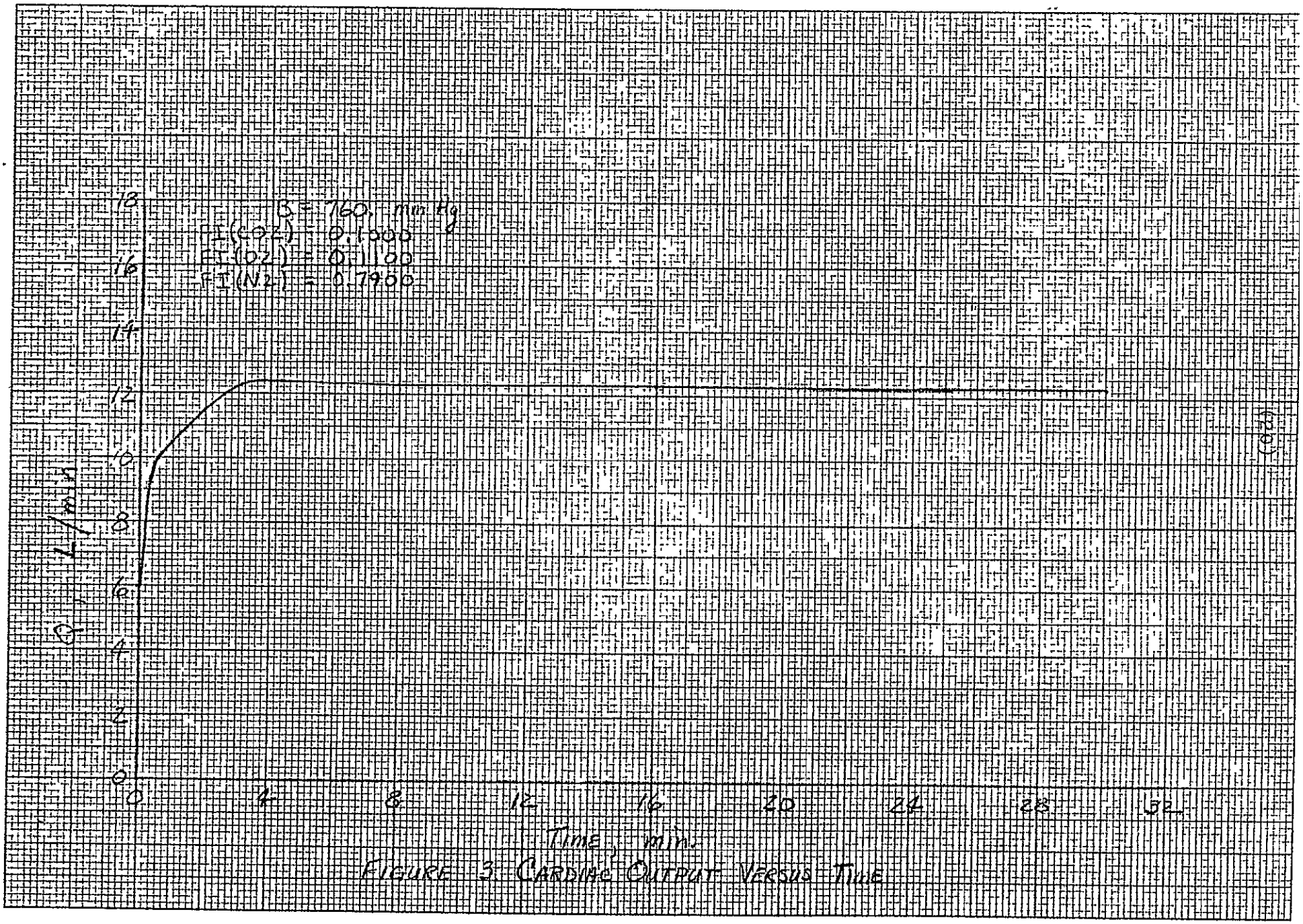

FIGURE 3. CARDIAC OUTPUT VERSUS TIME

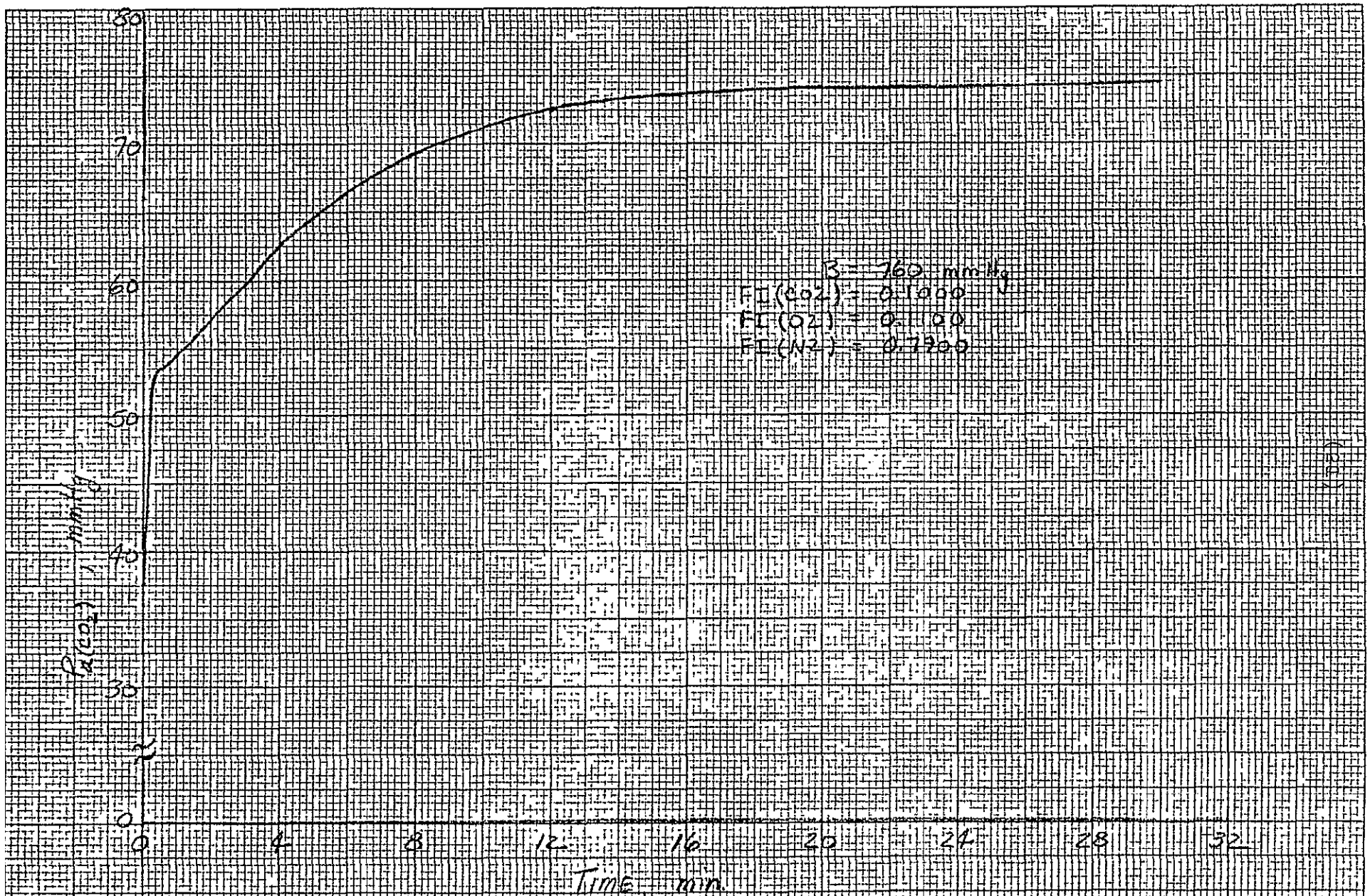

FIGURE 4. ARTERIAL PARTIAL PRESSURE OF CO_2 VERSUS TIME

concise and informative manner. There is a tremendous amount of data which will not be discussed or presented in graphical form. This is not mean't to deemphasize their importance. Only the variables which illustrate significant changes will be addressed. The reader should acquaint himself with the output data format and all the possible relationships between variables that can be generated. See General Electric TIR 741-MED-3008 and TIR 741-MED-3009.

With regard to inspired gaseous concentrations only the on-transient and related steady-state conditions are analyzed. The off-transient as related to the transition from exercise to the resting state is presented later in this section. Since the base run indicates an oscillatory response in the off-transient of some variables, parameter sensitivity analyses will no doubt prove enlightning within this time range.

The computer program is a modified version of Grodins' program similar to that used by Weissman (15). Although it has a subroutine which involves a work-exercise phenomenon, only the case of the resting subject is considered here.

Table 1 presents the input data format giving card number, symbol, normal initial value, and a brief discription of each parameter. In the discussion of each parameter variation, the card number, symbol, and new initial value (or % change in base initial value) will be given.

TABLE 1: INPUT DATA CARDS

Card No.	Symbol	Normal Initial Value	Description
1	FA(CO2)	.0527	Alveolar gas fractions (dry), volumetric fraction of gas, dimensionless
2	FA(O2)	.1514	
3	FA(N2)	.7959	
4	CB(CO2)	.6397	Concentration of gas in brain, liters (STPD)/liter brain
5	CB(O2)	.0011	
6	CB(N2)	.0097	
7	CT(CO2)	.6132	Concentration of gas in tissue compartment. Liters(STPD)/liter tissue
8	CT(O2)	.0014	
9	CT(N2)	.0097	
10	Q	6.0000	Cardiac output blood flow, liters/min., cerebral blood flow, liters/min.
11	QB	.7370	
12	PCSF(CO2)	47.8529	Partial pressure of gas in cerebrospinal fluid compartment, mmHg.
13	PCSF(O2)	36.0047	
14	PCSF(N2)	567.4731	
15	TMAX	30.0000	Length of computer run, min.
16	CENT SENS PT	0.0000	Central Sensitivity Partition. Weighting of the H+ concentration in CSF with that of venous blood in the brain. With C(16)=0, zero weight is given to venous blood at level of the brain and a weight of one is given to H^+ conc. in CSF.
17	HB	.2000	Blood oxygen capacity, liters (STPD)/liter blood
18	R1	.1000	Time constants for cardiac output response (R1) and cerebral blood flow response (R2) for changes in blood chemical composition.
19	R2	.1000	
20	CNT SENS COF	1.1380	Controller sensitivity weightings, i.e.,
21	CRTD BDY SCF	1.1540	

$$V_I = 1.1380\,[C(16)C_{a(H^+)}(t-\tau_{aB}) + (1.0-C(16))C_{CSF(H^+)}] + 1.1540\,C_{a(H^+)}(t-\tau_{ao}) + TERM\text{-}VI(N)$$

Card No.	Symbol	Normal Initial Value	Description
			where τ_{ao} = Blood transport delay from lung to carotid body, τ_{aB} = Blood transport delay from lung to brain, VI(N) = C(37), and TERM = function of $F_{A(O_2)}$.
22	KL	3.0000	Volumes of Lung (alveoli), brain, and tissue compartments, liters
23	KB	1.0000	
24	KT	39.0000	
25	MRB (CO2)	.0500	Metabolic rates by brain, liters (STPD)/min
26	MRB (O2)	.0500	
27	D (CO2)	81.9900	Diffusion coefficient for gas across "blood-brain", liters (STPD)/min per mmHg
28	D (O2)	4.3610	
29	D (N2)	2.5240	
30	B	760.0000	Barometric pressure, mmHg
31	FI(CO2)	.1000	Volumetric fraction of gas (dry inspired), dimensionless. This is the value for the Base Run that's utilized.
32	FI(O2)	.1100	
33	FI(N2)	.7900	
34	KCSF	.1000	Volume of cerebrospinal fluid, liters.
35	T	.0000	Initial time.
36	H	.0078	Size of computer time step, min.
37	VI(N)	87.5500	Constant that is involved in the controller equation (See C(21)). Determines the normal level of alveolar ventilation so that $P_{A(CO2)} \approx 40.0$ at rest, breathing air at sea level. When the controller sensitivity weightings are changed VI(N) should be altered accordingly.
38	VI(SS)	5.3900	Value used for normal resting alveolar ventilation. This is not used in the program if VI(N) is known.

Card No.	Symbol	Normal Initial Value	Description
39	PRINT AL TIM	0.5000	Output printed in these time increments. However, there is an over-riding statement that permits no increments greater than 0.5 min.
40	UNKNOWN	0.0000	Importance related to C(39), but doesn't seem to be of any real significance.
41	BHCO3 Blood	.5470	Standard bicarbonate content, liters CO_2 (STPD)/liter χ, 37°C where
42	BHCO3 Brain	.5850	
43	BHCO3 Tissue	.5850	
44	BHCO3 CSF	.5850	χ = Blood, brain, tissue, CSF.
45	RMT(CO2)	.1820	Metabolic rates by tissue, liters (STPD)/min.
46	RMT(O2)	.2150	
47	DJ1	.0000	Used in performing Dejours experiment (Not utilized in present runs). Brief description of Dejours work relating O_2 and CO_2 threshold effects is given in Grodins' paper (8).
48	DJ2	.0000	
49	*Col 1-6 WORK2	0.00	Work load (watts)
	Col 7-9		Blank
	Col 10-15 DURAT**	30.00	Run time for work load (min.)

*F6.2

**If DURAT is less than TMAX (Card 15) another work load card is read when print time exceeds DURAT.

B. Controlled System Parameter Variations-Barometric Pressure = 760 mmHg

Run No.	Card No.	Symbol	Revised Initial Values
107	C(18)	R1	.0700
	C(19)	R2	.0700
108	C(18)	R1	.1300
	C(19)	R2	.1300

Discussion: The values R1 and R2 correspond to the time constants r_1 and r_2 in the first order differential equations describing cardiac output and brain blood flow. By using 70% and 130% of the normal initial

values essentially the time that is required for the blood flows to reach their steady-state values was altered. The model was shown to be insensitive to this alteration for $t \geq 1$ min. There were slight variations in the initial transient ($0 \leq t \leq 1$), but even in this time period, the system seems fairly insensitive to these 30% variations. Cardiac output reaches its steady-state value in about 4 minutes, so in general its transient period is less than for some other variables.

Run No.	Card No.	Symbol	Revised Initial Values
112	C(42)	BHCO3 BRAIN	0.5660
	C(43)	BHCO3 TISSUE	0.5660
113	C(42)	BHCO3 BRAIN	0.5470
	C(43)	BHCO3 TISSUE	0.5470
114	C(42)	BHCO3 BRAIN	0.5850
	C(43)	BHCO3 TISSUE	0.5470
115	C(42)	BHCO3 BRAIN	0.5470
	C(43)	BHCO3 TISSUE	0.5850

Discussion: Refer to Figures 5-7. Grodins indicates that the standard bicarbonate content of the brain and tissue compartments of 0.5850 is too high. Several simulations were run from which some data are plotted in Figures 5-7. Physiologically speaking there is a lower limit placed upon possible values for C(42) and C(43). Neither can be less than the value of C(41), the bicarbonate content of the blood. This extreme limit was one of several chosen for evaluation. The model was found to be much more sensitive to changes in the bicarbonate content of the tissues than of the brain. This is likely to be related to the relative volume sizes of the two compartments in addition to the buffering and metabolism relationships. The most pronounced changes occured in the transients with the

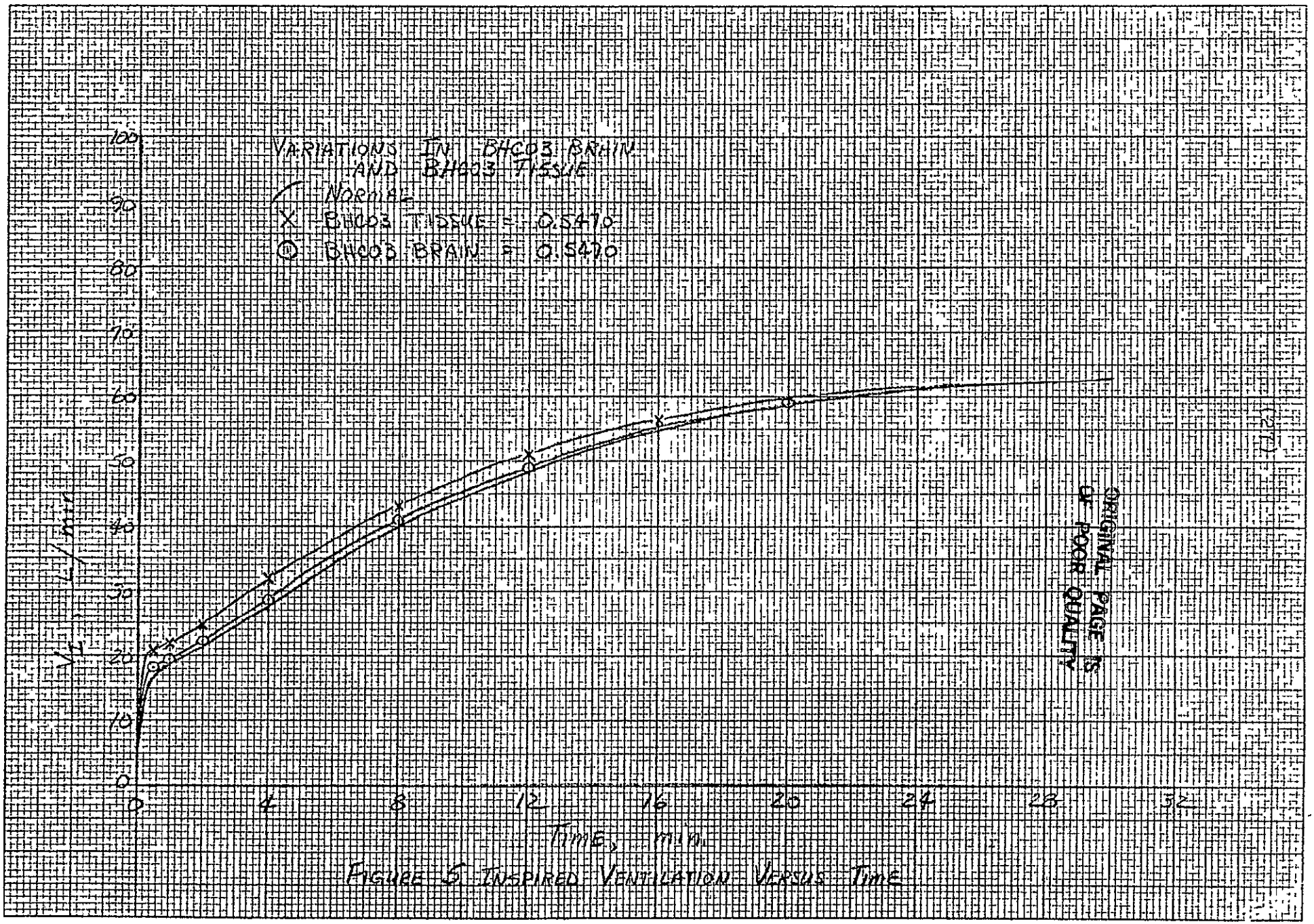

FIGURE 5 INSPIRED VENTILATION VERSUS TIME

ORIGINAL PAGE IS
OF POOR QUALITY

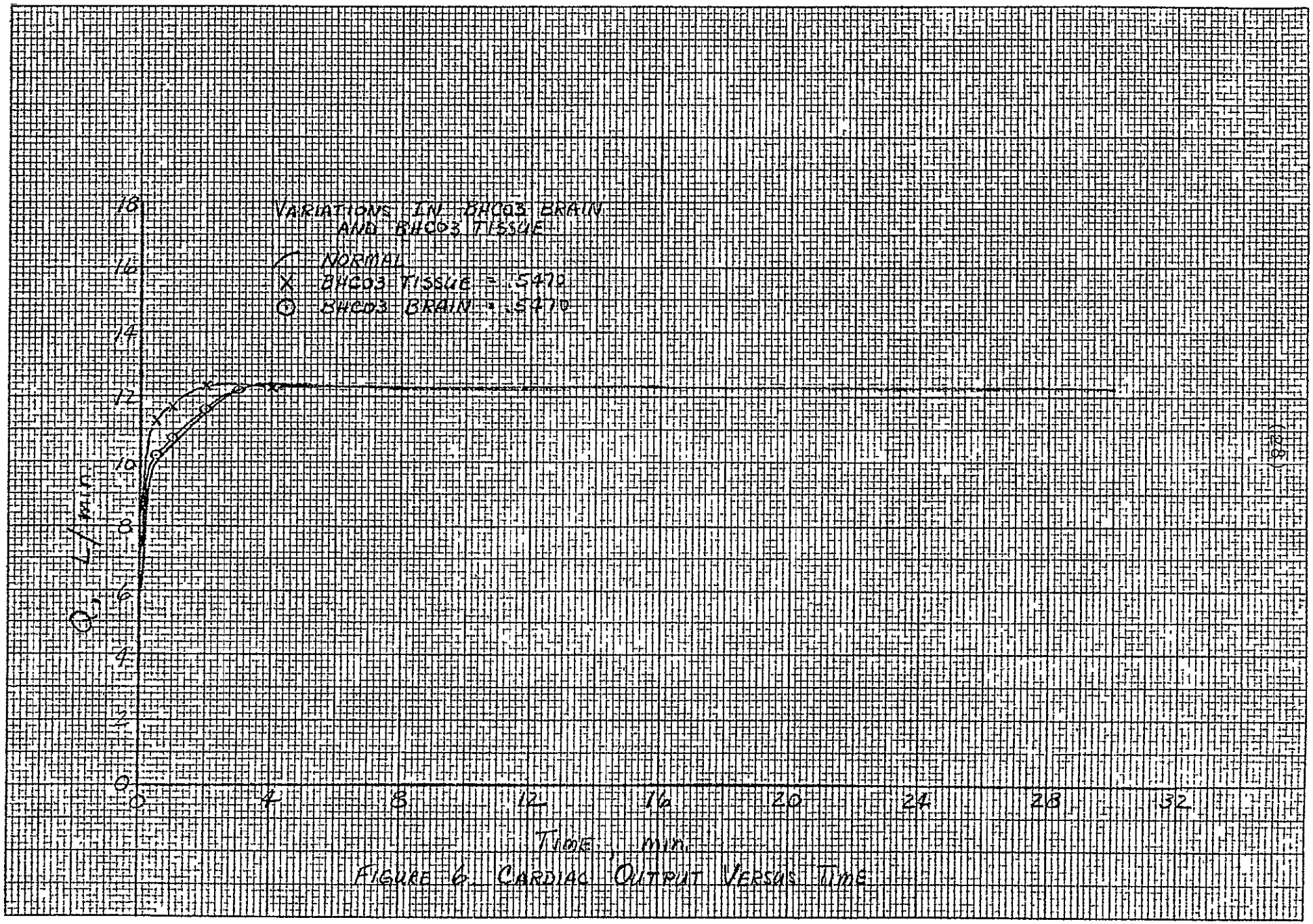

FIGURE 6. CARDIAC OUTPUT VERSUS TIME

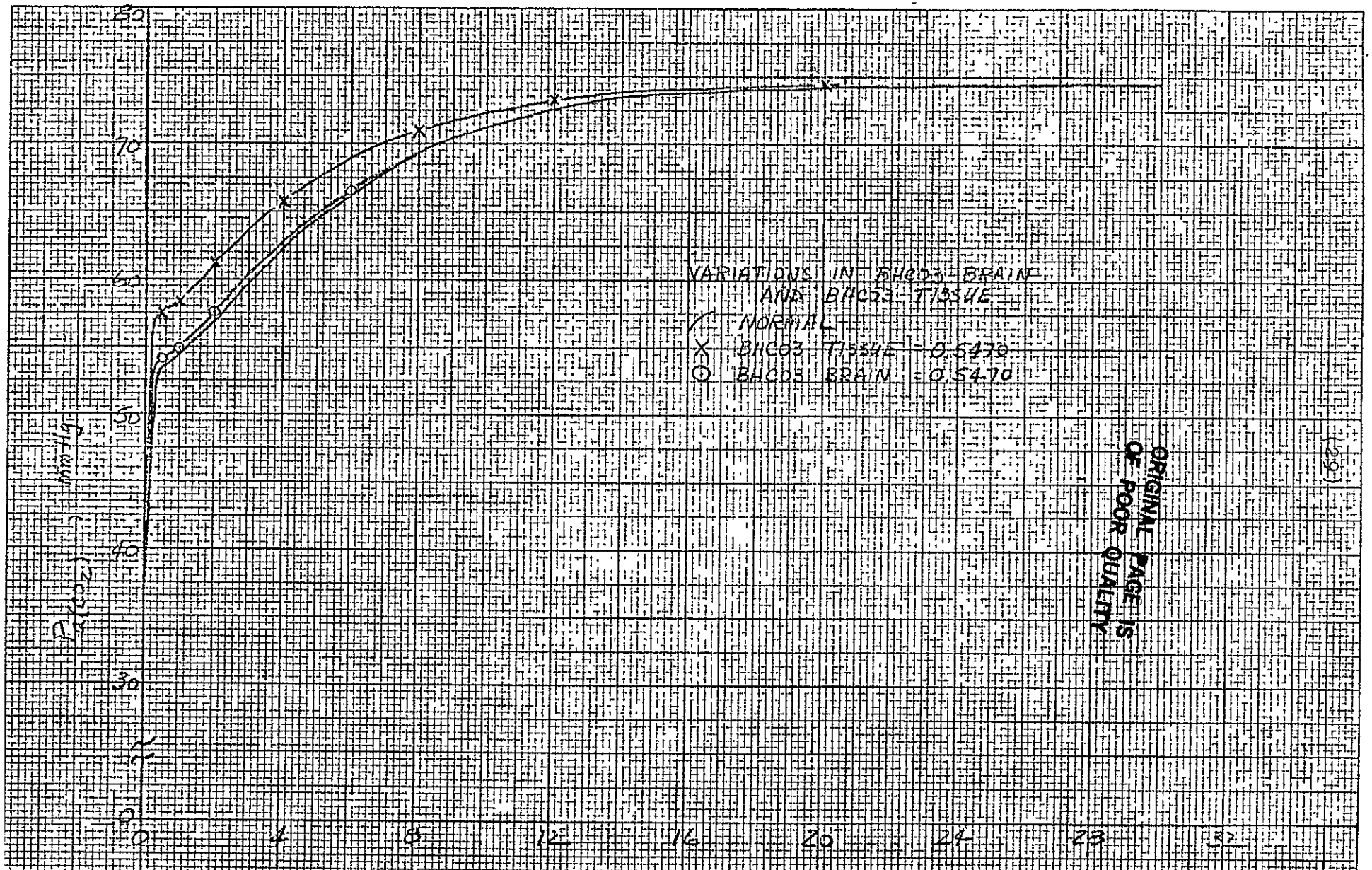

FIGURE 7. ARTERIAL PARTIAL PRESSURE OF CO_2 VERSUS TIME

ORIGINAL PAGE IS OF POOR QUALITY

steady-state responses remaining unaltered except for the H^+ concentrations related to the brain and tissue compartments, i.e., $C_{B(H^+)}$ and $C_{T(H^+)}$.

Run No.	Card No.	Symbol	Revised Initial Values
129	C(27)	D(CO2)	50% Normal = 40.9950
	C(28)	C(O2)	50% Normal = 2.1805
130	C(27)	D(CO2)	150% Normal =122.9850
	C(28)	D(O2)	150% Normal = 6.5415
131	C(27)	D(CO2)	50% Normal = 40.9950
	C(28)	D(O2)	50% Normal = 2.1805
	C(29)	D(N2)	50% Normal = 1.2620
132	C(27)	D(CO2)	150% Normal =122.9850
	C(28)	D(O2)	150% Normal = 6.5415
	C(29)	D(N2)	150% Normal = 3.7860

Discussion: Refer to Figures 8-9. The qualitative trends that these variations produced are very physiologically sound. Noting that the diffusion rate is directly proportional to the diffusion gradient, we have a direct change in the rate of CO_2, O_2, and N_2 passing across the brain-CSF barrier as we look at 50% and 150% variations in their diffusion coefficients. Since the blood-cerebrospinal fluid barrier is very impermeable to H^+, a change in the $C_{a(H^+)}$ has little effect upon the $C_{CSF(H^+)}$. However, $P_{a(CO2)}$ variations are detected in the CSF(18). The blood-cerebrospinal fluid barrier is highly permeable to CO_2; thus, a 50% or 150% variation in D(CO2) will be significant. In addition, when CO_2 enters the CSF compartment, $C_{CSF(H^+)}$ is increased via the formation of carbonic acid. This is reflected in the Henderson-Hasselbalch equation and provides for the CSF compartment to be very sensitive to CO_2 variations. One should not expect a significant change in V_I for variations of D(O2) or D(N2) since N_2 effects are not considered in the controller

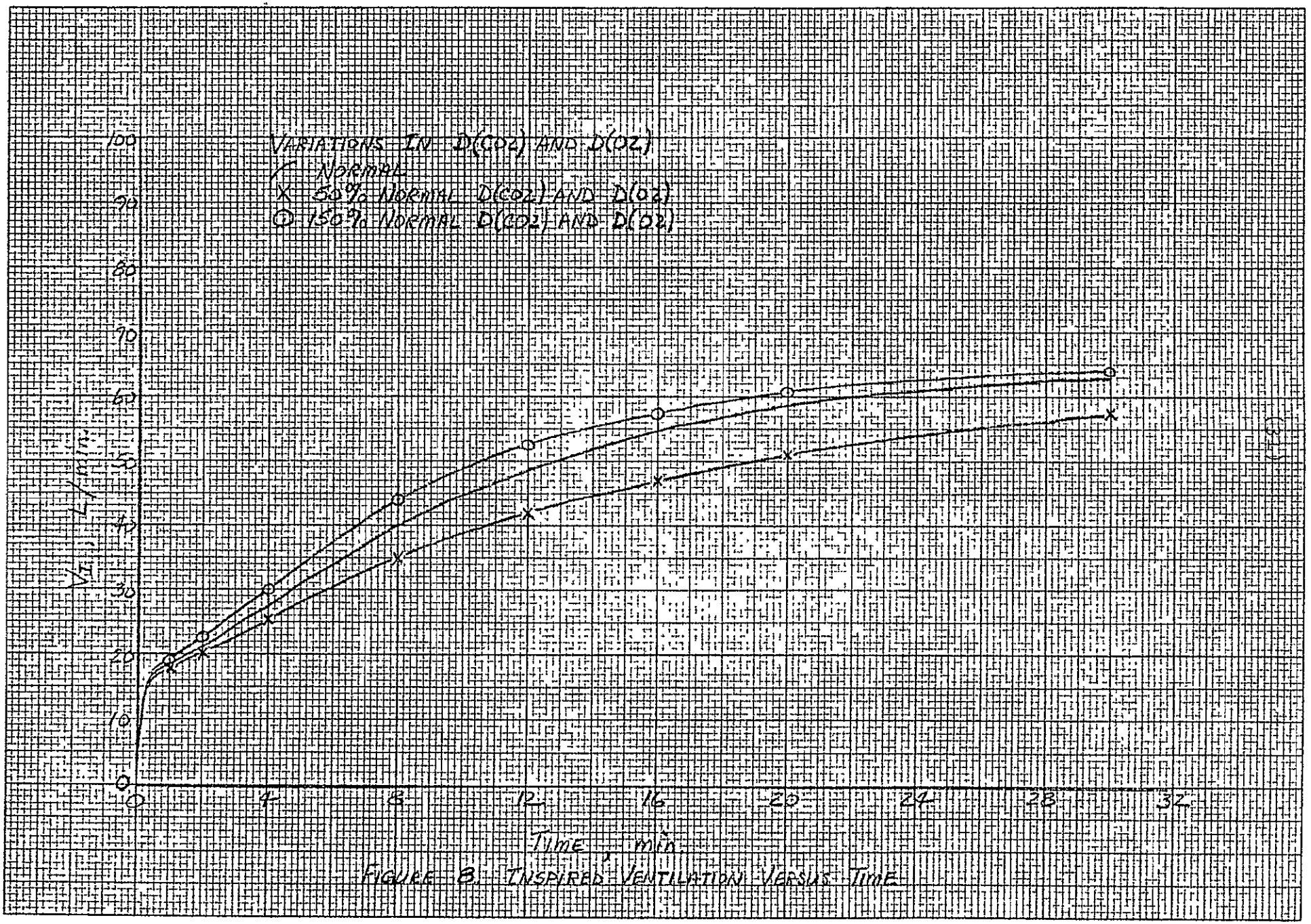

FIGURE 8. INSPIRED VENTILATION VERSUS TIME

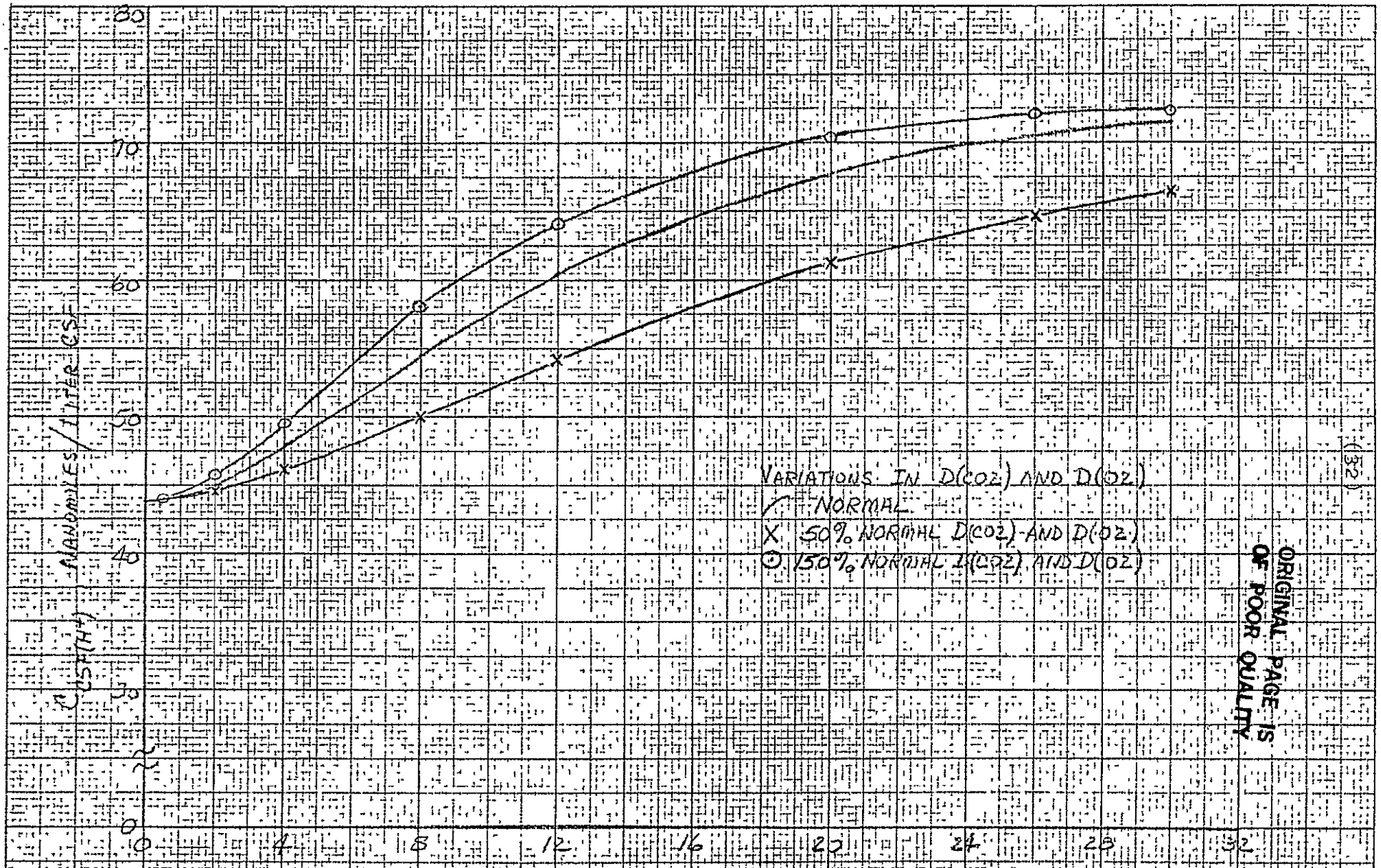

FIGURE 9. CEREBROSPINAL FLUID H^+ CONCENTRATION VERSUS TIME

ORIGINAL PAGE IS OF POOR QUALITY

equation and the simulated dependency upon O_2 would not significantly affect the $C_{CSF(H^+)}$ or $C_{a(H^+)}$ which directly controls V_I. The simulations support these conclusions in being very sensitive to D(CO2) variations and insensitive to D(O2) and D(N2) variations. Both an increase in the transient and steady-state responses were obtained for V_I and $C_{CSF(H^+)}$ with Run Nos. 130 and 132. Corresponding decreases were observed for Run Nos. 129 and 131.

C. Controlling System Parameter Weightings-Barometric Pressure = 760 mmHg.

Run No.	Card No.	Symbol	Revised Initial Values	
201	C(20)	CNT SENS COF	50% Normal =	0.5690
	C(37)	VI(N)		62.6399
202	C(20)	CNT SENS COF	90% Normal =	1.0242
	C(37)	VI(N)		82.5680
203	C(20)	CNT SENS COF	110% Normal =	1.2518
	C(37)	VI(N)		92.5321
204	C(20)	CNT SENS COF	150% Normal =	1.7070
	C(37)	VI(N)		112.4602

Discussion: Refer to Figure 10. The variation in C(20) corresponds to a variation in the weighting of $C_{CSF(H^+)}$ in the controller equation. As previously described respiratory control is very sensitive to alterations in the $C_{CSF(H^+)}$. There was a corresponding change made in C(37) so as to compensate for maintaining $P_{a(CO_2)} \approx 40$ mmHg at rest. If a new calculation for VI(N) was not made, the system would use the value of C(38) and then calculate a new value of VI(N). This step was bypassed with hopefully a good initial approximate calculation for VI(N).

No significant variations were observed in any compartmental H^+ concentration, $P_{a(O_2)}$, Q, or $P_{a(CO_2)}$. However, as illustrated

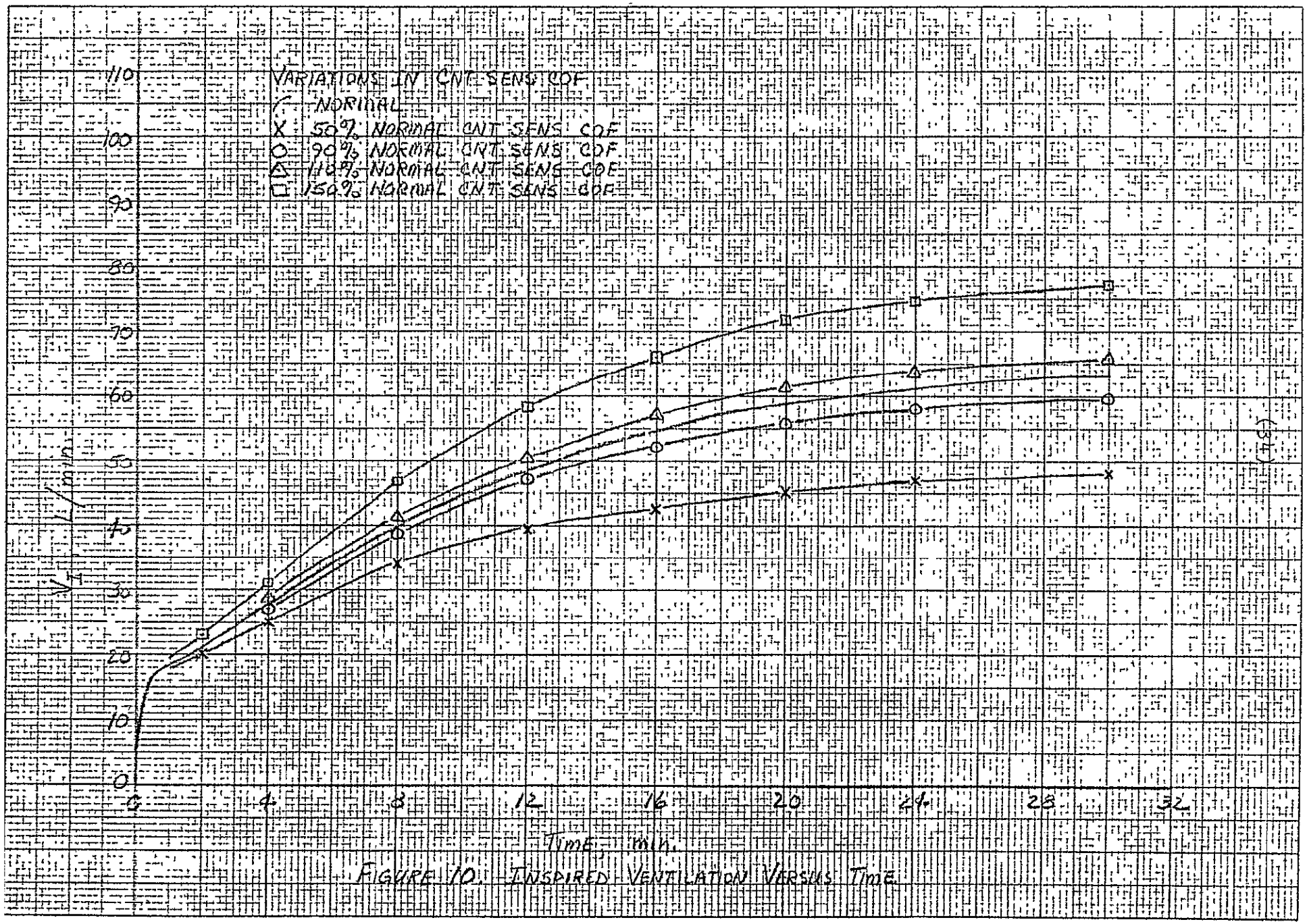

FIGURE 10. INSPIRED VENTILATION VERSUS TIME

in Figure 10, V_I is directly dependent upon C(20) although not responding rapidly in the initial transient.

Run No.	Card No.	Symbol	Revised Initial Values
205	C(21)	CRTD BDY SCF	50% Normal = 0.5770
	C(37)	VI(N)	65.9842
206	C(21)	CRTD BDY SCF	90% Normal = 1.0386
	C(37)	VI(N)	83.2368
207	C(21)	CRTD BDY SCF	110% Normal = 1.2694
	C(37)	VI(N)	91.8632
208	C(21)	CRTD BDY SCF	150% Normal = 1.7310
	C(37)	VI(N)	109.1158

Discussion: Refer to Figures 11-12. With consideration given to all the system variables the simulation seems to be more sensitive to variations in the carotid body sensitivity weighting, C(21), than the central sensitivity weighting, C(20). Here, the initial phase of the transient is modified with this modification significantly realized in the cardiac output, $0 \leq t \leq 4$ min. Although the steady-state values of the other variables are not altered appreciably, the system's initial transient variations in V_I and Q are reflected in the other variables' transient responses. The term VI(N) is used in the same manner as in Run Nos. 201-204. Physiologically speaking, one should expect the system to respond faster to changes at the carotid receptor sites than at the CSF site. Not illustrated in such a pronounced fashion, but certainly evident in Run Nos. 205-208, is the fact that the system that has the faster response seems to reach a steady-state value of lower magnitude than does the system with the slower response for all variables except V_I and Q.

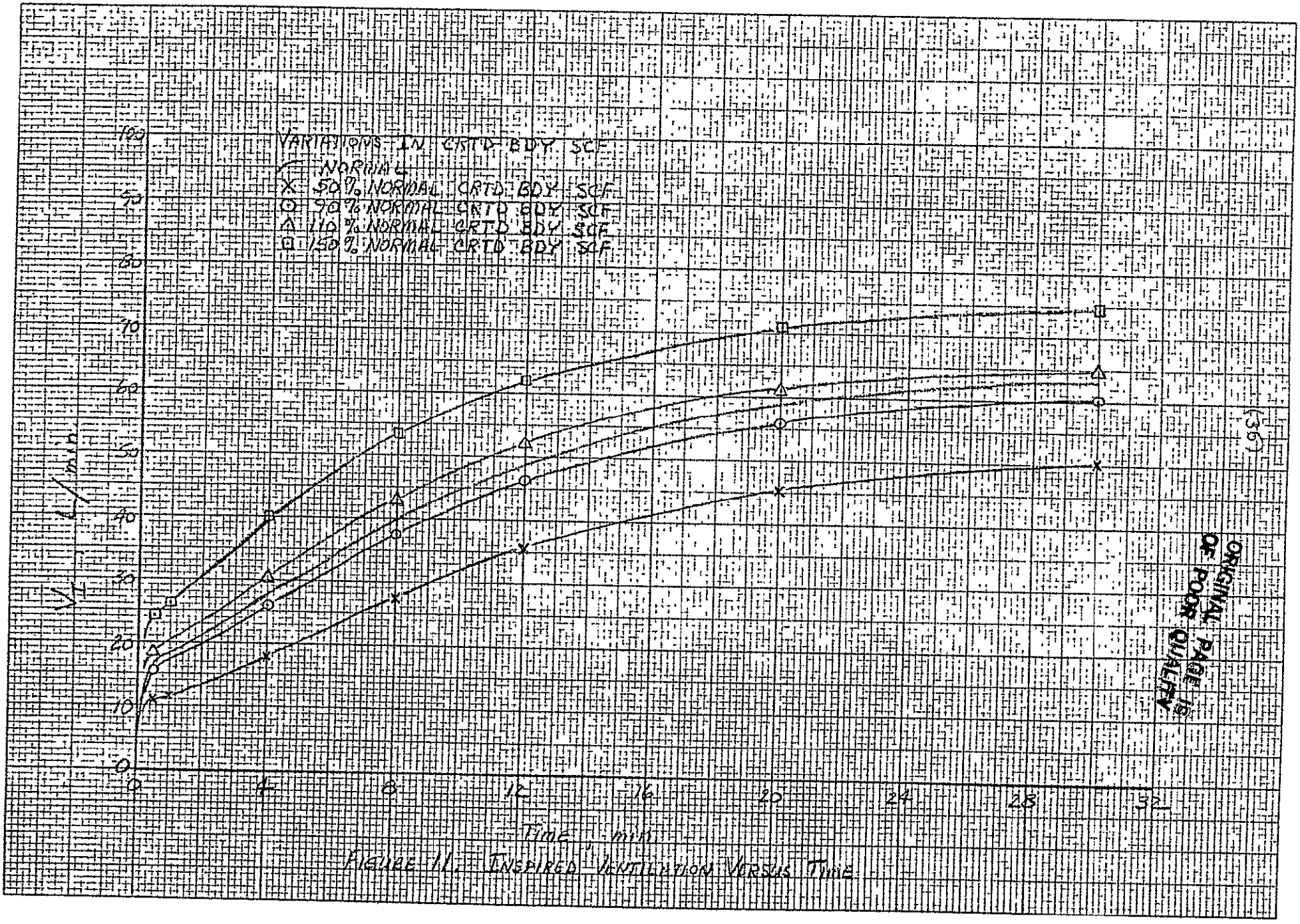

FIGURE 11. INSPIRED VENTILATION VERSUS TIME

ORIGINAL PAGE IS OF POOR QUALITY

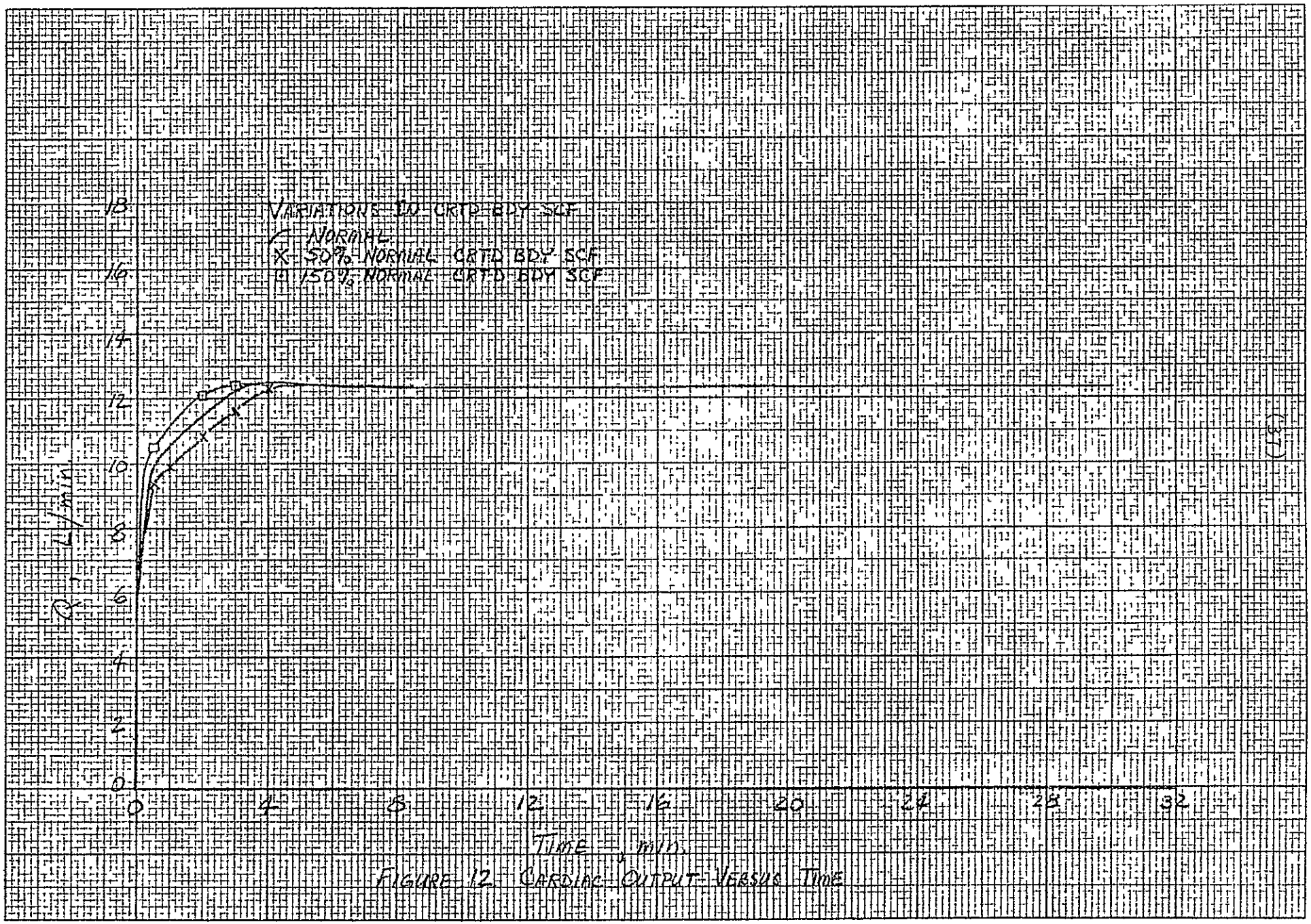

FIGURE 12 CARDIAC OUTPUT VERSUS TIME

Run No.	Card No.	Symbol	Revised Initial Values
209	C(20)	CNT SENS COF	50% Normal = 0.5690
	C(21)	CRTD BDY SCF	50% Normal = 0.5770
	C(37)	VI(N)	41.0741
210	C(20)	CNT SENS COF	50% Normal = 0.5690
	C(21)	CRTD BDY SCF	150% Normal = 1.7310
	C(37)	VI(N)	84.2057
211	C(20)	CNT SENS COF	150% Normal = 1.7070
	C(21)	CRTD BDY SCF	50% Normal = 0.5770
	C(37)	VI(N)	90.8944
212	C(20)	CNT SENS COF	150% Normal = 1.7070
	C(21)	CRTD BDY SCF	150% Normal = 1.7310
	C(37)	VI(N)	134.0260

Discussion: Refer to Figures 13-15. There are some interesting interacting phenomena that occur when both C(20) and C(21) are varied. From initial investigation of Figure 13, one might conclude that for both C(20) and C(21) equal to 50% or 150% of their normal values that the system's responses are additive. However, when the system's responses for independent variations in C(20) and C(21) are viewed and compared to Figure 13, it is noted that the responses are not additive, but convey interaction. A decrease in C(20) by 50% is more influencial than a concurrent increase in C(21) by 50%. In a similar manner, an increase in C(20) by 50% is more dominating than a concurrent decrease in C(21) by 50%. As steady-state conditions are approached the simulation becomes more dependent upon the CSF detecting system than the carotid body site. The opposite effect can be mentioned for the initial part of the transient. Here the carotid body site is more influential.

Figure 14 shows the effects of the extreme conditions upon cardiac output. Figure 15 showing the response of $P_{a(CO_2)}$ to the extreme variations of C(20) and C(21) illustrates that the

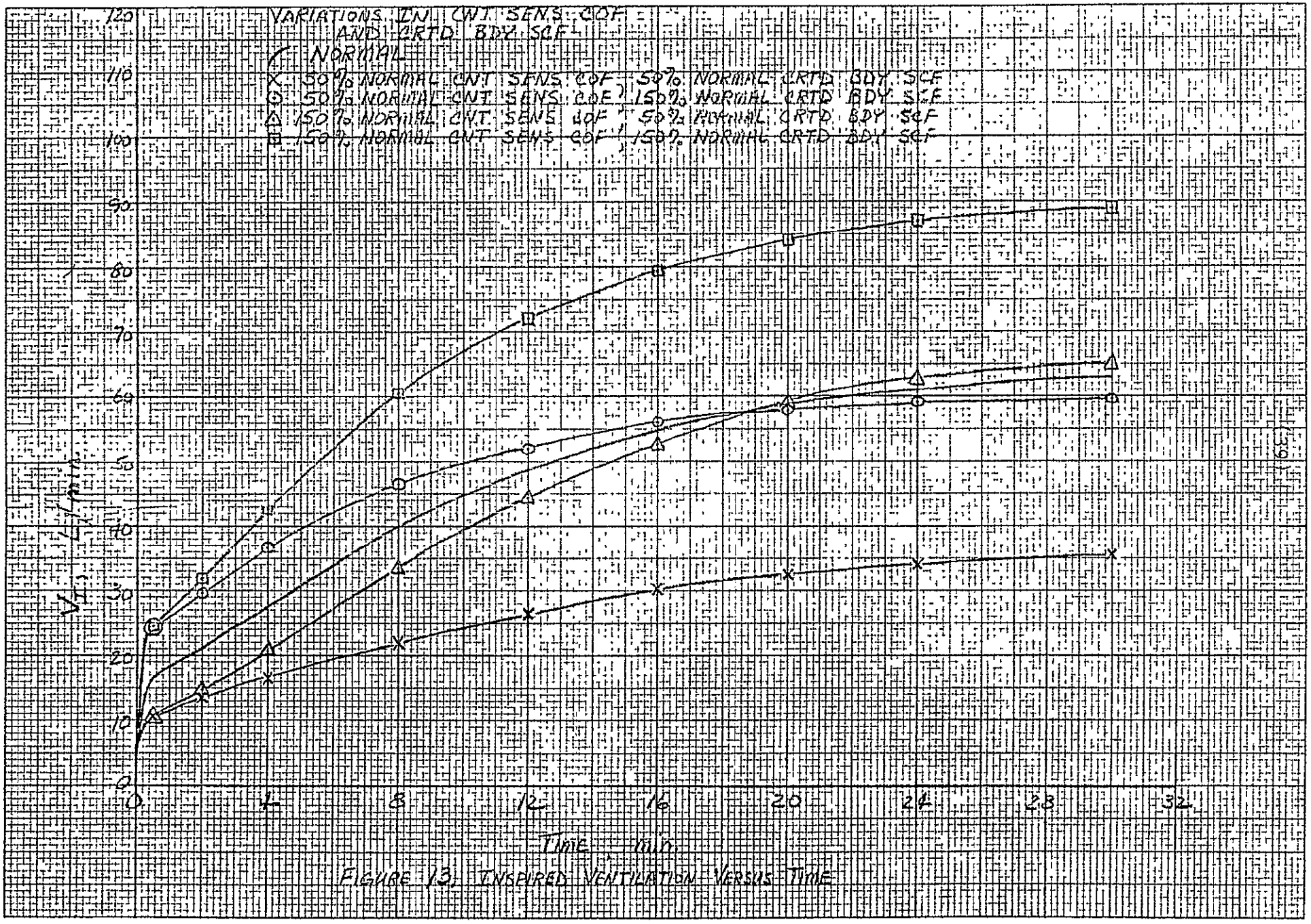

FIGURE 13. INSPIRED VENTILATION VERSUS TIME

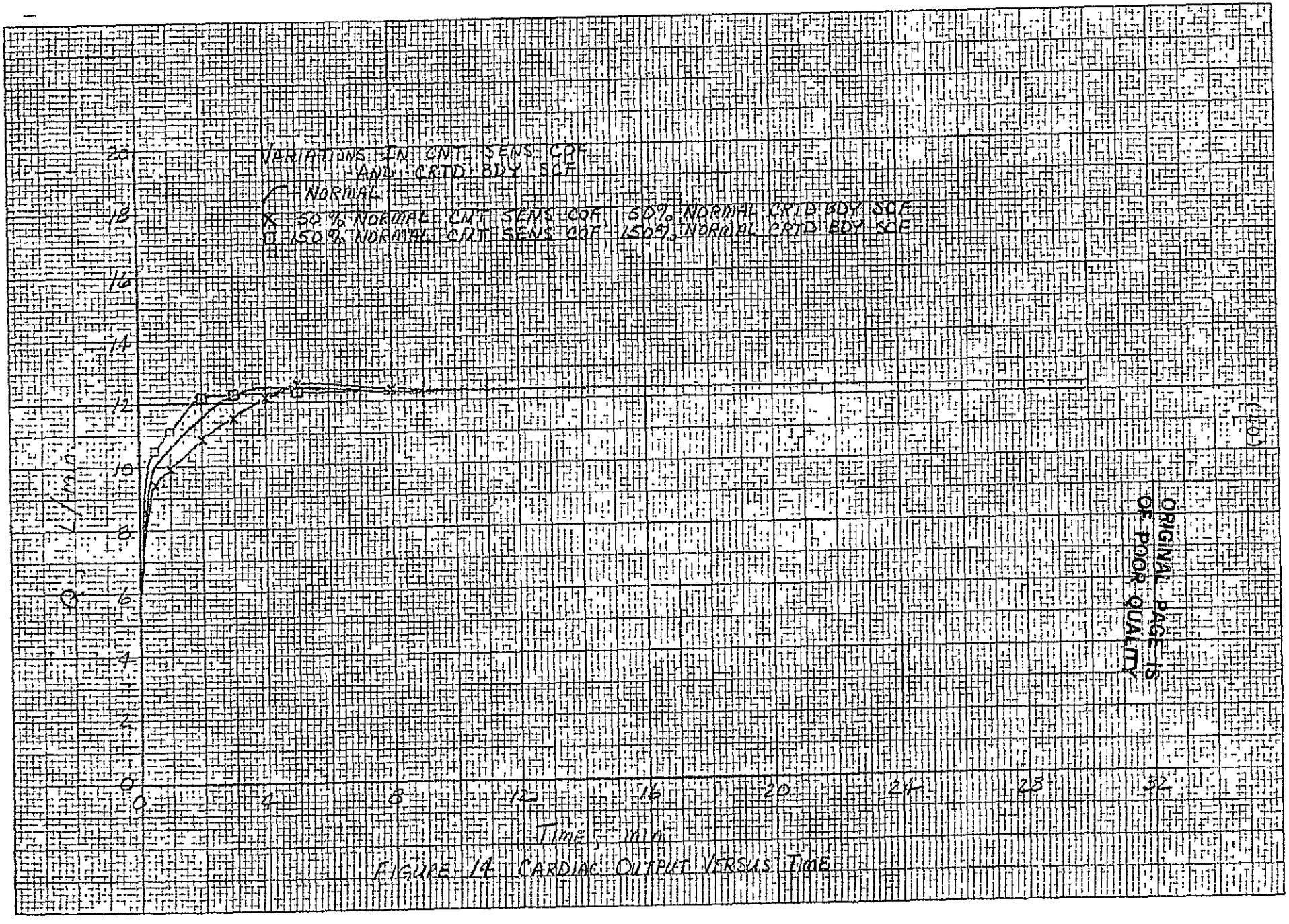

FIGURE 14 CARDIAC OUTPUT VERSUS TIME

ORIGINAL PAGE IS
OF POOR QUALITY

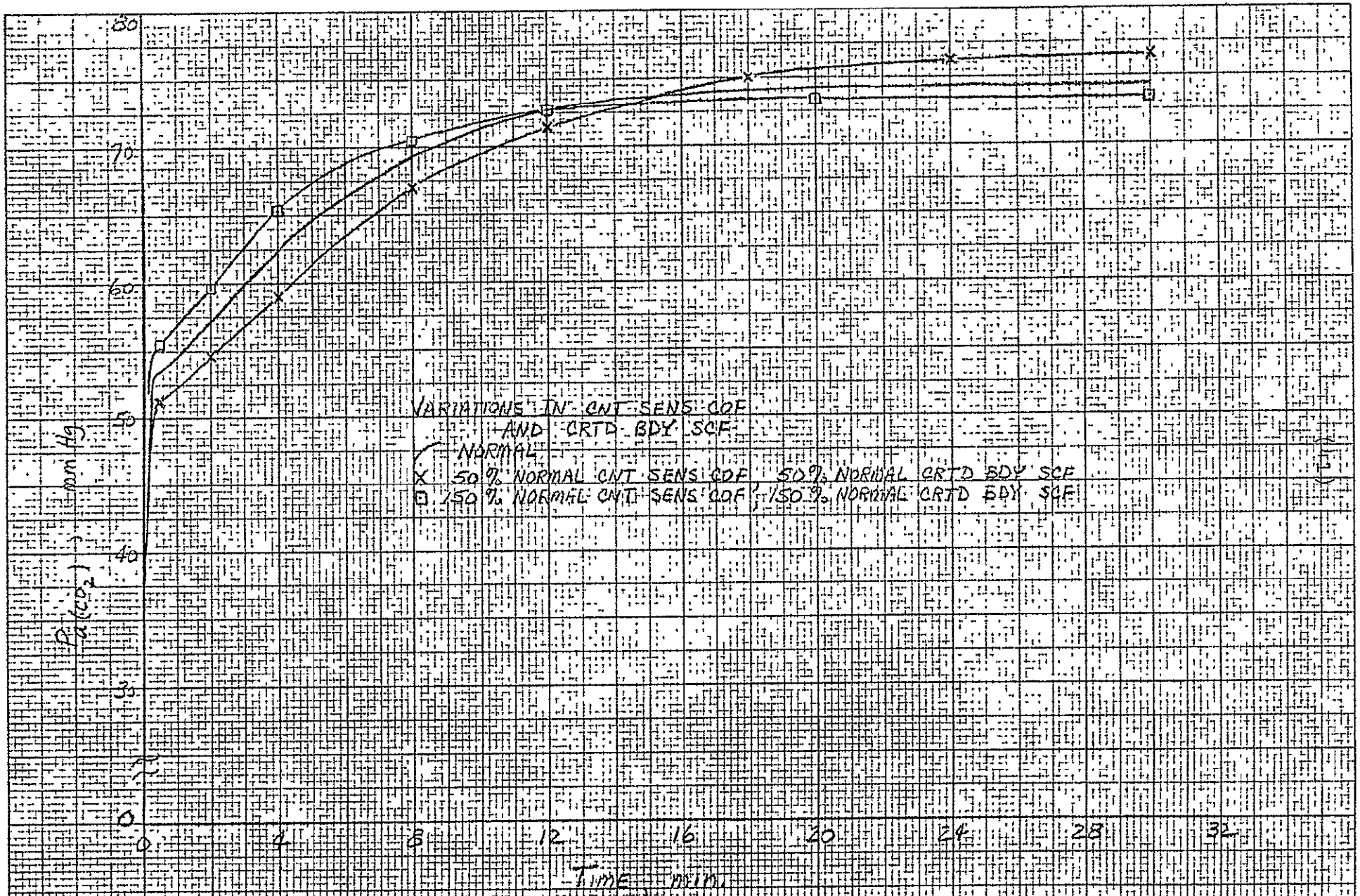

FIGURE 15. ARTERIAL PARTIAL PRESSURE OF CO_2 VERSUS TIME

faster responding system eventually reaches a lower steady-state value than the slower responding system. The variations in $P_{a(CO_2)}$ at steady-state are in agreement in that a larger steady-state $P_{a(CO_2)}$ is maintained when V_I is reduced and vice-versa.

Run No.	Card No.	Symbol	Revised Initial Values
116	C(16)	CENT SENS PT	0.1000
117	C(16)	CENT SENS PT	0.2000
118	C(16)	CENT SENS PT	0.4000
119	C(16)	CENT SENS PT	0.6000
120	C(16)	CENT SENS PT	0.8000

Discussion: Refer to Figure 16. The central sensitivity partition term is involved in a weighting of the response to H^+ concentrations in two compartments, namely the CSF and brain. Although CSF H^+ concentration is the dominant controller in the brain-CSF compartment, it has been suggested that venous brain H^+ concentrations are also involved in the controller function for ventilation. In addition, the latter responds more rapidly than the CSF detector system. With C(16) = 0, zero weighting is given to the venous blood at the level of the brain and a weighting of one is given to the H^+ concentration in the CSF. The form of the controller equation reflecting this condition is shown as

$$VI = 1.1380(C(16)C_{a(H^+)}(t-\tau_{aB}) + (1.0-C(16))\ C_{CSF(H^+)}) + 1.1540\ C_{a(H^+)}(t-\tau_{ao}) + TERM - VI(N).$$

All of the variables illustrated a faster response as C(16) was increased; however, a variation in steady-state response was realized only in the inspired ventilation. This feature is a direct reflection on the fact that in the steady-

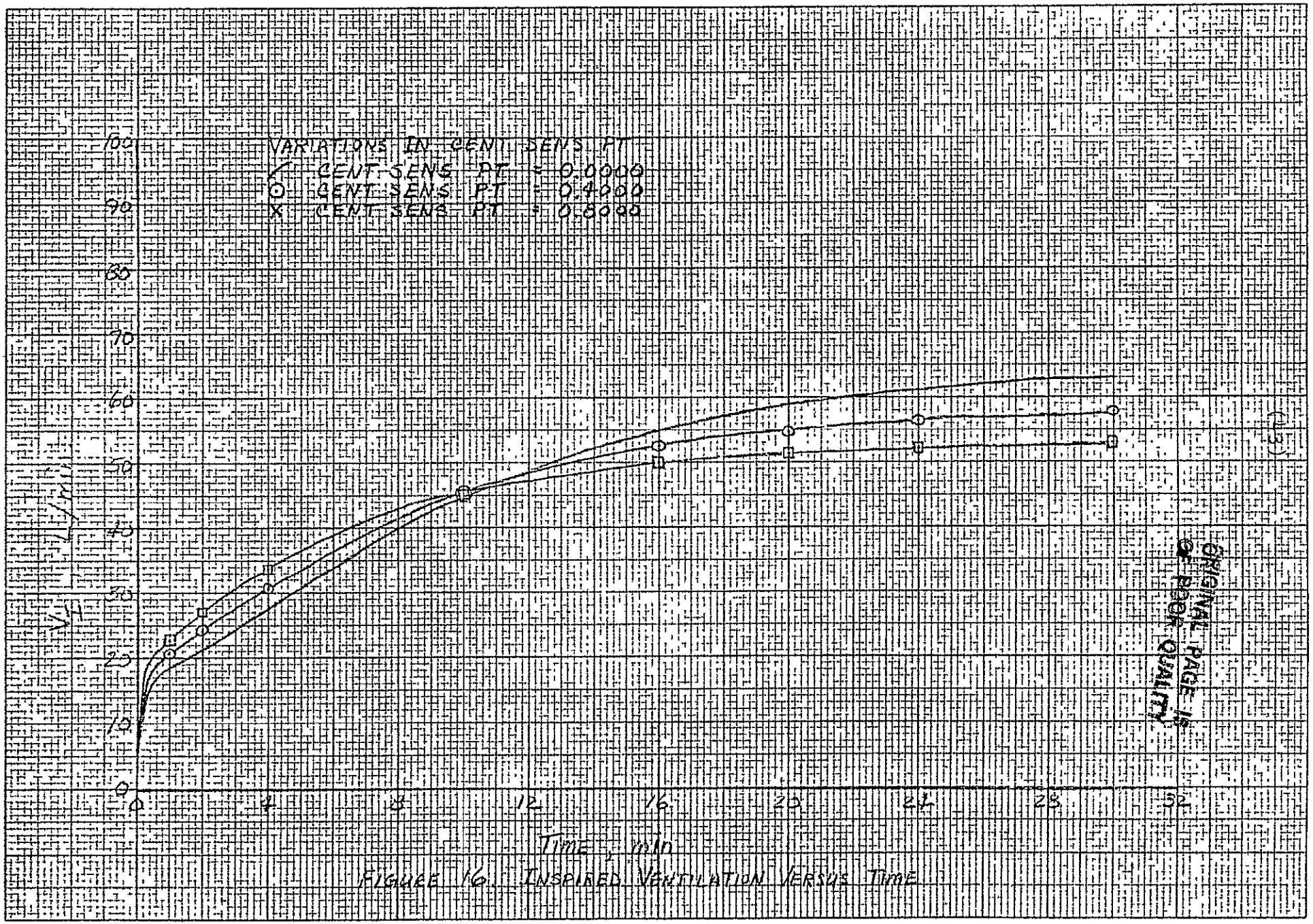

FIGURE 16. INSPIRED VENTILATION VERSUS TIME

ORIGINAL PAGE IS OF POOR QUALITY

state response the H^+ concentration in the arterial compartment, $C_{a(H^+)ss}$ = 59.5 nanomoles per liter blood, is less than in the CSF compartment, $C_{CSF(H^+)ss}$ = 71.5 nanomoles per liter CSF.

D. Comments on Simulated Skylab Conditions

The importance and usefulness of the model will be more evident in environmental simulations approaching the conditions of Skylab. From the simulations run for sea level conditions, barometric pressure = 760 mmHg, it was concluded that the most sensitive component of the system was the controlling equation. Thus the efforts of this section are concentrated on the controlling equation and its variable weightings both for the resting state and various exercise levels.

The first simulation effort involved a change of only the barometric pressure and inspired gaseous concentrations. Thus, these specific input data cards were altered to read as follows with the CO_2 concentration corresponding to 5 Torr,

Card No.	Symbol	Revised Initial Values
C(30)	B	260.0000
C(31)	FI(C02)	.0192
C(32)	FI(02)	.7000
C(33)	FI(N2)	.2808

With the above conditions for the simulations, the subject was introduced into the new environmental conditions with no preconditioning period. Consequently, no faithful results could be associated with the transient solution. The steady-state conditions that were obtained for all the variables were of value since they were required to establish the appropriate initial values for all the simulations using the above conditions.

In a sense, the use of these steady-state values compensated for the preconditioning period. The transient period for most of the variables appeared to be less than 5 minutes; therefore, a simulation run of 25-30 minutes produced good steady-state values. Table 2 shows the comparison of the initial values for the variables at normal environmental sea level conditions versus Skylab conditions. The variables associated with N_2 were altered the most.

TABLE 2: COMPARISON OF INPUT DATA CARDS FOR SEA LEVEL VERSUS SKYLAB CONDITIONS

Card No.	Symbol	Initial Value for Normal Environmental Conditions	Initial Value for Skylab Conditions
1	FA(CO2)	.0527	.1783
2	FA(O2)	.1514	.5336
3	FA(N2)	.7959	.2881
4	CB(CO2)	.6397	.6413
5	CB(O2)	.0011	.0012
6	CB(N2)	.0097	.0011
7	CT(CO2)	.6132	.6153
8	CT(O2)	.0014	.0015
9	CT(N2)	.0097	.0012
10	Q	6.0000	6.0000
11	QB	.7370	.7496
12	PCSF(CO2)	47.8529	48.1202
13	PCSF(O2)	36.0047	36.6316
14	PCSF(N2)	567.4731	70.6804
15	TMAX	30.0000	30.0000

Card No.	Symbol	Initial Value for Normal Environmental Conditions	Initial Value for Skylab Conditions
16	CENT SENS PT	0.0000	.0000
17	HB	.2000	.2000
18	R1	.1000	.1000
19	R2	.1000	.1000
20	CNT SENS COF	1.1380	1.1380
21	CRTD BDY SCF	1.1540	1.1540
22	KL	3.0000	3.0000
23	KB	1.0000	1.0000
24	KT	39.0000	39.0000
25	MRB(CO2)	.0500	.0500
26	MRB(O2)	.0500	.0500
27	D(CO2)	81.9900	81.9900
28	D(O2)	4.3610	4.3610
29	D(N2)	2.5240	2.5240
30	B	760.0000	260.0000
31	FI(CO2)	.1000	.0192
32	FI(O2)	.1100	.7000
33	FI(N2)	.7900	.2808
34	KCSF	.1000	.1000
35	T	.0000	.0000
36	H	.0078	.0078
37	VI(N)	87.5500	87.5500
38	VI(ss)	5.3900	5.3900
39	PRINT AL TIM	.5000	.5000
40	UNKNOWN	.0000	.0000
41	BHCO3 BLOOD	.5470	.5470
42	BHCO3 BRAIN	.5850	.5850

Card No.	Symbol	Initial Value for Normal Environmental Conditions	Initial Value for Skylab Conditions
43	BHCO3 TISSUE	.5850	.5850
44	BHCO3 CSF	.5850	.5850
45	RMT(CO2)	.1820	.1820
46	RMT(O2)	.2150	.2150
47	DJ1	.0000	.0000
48	DJ2	.0000	.0000

One of the goals of the Skylab experiments is to evaluate the subject's performance at various exercise levels. The base run to which the succeeding parameter sensitivity analyses were compared incorporates the exercise phenomenon. Exercise levels of five-minute intervals were used. The work loads and corresponding time intervals were described as

Time Interval	Work Load *
$0 \leq t < 5$ min	0 watts
5 min $\leq t < 10$ min	50 watts
10 min $\leq t < 15$ min	100 watts
15 min $\leq t < 20$ min	150 watts
20 min $\leq t < 30$ min	0 watts

At 5, 10, and 15 minutes an on-transient of all the variables may be observed. The off-transient or return to the resting state is contained in the interval from 20 to 30 minutes.

E. Controlling System Parameter Weightings - Barometric Pressure = 260 mmHg

Although significant results were obtained for all system variables only a representative number of outputs were plotted. Inspired ventilation, cardiac output, an example of compartmental

* Note card No. 49 on page 25 for input data format

H^+ concentration ($C_{CSF(H^+)}$), and an example of CO_2 partial pressure in the blood ($P_{a(CO_2)}$) were used. Also data were plotted illustrating the interrelationship between O_2 partial pressure in the blood ($P_{a(O_2)}$) and cardiac output, Q.

Run No.	Card No.	Symbol	Revised Initial Value
303	C(16)	CENT SENS PT	0.4000
304	C(16)	CENT SENS PT	0.8000

Discussion: Refer to Figures 17-20. From Figure 17 one can see that when more weighting is given to the H^+ concentration in the venous blood of the brain than in the CSF compartment there is an increase in oscillation in the V_I response to exercises. All exercise levels produce a slightly lower steady-state response for V_I when CENT SENS PT is increased. The decrease in exercise level to the resting state is not significantly altered by variations in CENT SENS PT. Cardiac output, Figure 18, is unaffected except possibly for the off-transient where a slight oscillation is observed.

The oscillations are more pronounced for $20 \leq t \leq 30$ minutes in Figures 19-20. Throughout the entire simulation an increase in the CENT SENS PT correspondingly raises the H^+ concentration in the CSF compartment and the partial pressure of CO_2 in the blood regardless of the exercise level.

In going from the resting state to the first exercise level the arterial CO_2 tension is reduced indicating that the increase in inspired ventilation for this level of exercise is more than adequate. However, as the exercise level is increased

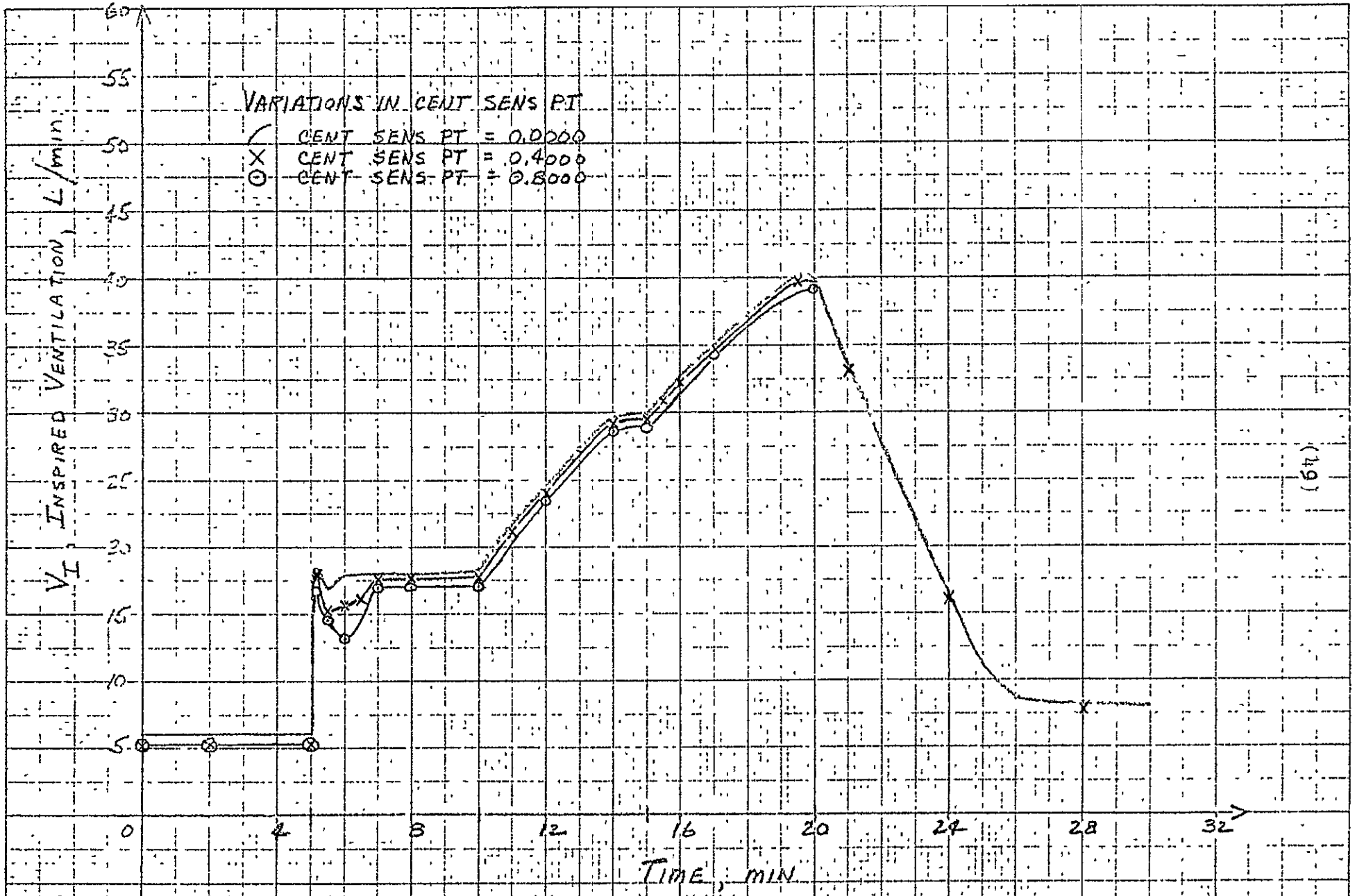

FIGURE 17. INSPIRED VENTILATION VERSUS TIME FOR VARIATIONS IN SYSTEM PARAMETERS UNDER SKYLAB CONDITIONS AND EXERCISE

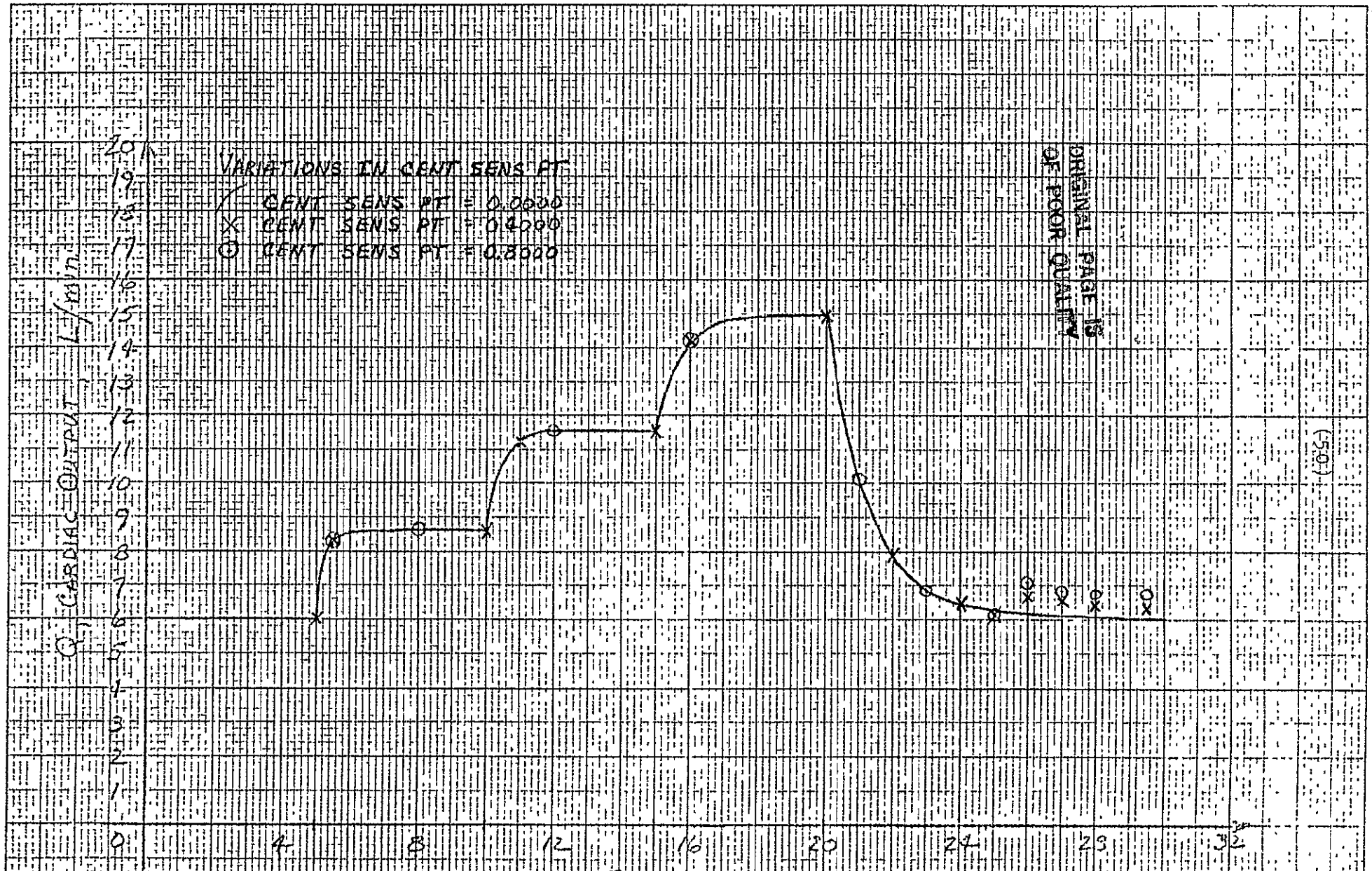

FIGURE 18. CARDIAC OUTPUT VERSUS TIME FOR VARIATIONS IN SYSTEM PARAMETERS UNDER SKYLAB CONDITIONS AND EXERCISE

ORIGINAL PAGE IS OF POOR QUALITY

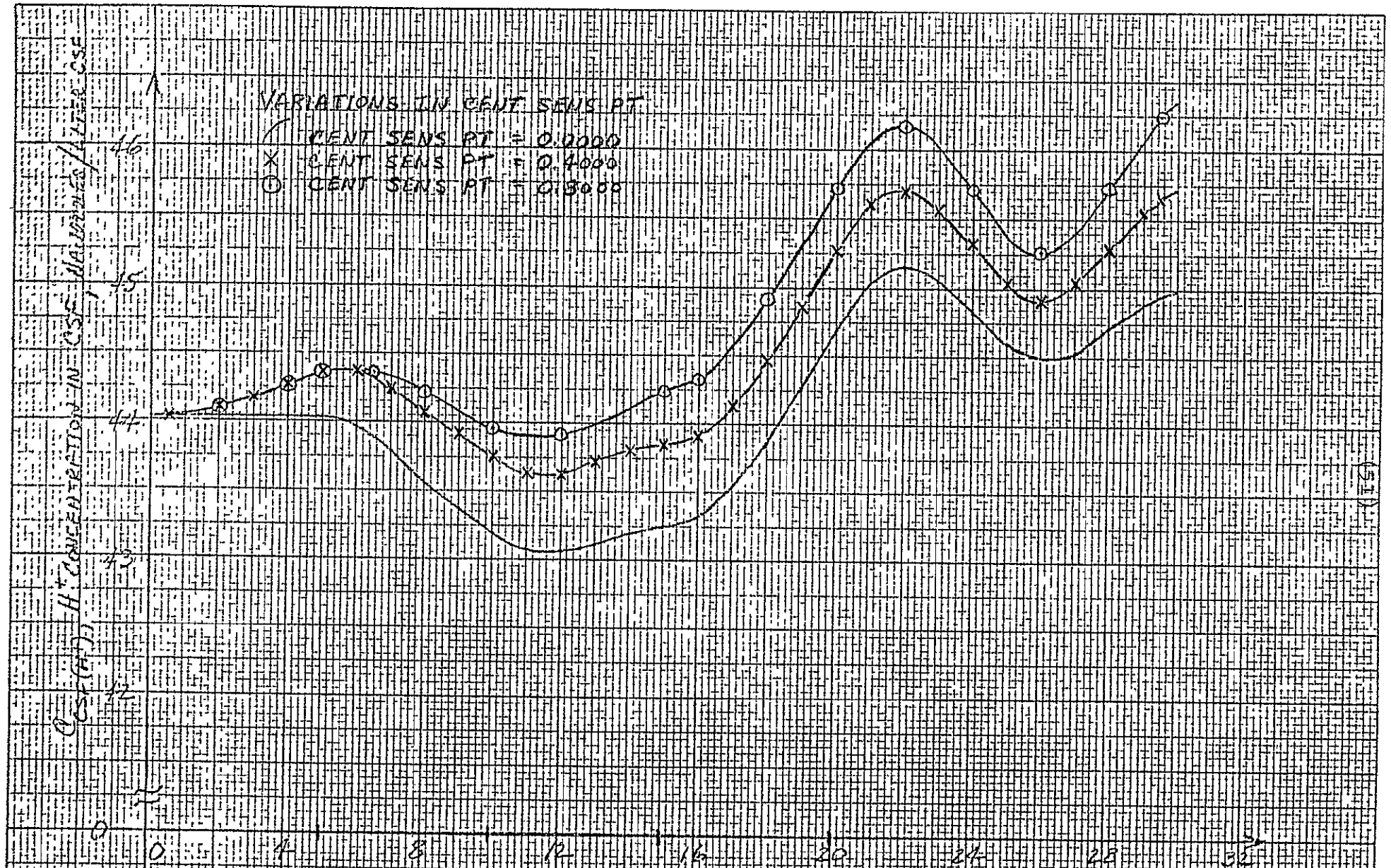

FIGURE 19. H^+ CONCENTRATION IN CSF VERSUS TIME FOR VARIATIONS IN SYSTEM PARAMETERS UNDER SKYLAB CONDITIONS AND EXERCISE

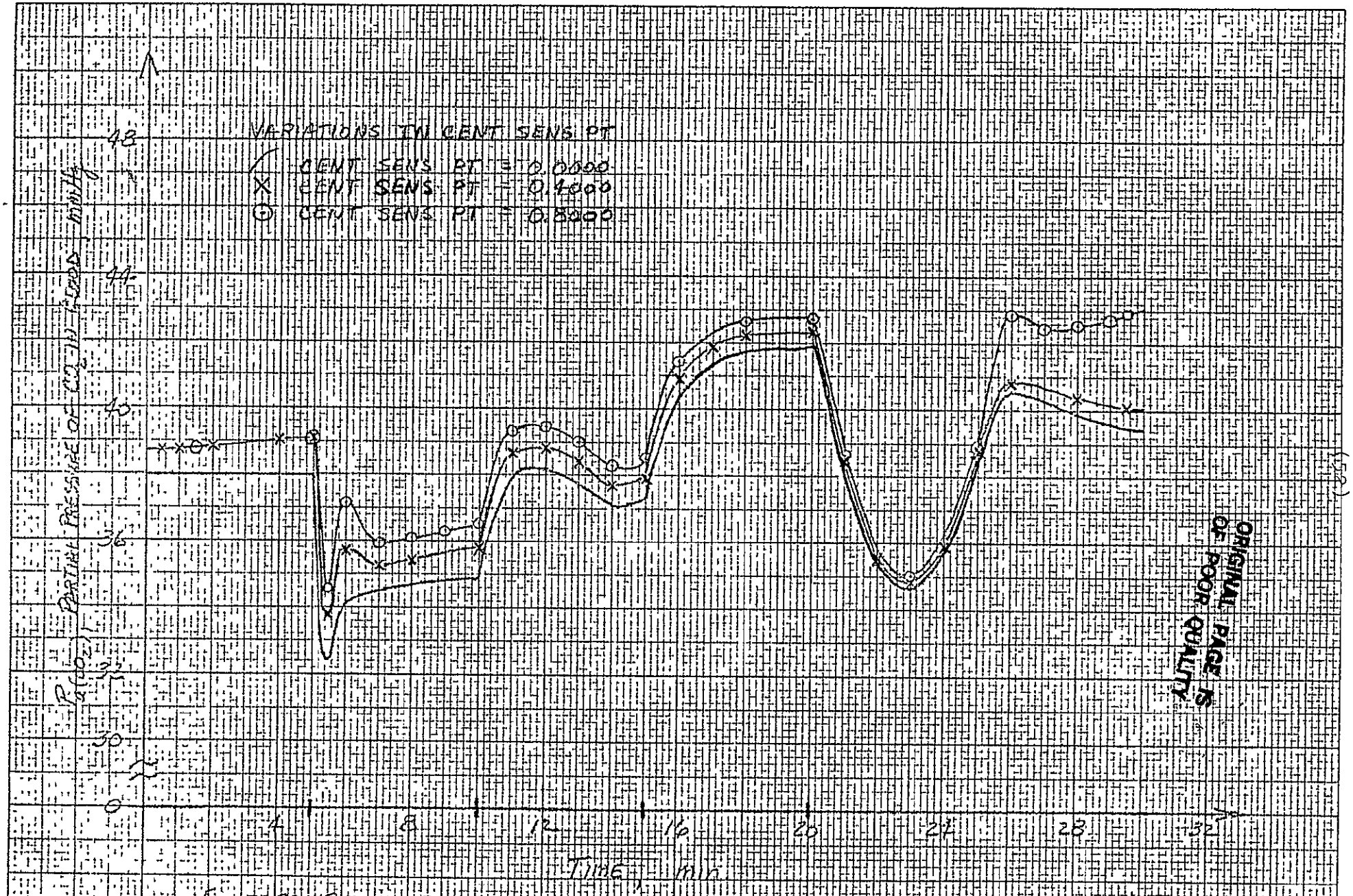

FIGURE 20. PARTIAL PRESSURE OF CO_2 IN BLOOD VERSUS TIME FOR VARIATIONS IN SYSTEM PARAMETERS UNDER SKYLAB CONDITIONS AND EXERCISE

ORIGINAL PAGE IS OF POOR QUALITY

beyond the 50 watts both the arterial CO_2 tension and H^+ concentration in the CSF compartment is increased. This justifies the statement that the ventilation rate is not as efficient for increased exercise. Also from Figure 17 it is evident that the ventilation rate increase does not respond as swiftly for higher exercise levels. The more weighting that is given to the H^+ concentration sensing in the venous blood of the brain, the higher the relative arterial CO_2 tension is for any instant of time. As expected the level of the H^+ concentration in the CSF compartment is higher when the CENT SENS PT is increased.

Run No.	Card No.	Symbol	Revised Initial Value
313	C(20)	CNT SENS COF	50% Normal = 0.5690
	C(37)	VI(N)	62.6399
314	C(20)	CNT SENS COF	150% Normal = 1.7070
	C(37)	VI(N)	112.4602

Discussion: Refer to Figures 21-24. There was no significant deviation from the base run for the variations in the weighting of the H^+ concentration in the CSF compartment. A slight variation occurred in the arterial CO_2 tension response when the initial exercise level was implemented. Under the existing environmental conditions (low inspired CO_2 concentration) the system is insensitive to various weightings of $C_{CSF(H^+)}$. Of course this fact is evident since from Figure 24 it is shown that $C_{CSF(H^+)}$ does not deviate very much from the base run.

ORIGINAL PAGE IS
OF POOR QUALITY

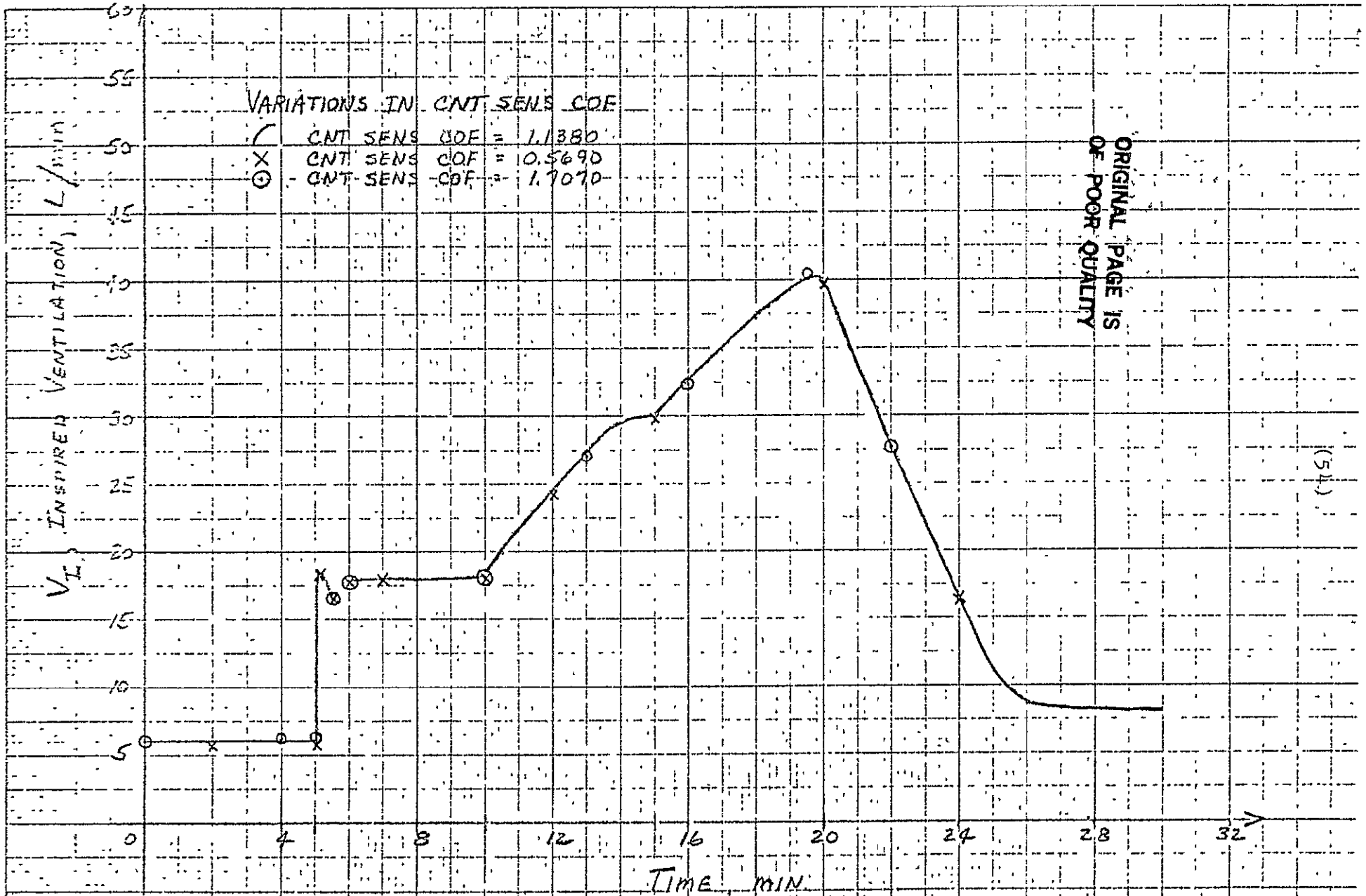

FIGURE 21. INSPIRED VENTILATION VERSUS TIME FOR VARIATIONS IN SYSTEM PARAMETERS UNDER SKYLAB CONDITIONS AND EXERCISE

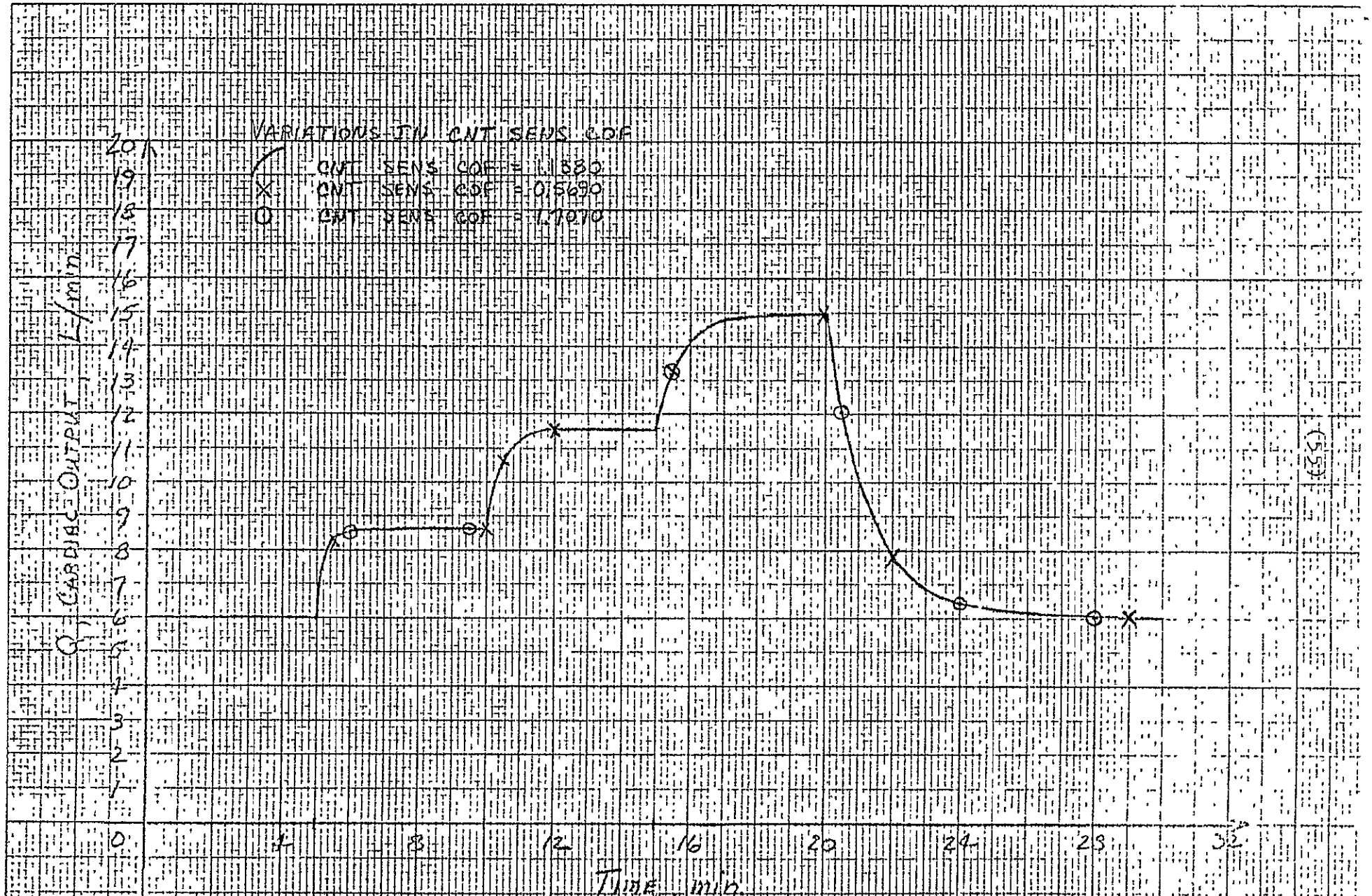

FIGURE 22. CARDIAC OUTPUT VERSUS TIME FOR VARIATIONS IN SYSTEM PARAMETERS UNDER SKYLAB CONDITIONS AND EXERCISE

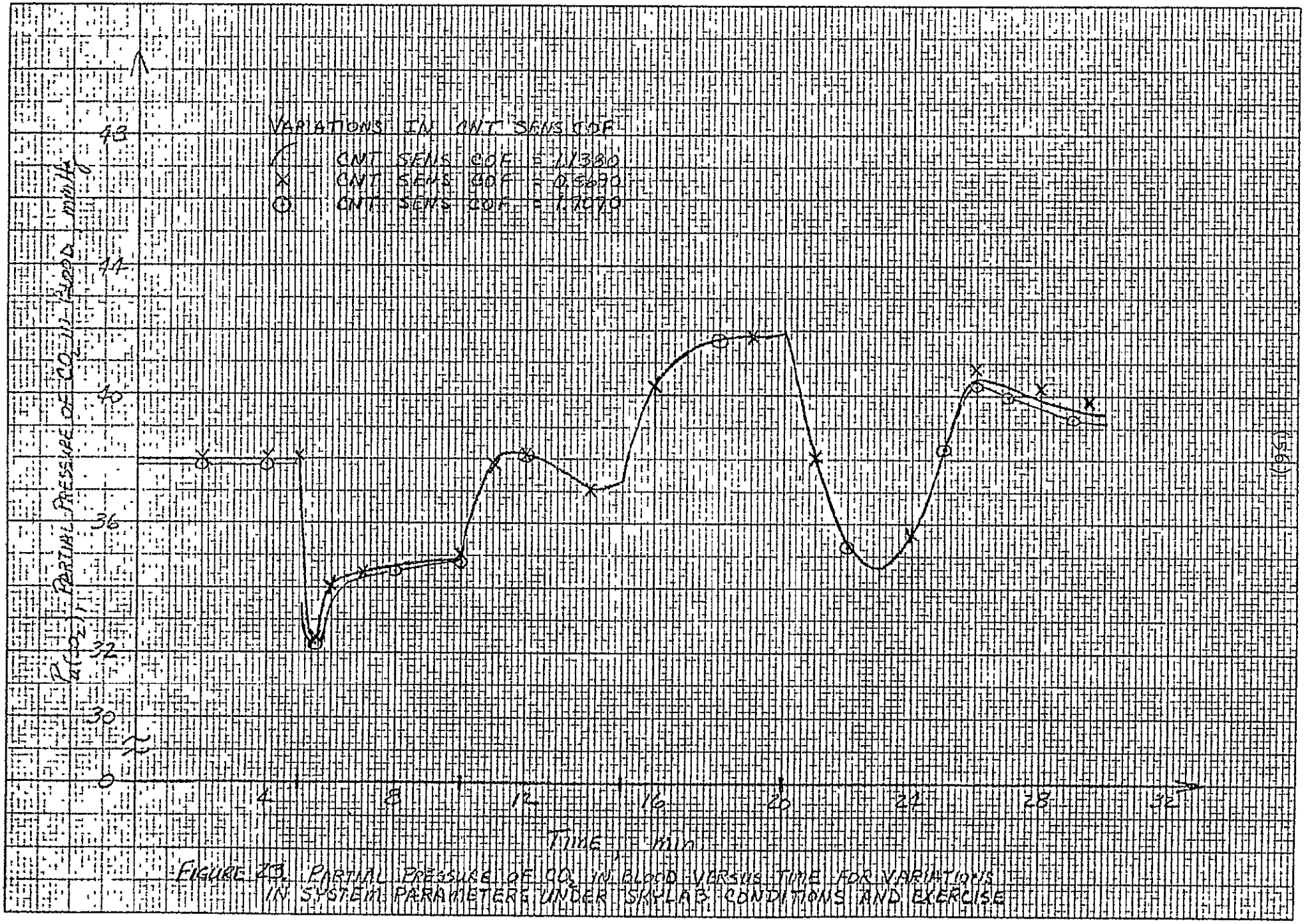

FIGURE 23. PARTIAL PRESSURE OF CO_2 IN BLOOD VERSUS TIME FOR VARIATIONS IN SYSTEM PARAMETERS UNDER SKYLAB CONDITIONS AND EXERCISE

(96)

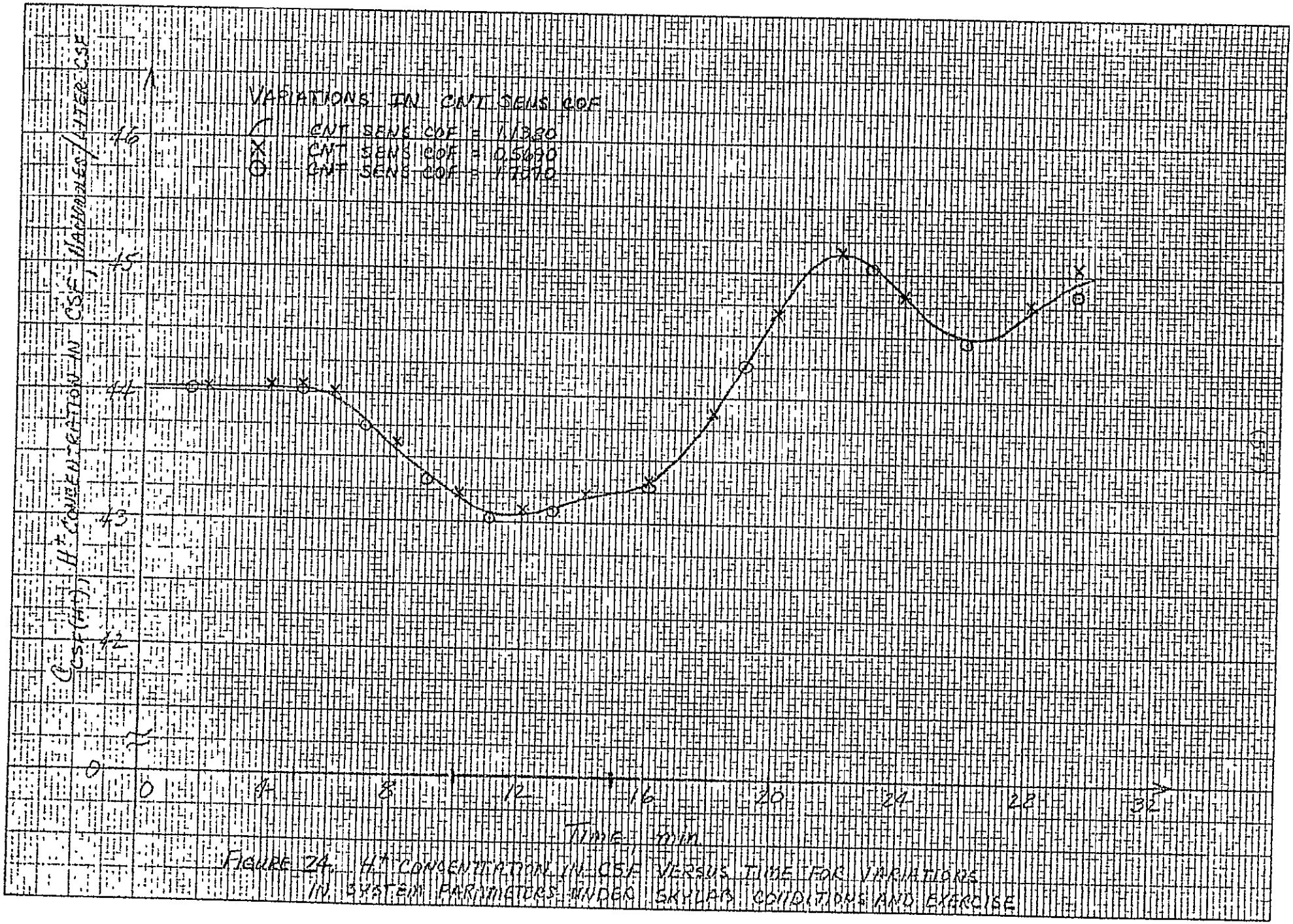

FIGURE 24. H^+ CONCENTRATION IN CSF VERSUS TIME FOR VARIATIONS IN SYSTEM PARAMETERS UNDER SKYLAB CONDITIONS AND EXERCISE

 ORIGINAL PAGE IS
OF POOR QUALITY

Run No.	Card No.	Symbol	Revised Initial Value
323	C(21)	CRTD BDY SCF	50% Normal = 0.5770
	C(37)	VI(N)	65.9842
324	C(21)	CRTD BDY SCF	150% Normal = 1.7310
	C(37)	VI(N)	109.1158

Discussion: Refer to Figures 25-28. The arterial CO_2 tension in Figure 27 displayed the most sensitivity toward variations in the weighting of the H^+ concentration at the carotid bodies. An increase in the CRTD BDY SCF weighting produced a more pronounced oscillation in the transient response of V_I when the first exercise level was simulated. Basically, the carotid bodies' receptor site is a faster responding system component than the CSF component; therefore, it is not too surprising to observe slightly more sensitivity for similar variations in CRTD BDY SCF than in CNT SENS COF.

Many times it is more instructive to analyze the relationship between two variables instead of viewing the variables on a time basis. The two variables chosen are $P_{a(O_2)}$ and Q as shown in Figures 29 and 30. The two curves can be explained by following through a sequence of events corresponding to the letters A through H. Figure 29 corresponds to a deemphasis in the H^+ concentration weighting at the carotid bodies' site while Figure 30 corresponds to an increase in the same weighting factor.

Time is measured along the curve connecting the letters with t=0 at point A and t=30 minutes at point H. The sequence of events which relate to the exercise changes can be described as follows.

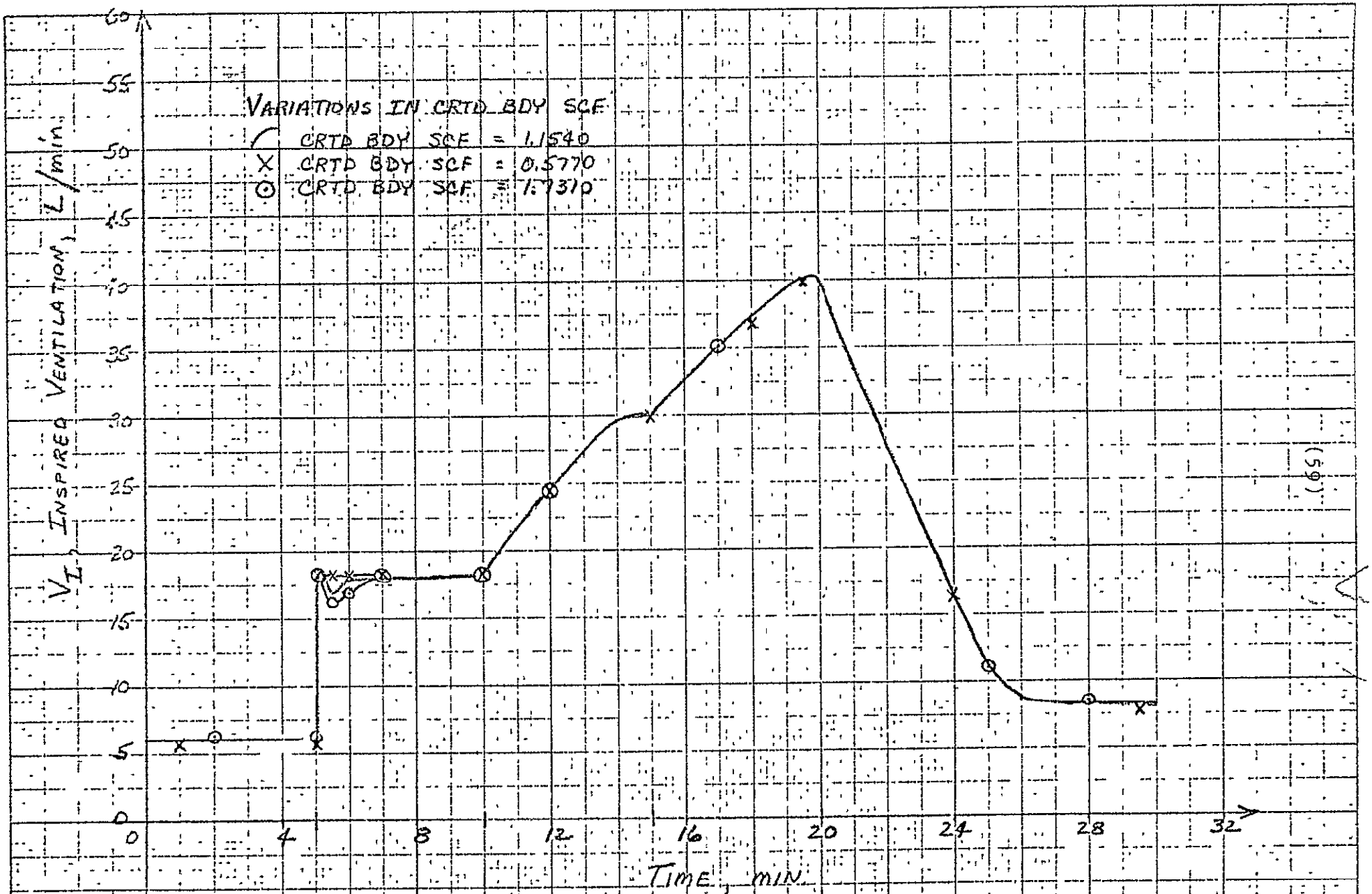

FIGURE 25. INSPIRED VENTILATION VERSUS TIME FOR VARIATIONS IN SYSTEM PARAMETERS UNDER SKYLAB CONDITIONS AND EXERCISE

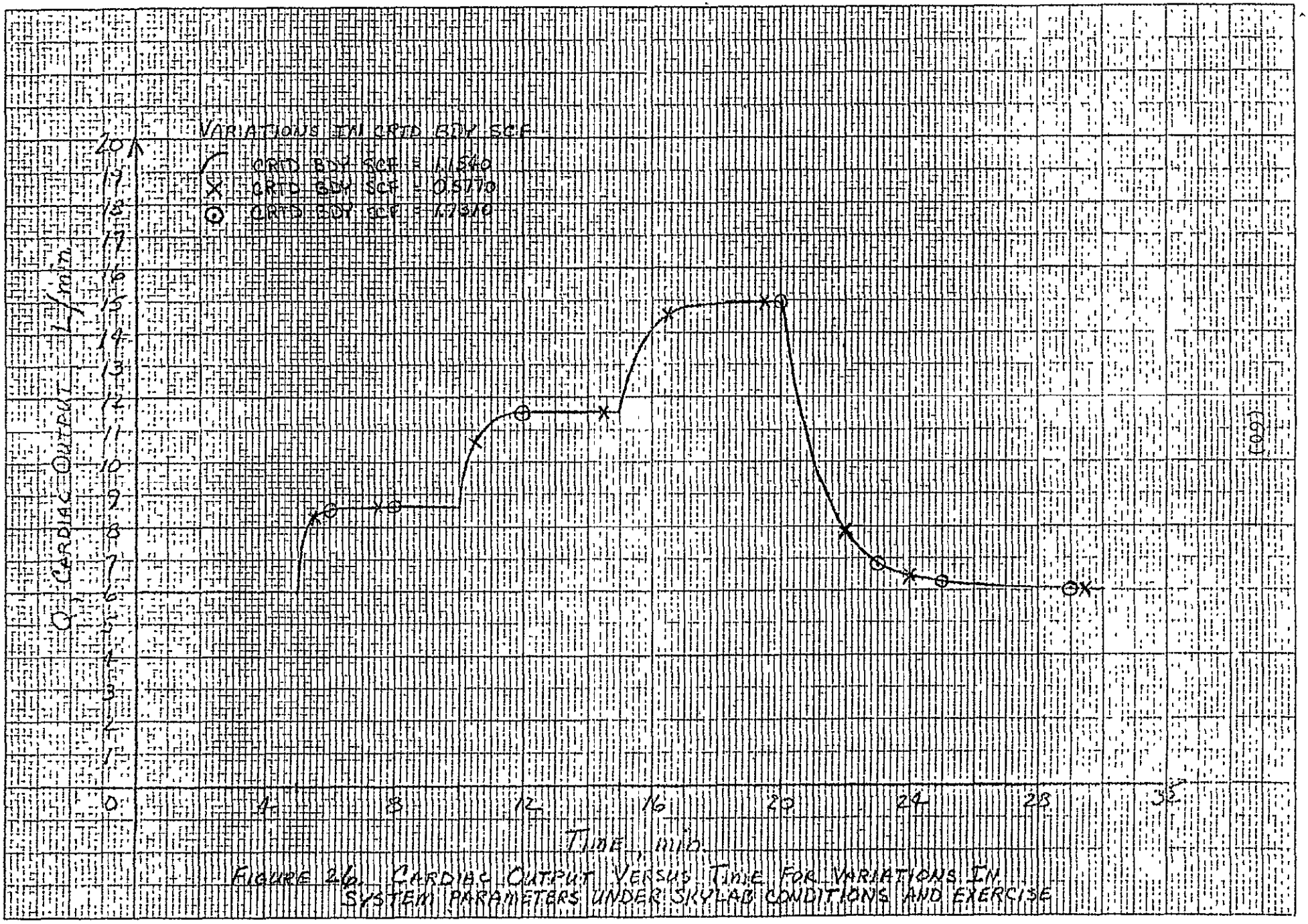

FIGURE 26. CARDIAC OUTPUT VERSUS TIME FOR VARIATIONS IN SYSTEM PARAMETERS UNDER SKYLAB CONDITIONS AND EXERCISE

ORIGINAL PAGE IS
OF POOR QUALITY

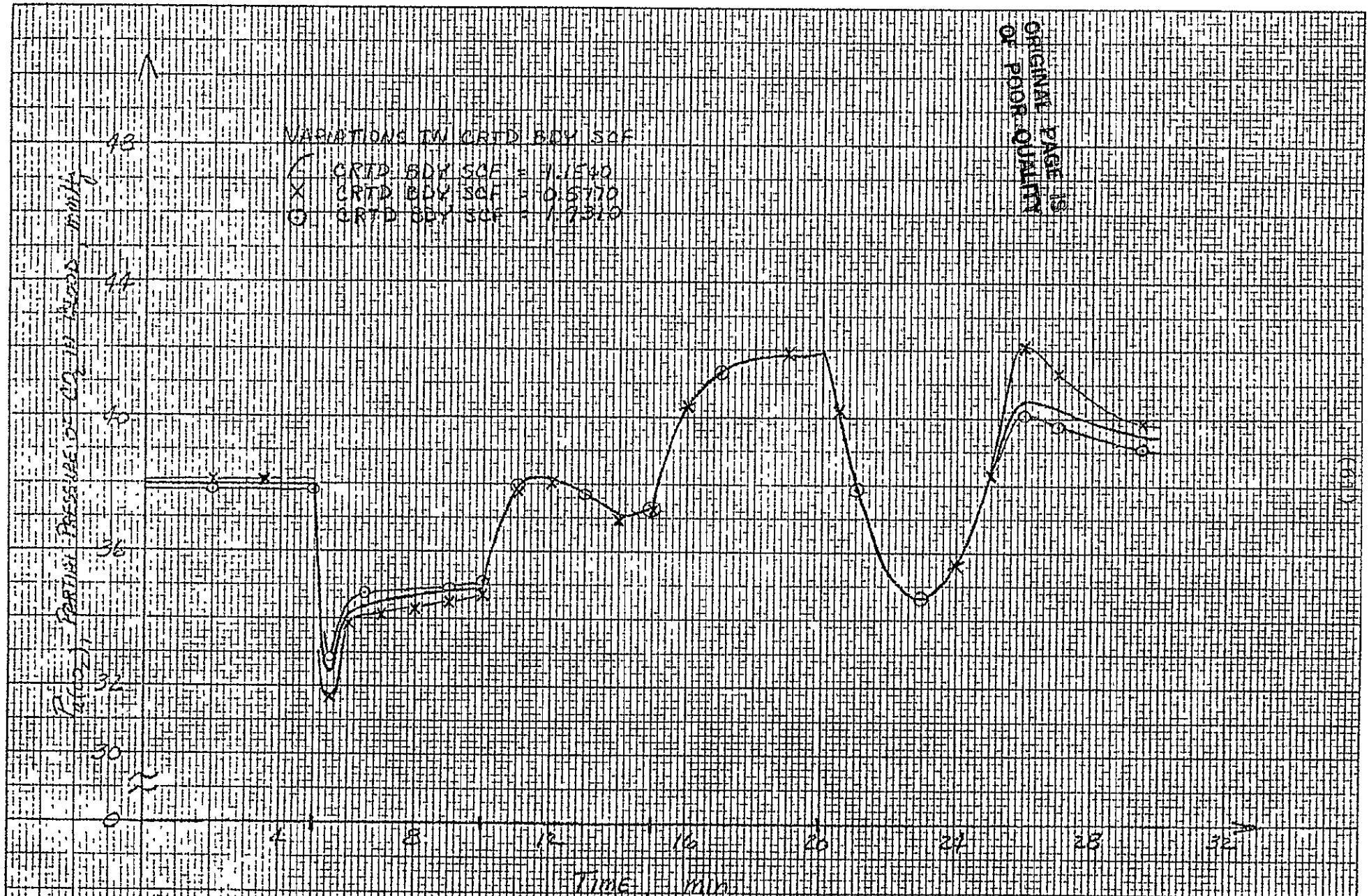

FIGURE 27. PARTIAL PRESSURE OF CO_2 IN BLOOD VERSUS TIME FOR VARIATIONS IN SYSTEM PARAMETERS UNDER SKYLAB CONDITIONS AND EXERCISE

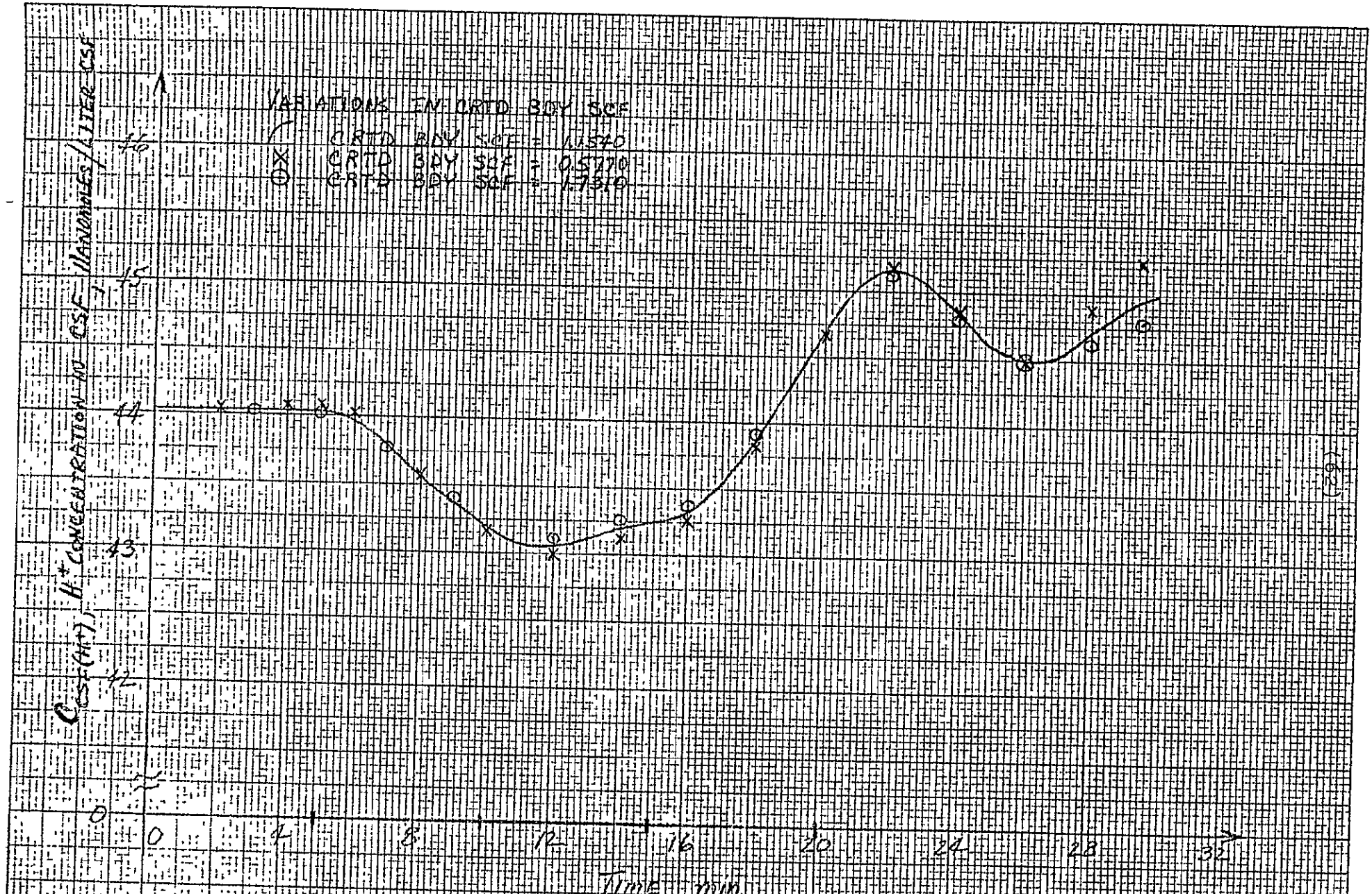

FIGURE 28. H^+ CONCENTRATION IN CSF VERSUS TIME FOR VARIATIONS IN SYSTEM PARAMETERS UNDER SKYLAB CONDITIONS AND EXERCISE

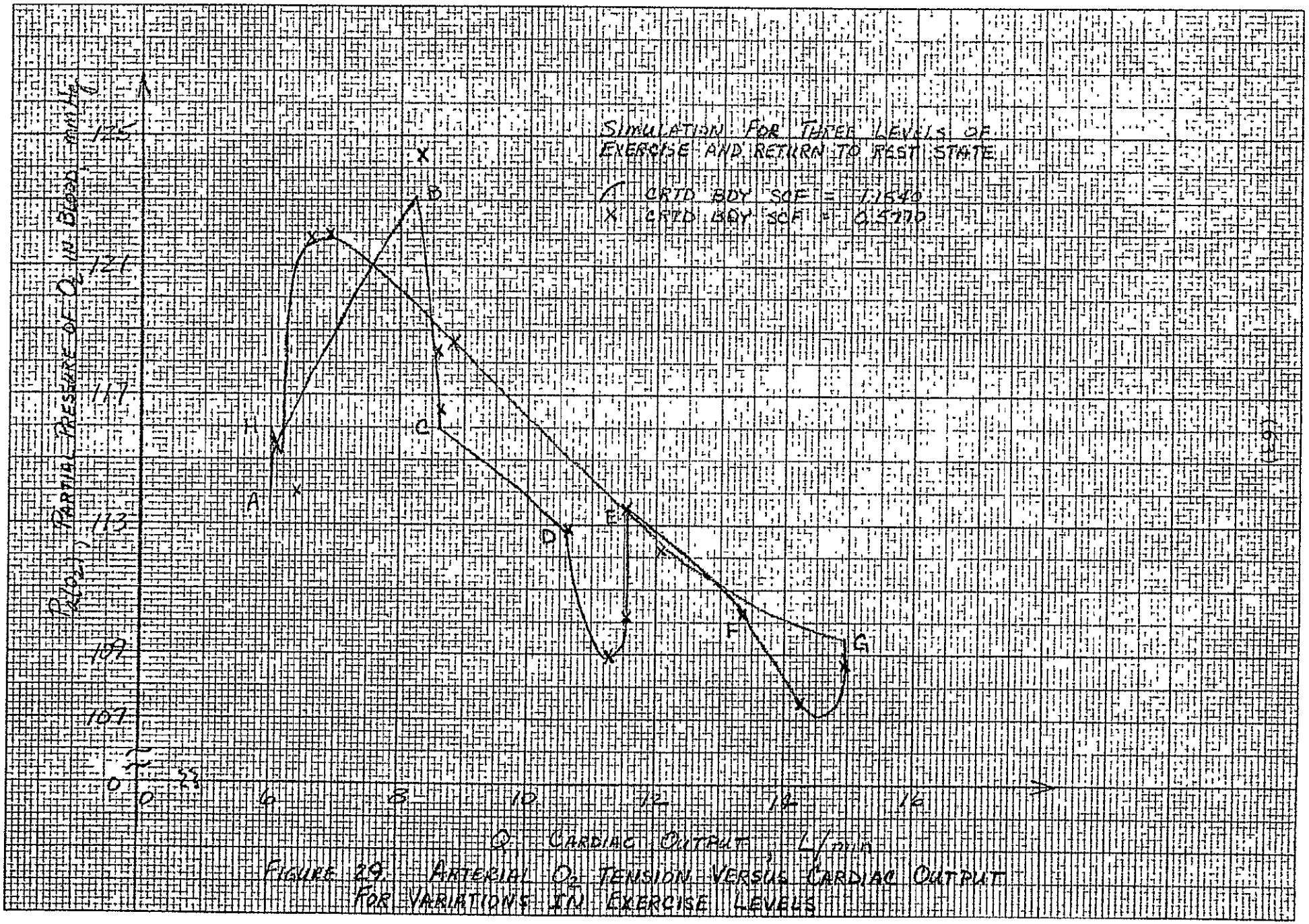

FIGURE 29. ARTERIAL O_2 TENSION VERSUS CARDIAC OUTPUT FOR VARIATIONS IN EXERCISE LEVELS

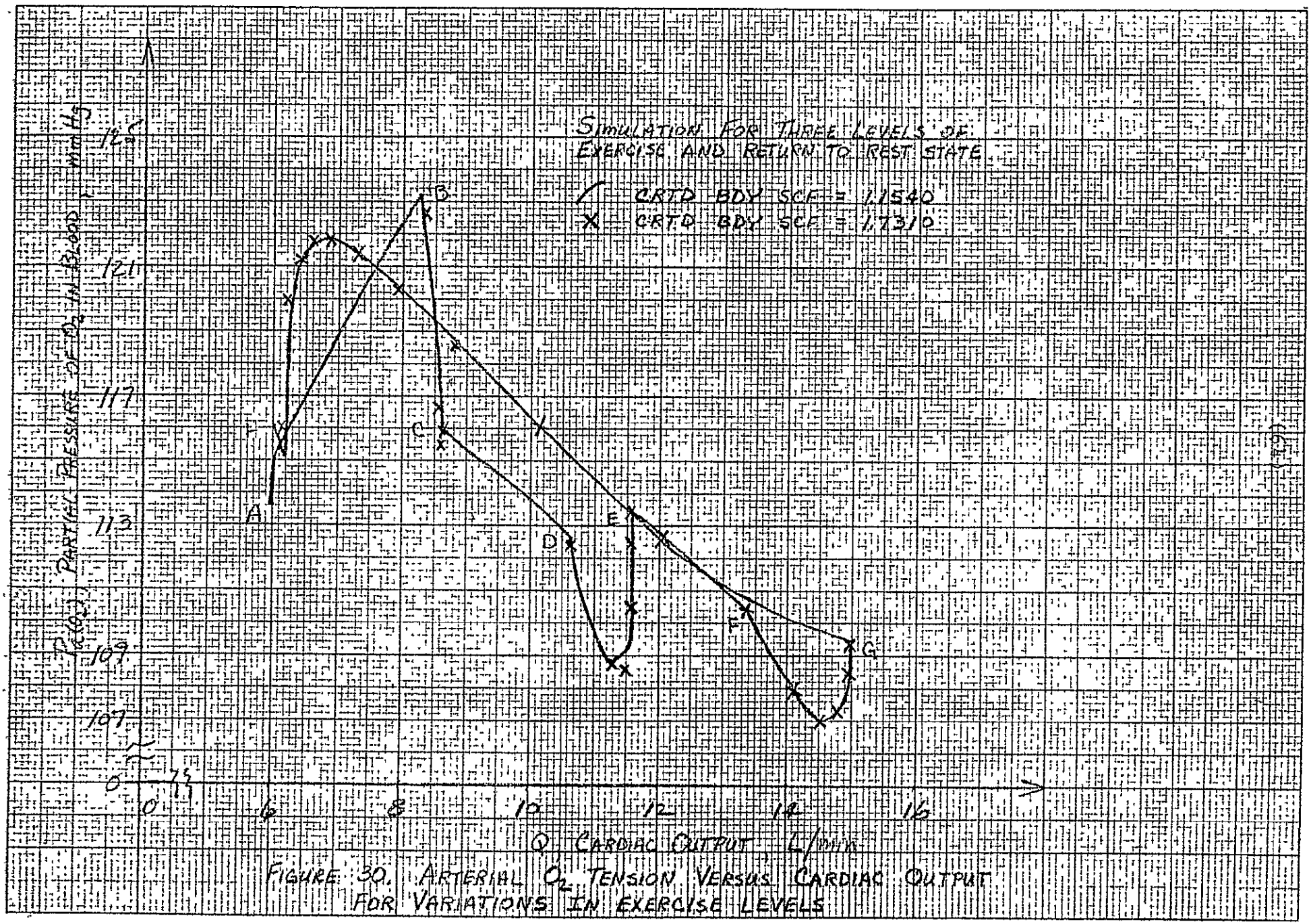

FIGURE 30. ARTERIAL O_2 TENSION VERSUS CARDIAC OUTPUT FOR VARIATIONS IN EXERCISE LEVELS

Interval A-C: 5-10 minutes. Work load = 50 watts

Interval C-E: 10-15 minutes. Work load = 100 watts

Interval E-G: 15-20 minutes. Work load = 150 watts

Interval G-H: 20-30 minutes. Work load = 0 watts (return to resting state).

Intervals A-B, C-D, and E-F correspond to very short time segments. All three of these intervals are less than ½ minute in length. As the exercise level increases, the cardiac output increases and the partial pressure of O_2 in the blood decreases. Both Figures 29 and 30 illustrate a recovery in $P_{a(O_2)}$ for the exercise levels. The steady-state values of $P_{a(O_2)}$ and Q for the three exercise levels correspond to points C,E, and G. When the maximum exercise level is reduced to the resting state, the two variables take on values along the curve from point G to point H.

The recovery phenomenon referred to in the previous paragraph can be physiologically described as follows. Basically, an increase in exercise promotes an increase in cardiac output. The increase in cardiac output along with an increase in the ventilation rate is not adequate to maintain the arterial O_2 tension at a constant level for the exercise steps of 100 and 200 watts. The increase in ventilation rate is more than adequate for the first exercise level since there is an increase in both cardiac output and arterial O_2 tension. After the cardiac output approaches its steady-state value for each exercise level the arterial O_2 tension recovers as shown by the curves approaching points E and G.

IV. CONCLUSIONS AND RECOMMENDATIONS

Upon performing some preliminary studies as described in the previous sections, it appears that Grodins' Respiratory Control Model can be made adaptable to the research efforts of the Environmental Physiology Branch of the Biomedical Research Division, NASA-MSC. There are several facets of the program that need to be altered which will provide for a more complete physiological representation. On the surface there appears to be potential benefits from the incorporation of other research efforts, i.e., Milhorn's models, while utilizing the basic framework of Grodins' model. This phase of the project will be considered later.

The parameter sensitivity analyses need to be extended to include combinations of parameter variations and also to critically evaluate the off-transient ($t \geq 30$ min) conditions. A test for the physiological constraints of the model with regard to CO_2 input levels would be an important investigative effort. Levels of inspired CO_2 are physiologically correlated with ventilation rates, coma, anesthetized states, and death. The model should perform in a similar manner. If not, CO_2 limits must be specified.

The most flexible feature of the entire system is the controller equation. There needs to be a continuing effort in the modification of the existing controller equation and in the evaluation of other controller equations. This is especially important in view of integration of the respiratory system model with other physiological systems. The controller equation will

be a very important link in the total system providing some of the interface capabilities between the cardiovascular, thermal, and body fluid systems with the respiratory system for both the resting and exercising subject.

To perform with any acceptable degree of fidelity, the system must be closely correlated to the salient physiological functionings. Variations in the solubility coefficients of the gases for each compartment and a reduction of the bicarbonate content of the brain and tissue compartments, seem to be desirable. The model includes no general description of the control of cardiac output and regional blood flow. Certainly the regional blood flow feature will be important when the system is interfaced with the body fluid and cardiovascular systems.

As mentioned in Section II.A, respiratory frequency which is now defined as

$$FREQ = 8.1 + 7.815\ (RMT(02) + RMB(02))$$

should be expanded to illustrate other physiological dependencies in addition to O_2 metabolic rates of the tissue and brain compartments. In a similar manner, heart rate, defined as

$$HRATE = 43.8\ (RMT(02) + RMB(02)) + 54.5$$

should be expanded to include relationships involving stroke volume, regional blood flow, increased work load, and perhaps a proper weighting of parasympathetic and/or sympathetic stimulations.

Probably the most important element of the simulation is the adaptation of the model to particular individuals. This

will require a better defined set of initial parameter values in addition to relating these parameter values to the desired environmental conditions.

At present there is a feeling of skepticism with regard to the exercise portion of the simulation in that it doesn't relate to the actual physiological processes involved. There is supportive experimental evidence that indicates the initial transient ventilation response due to a change in the exercise level under stable environmental conditions is created primarily by neurological control (18). With the present simulation, a change in the exercise level causes a change in the metabolic rates of CO_2 and O_2 in the brain compartment which via chemical control is reflected in the ventilation rate. A control mechanism which appropriately weights the neural and chemical processes is being studied. This postulated change will also be related to the functions describing heart and respiratory rates during exercise.

Investigation will continue in the forementioned areas with the goal being to develop a model that is physiologically sound and compatible with the research of the Environmental Physiology Branch. Specific system alterations will be given upon further evaluation of experimental data related to exercise levels and after a more thorough investigation of Milhorn's research.

V. APPENDIX

The following material is a description of the mathematical development of Grodins' program (8) excluding the exercise simulation component. The description involves

(A) Compartment material balance equations
(B) Alveolar-arterial concentration equilibria
(C) Venous blood-brain equilibria
(D) Venous blood-tissue equilibria
(E) Cardiac output and brain blood flow
(F) Blood transport time delays
(G) Controller equation
(H) Differential-difference equations.

All of the explanations including equation numbers refer to Grodins' paper (8).

A. Compartment Material Balance Equations

Equations 1.1-1.3 of Grodins' model (8) will not be duplicated. This format will be carried throughout the ensuing discussion. These three equations describe the time rate of change in the nondimensional volumetric fraction of CO_2, O_2, and N_2 in the lung compartment. They are first order differential equations containing the following terms. Each equation contains the difference between two product terms. One of the terms is the product of the inspiratory gas flow rate multiplied by the volumetric fraction of each gas in dry inspired air. The other term is similar in that it is the product of the expiratory gas flow rate multiplied by the volumetric fraction of each gas in dry alveolar gas. Evident from these two terms is the fact that water vapor is not considered in this gaseous exchange relationship. The difference between the venous and

arterial concentrations of each gas is multiplied by the total cardiac output. One should note that the concentration terms have units of liters per liter blood. Another coefficient relating barometric pressure and water vapor pressure of the blood multiplies the concentration differences. All of the terms are divided by the volume of the lung compartment yielding the proper volumetric fraction of gas per minute.

Expressions of the time rate of change of each gas in the brain and tissue compartments are defined by Equations 1.4 - 1.9. The metabolic rates of CO_2 and O_2 have opposite effects in both the brain and tissue compartments. Both are considered constants in each compartment. The metabolic rate of CO_2 increases the rate of change in concentration of CO_2 while the metabolic rate of O_2 decreases the rate of change in concentration of O_2. There is no metabolic rate term associated with the nitrogen gas. This concept corresponds to the basic assumptions in the previous sections. The difference between the arterial and venous concentrations of each gas in the brain compartment, Equations 1.4 - 1.6, is multiplied by the blood flow in the brain, thus altering the rate of change in the concentrations of each gas. Also, within the brain compartment there is a membrane separating the CSF subcompartment from the brain. The membrane is permeable to all three gases, being about 20 times more premeable to CO_2 than O_2 as depicted by the relative magnitudes of the diffusion coefficients. The product of the difference

between the partial pressures of each gas in the brain and CSF and the diffusion coefficient correspondingly alters the rate of change in concentration of that gas in the brain compartment. The brain - CSF interface is described in the manner that contributes to a positive alteration in the rate of change in the concentration of a gas if the partial pressure of that gas is greater in the CSF compartment than in the brain compartment.

In addition to the metabolic term described above, the rate of change in concentration of each gas in the tissue compartment, Equations 1.7 - 1.9, is a function of the tissue blood flow. Tissue blood flow is defined as the difference between cardiac output and brain blood flow. This difference is then multiplied by the gas concentration difference between the arterial and venous sides of the tissue compartment. Once again, the volumes of each compartment are entered into Equations 1.4 - 1.9 to provide the proper dimensions of liter per liters of blood per minute.

The partial pressure of each gas in the CSF compartment can be described by a first order differential equation as in Equations 1.10 - 1.12. The time rate of change in the partial pressure of each gas is a function of the diffusion coefficient across the blood-brain barrier, the volume of the CSF compartment, a conversion factor relating atmospheres and mmHg, the solubility coefficient of the gas in the CSF, and the difference between the partial pressure of the gas across the blood-brain barrier. As expected, the dimensions

of Equations 1.10 - 1.12 are mmHg per minute. It should be noted that the solubility coefficient of each gas is given in units of liter per liters per atmosphere and evaluated at 37 °C. These coefficients are not altered between compartments and satisfy Henry's Law for the environmental conditions being considered. The constant k is a conversion factor.

From the initial assumptions associated with the lung compartment it is obvious that a change in the volumetric fraction of one gas is related to the sum of the changes in the volumetric fractions of the other two gases. Therefore, the <u>algebraic</u> sum of $F_{A(CO_2)} + F_{A(O_2)} + F_{A(N_2)}$ is zero, which leads to Equation 2.1(8). Both V_E and V_I are needed for the solution of the system. Thus, Equation 2.1 gives a relationship from which V_E can be written in terms of V_I or vice versa. V_I is an output of the controlling system. The expired ventilation, V_E, is a function of the concentration differences of each gas multiplied by the total cardiac output and a nondimensional coefficient related to the barometric pressure.

This is a reasonable relationship if one considers that the output flow rate is equal to the input flow rate plus alterations that might occur in the metabolic processes relating CO_2, O_2, and N_2. The latter is tempered by the cardiac output and the difference between the input-output concentrations of each gas.

B. Alveolar - Arterial Concentration Equilibria

There are probably several methods for building up the necessary interrelationships between variables so as to solve the final system of differential-difference equations. Grodins' next step in the development is to formulate expressions for the alveolar-arterial concentration equilibria for the gases in the blood at the lung exit (Equation 3.1 - 3.7). The Haldane effect which illustrates the dependence of the concentration of CO_2 upon variations in O_2 concentration is included. Also included is the description of the dual role that variations in CO_2 concentration play upon the concentration of O_2. This latter dependency is termed the Bohr effect.

The concentration of CO_2, Equation 3.1, is comprised of a constant bicarbonate term, the last term being a weighting of the effect of the partial pressure of CO_2, and the two middle terms being chemically combined relationships. Although not readily explainable because of the coefficients involved, the second term is a weighting of the difference between the blood oxygen capacity and the concentration of oxyhemoglobin (liters of O_2 per liter blood). The third term attempts to describe the product effect of the presence of O_2 and CO_2 with the O_2 associated with the Hb term and CO_2 described by the logarithm of CO_2 arterial concentration and dry alveolar gas concentration difference divided by a weighted arterial partial pressure of CO_2.

The expression for $C_{a(O_2)}$, Equation 3.2, contains an empirical relationship describing the O_2 dissociation curve and the Bohr effect. The concentration of oxyhemoglobin is described by an empirical form containing an exponential term which is dependent upon the pressure of CO_2 whose involvement becomes evident through the pH term. An explanation of the derivation for pH_a is in order. The normal form for the Henderson-Hasselbalch equation is

$$pH = pK + \log\left(\frac{HCO^-_3}{CO_2}\right) .$$

Grodins has defined pH_a as

$$pH_a = - \log C_{a(H^+)}$$

with the units of $C_{a(H^+)}$ being nanomoles per liter. Thus

$$pH_a = - \log [C_{a(H^+)} (10)^{-9}]$$

$$pH_a = - \log [C_{a(H^+)}] - \log [10^{-9}]$$

$$pH_a = 9 - \log [C_{a(H^+)}].$$

To relate this development to the Henderson-Hasselbalch equation requires the terms of Equation 3.6 to be regarded as physiological equivalent to the terms in the Henderson-Hasselbalch equation, i.e.,

$$pK \Leftrightarrow \log K'$$

and $$\frac{HCO^-_3}{CO_2} \Leftrightarrow \frac{k\alpha_{CO_2} (B-47) F_{A(CO_2)}}{C_{a(CO_2)} - k\alpha_{CO_2} (B-47) F_{A(CO_2)}}$$

These analogies have been developed by several researchers for various body compartments; one example being given by Bradley et al. (19).

Since only physically dissolved nitrogen is considered, the arterial concentration of N_2, $C_{a(N_2)}$, can be defined by the simple expression in Equation 3.7. The development describing the alveolar-arterial concentration equilibria and the development in the following section concerning the blood-brain equilibria are probably the most complex, both mathematically and physiologically speaking, of any segment of the respiratory control model.

C. Venous Blood-Brain Equilibria

The expressions of the concentration of CO_2 in the brain and venous blood reflect the original assumptions in that the brain concentration is not dependent upon Hb and HbO_2 effects, while the venous blood is described in exactly the same manner as the alveolar-arterial CO_2 concentration. One other variation is that the standard bicarbonate content differs in the two expressions (Equations 4.1 and 4.2). The bicarbonate content of the brain, $(BHCO_3)_B$, must always be greater than or equal to the bicarbonate content of the blood, $(BHCO_3)_b$. This particular relationship between these two parameters is one which needs to be altered so as to more precisely simulate physiological conditions.

The O_2 concentration in the brain, $C_{B(O_2)}$, is given as

$$C_{B(O_2)} = k\alpha_{B(O_2)} P_{B(O_2)}.$$

This agrees with the form for $C_{B(N_2)}$ which is given as

$$C_{B(N_2)} = k\alpha_{B(N_2)} P_{B(N_2)}.$$

These two relationships are utilized because in the brain compartment only physically dissolved O_2 and N_2 are considered.

The concentration of O_2 in the blood at the brain exit is also a function of the oxyhemoglobin concentration. This particular involvement is described by Equations 4.3 - 4.7. As in the previous section, the oxyhemoglobin concentration is an empirical form containing an exponential term which is dependent upon the venous blood pH, pH_{vB}. As before, to relate this development to the Henderson-Hasselbalch equation, from Equation 4.7

$$pK \Leftrightarrow \log K'$$

and $$\frac{HCO_3^-}{CO_2} \Leftrightarrow \frac{k\alpha_{CO_2} P_{B(CO_2)}}{C_{vB(CO_2)} - k\alpha_{CO_2} P_{B(CO_2)}} .$$

The first expression in Equation 4.8 states that the concentration of N_2 in the venous blood leaving the brain is proportional to the concentration of N_2 in the brain. However, in the present simulations the coefficient is unity since the solubility coefficient any gas is the same for all compartments. This is another relationship between parameters that needs to be altered to more closely represent the physiology involved.

D. Venous Blood - Tissue Equilibria

As is suggested by Grodins (8) the CO_2, O_2, and N_2 relationships between the tissue compartment and the tissue venous blood are derived under the same basic assumptions as those of the venous blood-brain equilibria. Thus one can develop an analogous set of relationships for the tissue compartment as for the brain compartment. Since the physically dissolved concepts,

the metabolic relationships, and the empiricisms are analogous, then the overall system sensitivities to variations within the two compartments must be closely tied to the relative magnitudes of the compartmental volumes. This conjecture appears to be justified in some of the computer simulations.

E. Cardiac Output and Brain Blood Flow

Both cardiac output and brain blood flow are defined to be dependent upon variations in the partial pressures of arterial O_2 and CO_2. The first order differential equations that describe these two flow patterns are similar. Looking at the differential equation for cardiac output, Equation 7.1, it can be rewritten as

$$r_1 \dot{Q} + Q = f_Q.$$

The function, f_Q, can be considered the forcing function for the differential equation. Note that by Equation 7.2, f_Q is a collection of terms dependent upon the normal cardiac output, a variation in the blood flow due to O_2 and a corresponding variation due to CO_2. Let's ignore any physiological significance of the differential equation. The solution, $Q(t)$, can be considered as the sum of two components, $Q_c(t)$ and $Q_p(t)$. $Q_c(t)$ is the solution of the differential equation if $f_Q=0$. Such a solution would take the form of

$$Q_c(t) = K\varepsilon^{-t/r_1}$$

where K would be determined from the initial value $Q(t)$. The other component of the solution, $Q_p(t)$, is determined from the form of the forcing function f_Q. A simple example would be

to ignore any effects of O_2 and CO_2 and consider $f_Q = Q_N$. By the classical solution of differential equations, it is readily shown that

$$Q_p(t) = \text{Constant} = Q_N.$$

The total solution would be

$$Q(t) = Q_c(t) + Q_p(t)$$

$$\text{or} \quad Q(t) = K\varepsilon^{-t/r_1} + Q_N.$$

Suppose that at time $t = 0$ seconds, $Q(t)\Big|_{t=0} = Q(0)$. Then

$$K = Q(0) - Q_N.$$

and the total solution would be

$$Q(t) = (Q(0) - Q_N)\varepsilon^{-t/r_1} + Q_N.$$

A graphical description showing two values of $Q(0)$ relative to Q_N would appear as in Figure 1.

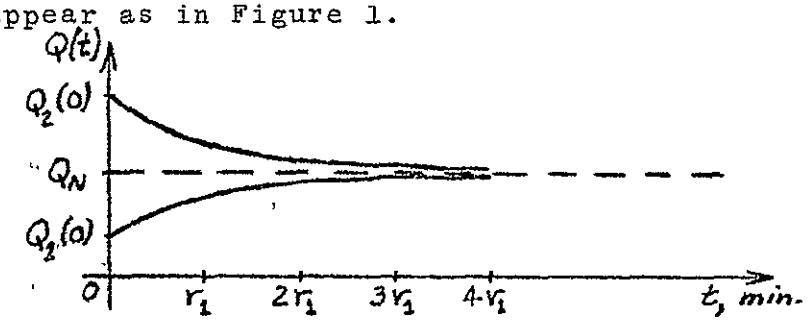

Figure 1. Sample of first order response

Up to this point the mathematical description of cardiac output depends upon the value of the initial condition, the normal resting value, and a time constant which attempts to drive the solution to a physiologically meaningful representation. Fortunately, by the addition of an empirical relationship describing $\Delta Q_{(O_2)}$ and a linear relationship describing $\Delta Q_{(CO_2)}$ both defined over specified limits for $P_{a(O_2)}$ and $P_{a(CO_2)}$ respectively, Grodins has mathematically formulated a more

precise description of $Q(t)$. There is a factor $\Delta Q_{(O_2)}$ contributing to the forcing function only when $P_{a(O_2)} < 104$ mmHg.

The computer program deviates from the paper in the mathematical description of the dependency of $\Delta Q_{(CO_2)}$ upon $P_{a(CO_2)}$. Equation 7.6 has been altered to read

$$\Delta Q_{(CO_2)} = 6 \text{ for } Y \geq 60$$

and $$\Delta Q_{(CO_2)} = 0 \text{ for } Y \leq 40.$$

These factors are described by Equations 7.3 and 7.5.

The same form of differential equation describes the brain blood flow except that the forcing function components related to $P_{a(CO_2)}$ and $P_{a(O_2)}$ are different. The same range of $P_{a(O_2)}$ is considered, but the empirical relationship is different than the one used for cardiac output. On the other hand, $P_{a(CO_2)}$ is a contributing factor for all of its possible values except for 38 mmHg $\leq P_{a(CO_2)} \leq$ 44 mmHg. In this range, brain blood flow is not dependent upon $P_{a(CO_2)}$. Variations in the time constants r_1 and r_2 are considered in some computer simulations involving parameter sensitivities.

F. <u>Blood Transport Time Delays</u>

As with any physically dynamic system involving flow dynamics or transfer of information, there are time delays in signal transmission. The time delays of the respiratory model are associated with the blood flow between compartments. The notation used for the time delays can be readily described by Figure 2 which indicates the shape of the delayed waveform and the notation used.

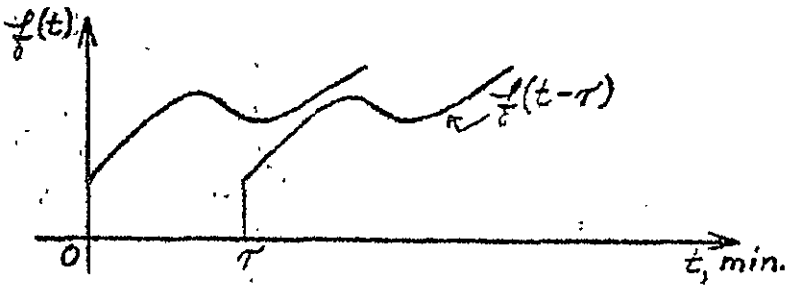

Figure 2. Function, f(t), delayed by τ minutes

In the simulation the time delay, τ, corresponds to delays between lung and brain compartments, between lung and tissue compartments, between tissue and lung compartments, and between the lung compartment and the carotid body receptor. These are very necessary terms and their incorporation in the system equation enhances the confidence placed upon the dynamics of the simulation. Concentrations of the three gases at the entrances of the brain, tissue, and lung compartments are defined in terms of the appropriate time delays by Equations 8.1 - 8.9. To further refine these time delays, they are not considered to be predetermined constants, but are time dependent in that they are functions of cardiac output, brain blood flow, and vascular segment volumes. This reasoning is very sound since the blood flow dynamics obviously affect relative site gas concentrations. These time delays which are continuously being recalculated in the computer program are defined by Equations 8.10 - 8.14. From the integral representations it is clear that when steady-state conditions are reached, i.e., Q and Q_B become constants, the time delays will become constants also. This is also justified by observing the computer print-out.

G. Controller Equation

The controller equation is the system's feature that provides the feedback mechanism. Many different forms for the

controller equation can be postulated. To completely understand the simulation's potentials, a concentrated effort should be given to investigation of other controller equations. This reasoning is amplified by Grodins' comments and consequently special emphasis is placed upon its evaluation in the study. At this point one might ask the following question. What is the purpose of the controller equation? This question might be answered best by observing the block diagram of a respiratory feedback system in Figure 3.

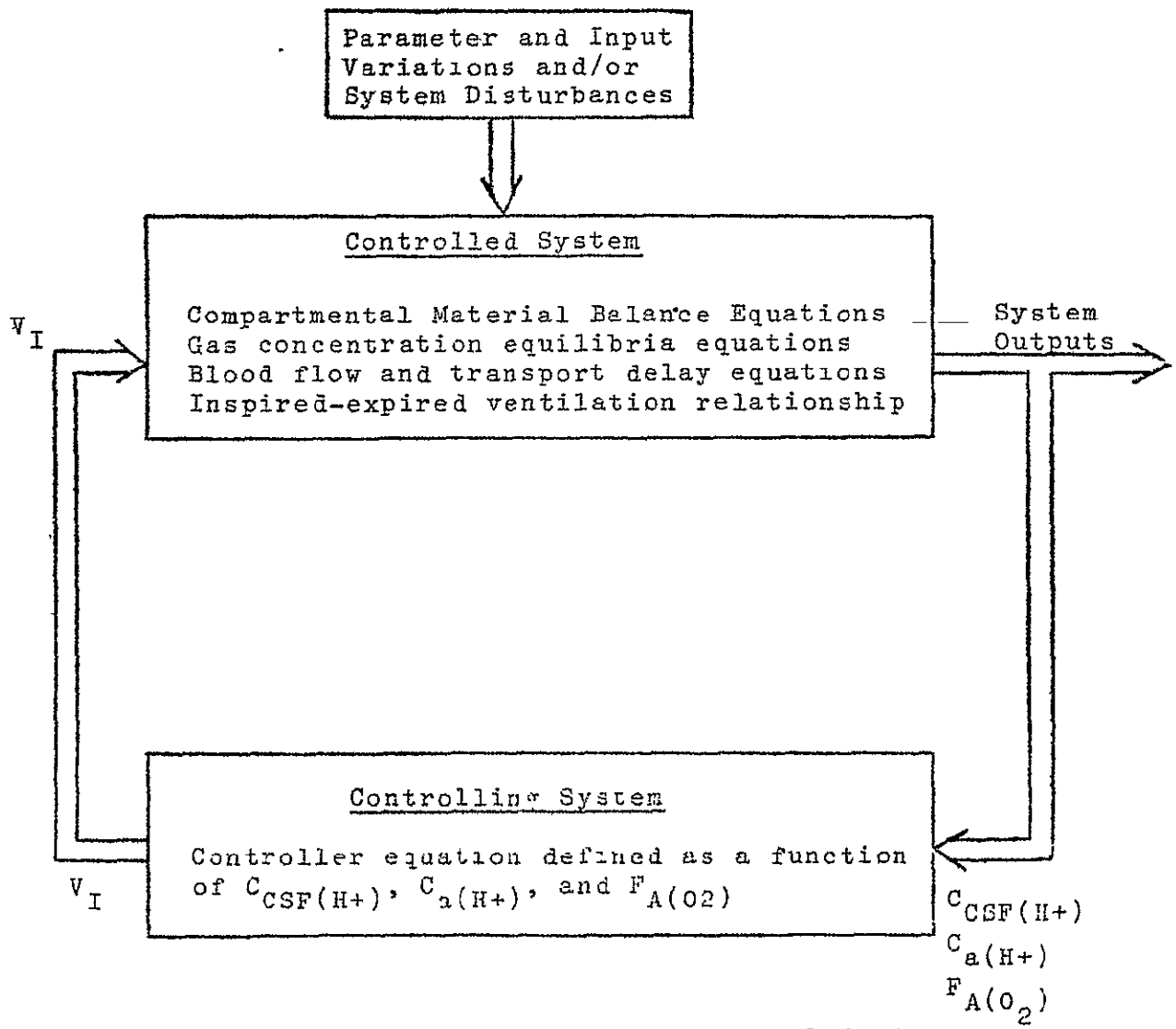

Figure 3. Respiratory Feedback Control System

The controller equation as described by Equation 9.2 uses only three of many outputs of the controlled system. At this point the thesis is that $C_{CSF(H^+)}$, $C_{a(H^+)}$, and $F_{A(O_2)}$ are the three factors which determine the inspired ventilation, V_I. The inspired ventilation is then used to determine V_E and is also used in the controlled system's equations. Thus, the feedback path is completed. Also, it is very instructive to note that the arterial H^+ concentration and alveolar oxygen volumetric fraction are not detected until τ_{ao} minutes after the arterial blood leaves the lungs. This feature simulates the time elapsed while the blood is flowing to the carotid receptors from the lung compartment. The H^+ concentration in the CSF subcompartment is described by Equation 6.1. In the same manner as the pH calculations are performed in the other compartments a comparison of terms in the Henderson-Hasselbalch equation with those of Equation 6.1 yields

$$pK \Leftrightarrow \log K'$$

$$\text{and } \frac{HCO_3^-}{CO_2} \Leftrightarrow \frac{k\alpha_{CSF(CO_2)}\ P_{CSF(CO_2)}}{(BHCO_3)_{CSF}} .$$

Once the decision has been made as to the variables which are used as inputs to the controlling equation, a proper weighting of these variables is made so as to drive the total system's responses to correlate with experimental data. This necessarily requires empirical formulations. Although not explained in the paper the computer program has the capability of weighting the influence of the H+ concentration in the CSF compartment to the

H+ concentration of the venous blood of the brain compartment. This weighting is evaluated in some of the computer simulations. Great care should be expended so as not to critically violate known physiological features.

H. Differential-Difference Equations

It is now apparent that many mathematical relationships have been developed relating alveolar-arterial concentration equilibria, venous blood-brain and venous blood-tissue equilibria, blood flow rates to all the compartments, and the transport time delays. The next task is to assemble these relationships in a meaningful set of equations from which solutions for the system's variables can be obtained. Grodins (8) has accomplished this by utilizing the framework of the compartmental mass balance equations. Although it is not necessary to completely describe the culminated effort in Equations 10.1 - 10.9 and Equation 11.1, perhaps it would be instructive to comment upon the substitutions for one of these equations, i.e., Equation 10.5. Equation 10.5 has the basic structure of Equation 1.5. For convenience these two equations are repeated here.

Equation 1.5:

$$\mathring{C}_{B(O_2)} = \frac{1}{K_B}\left[-MR_{B(O_2)} + Q_B\left(C_{aB(O_2)} - C_{vB(O_2)}\right) - D_{O_2}\left(P_{B(O_2)} - P_{CSF(O_2)}\right)\right]$$

Equation 10.5:

$$\mathring{C}_{B(O_2)} = \frac{1}{K_B}\left[-MR_{B(O_2)} + Q_B\left(\overbrace{\left(k\alpha_{O_2}(B-47)F_{A(O_2)} + C_{a(HbO_2)}\right)(t-\tau_{aB})}^{[A]} - \overbrace{\left(\frac{\alpha O_2}{\alpha B(O_2)}\right)C_{B(O_2)} - C_{vB(HbO_2)}}^{[B]}\right) - D_{O_2}\left(P_{B(O_2)} - P_{CSF(O_2)}\right)\right]$$

Remember we are looking at the brain compartment site. Here, from Equation 8.2,

$$C_{aB(O_2)}(t) = C_{a(O_2)}(t - \tau_{aB}).$$

Noting from Equation 3.2 that

$$C_{a(O_2)} = k\alpha_{O_2}(B\text{-}47)\, F_{A(O_2)} + C_{a(HbO_2)}$$

and delaying this expression by τ_{aB} minutes corresponding to realizing the alveolar-arterial concentration at the brain site we have the bracketed term [A].

Since we do not need to delay the venous blood-brain O_2 concentration Equation 4.3,

$$C_{vB(O_2)} = \left(\frac{\alpha O_2}{\alpha B(O_2)}\right) C_{B(O_2)} + C_{vB(HbO_2)} ,$$

is substituted. This substitution corresponds to bracketed term [B]. All other terms remain the same in forming the differential-difference equation.

VI. BIBLIOGRAPHY

1. Bellville, J.W., G. Fleischli, and J.G. Defares, A method of studying regulation of respiration - the response to sinusoidally varying CO_2 inhalation. Computers and Biomedical Research 2:pp. 329-349, 1969.

2. Fry, D.L., A preliminary lung model for simulating the aerodynamics of the bronchial tree. Computers and Biomedical Research 2:pp. 111-134, 1968.

3. Mead, J., Contribution of compliance of airways to frequency-dependent behavior of lungs. Journal of Applied Physiology 25: No. 5, pp. 670-673, 1969.

4. Saidel, G.M., T.C. Militano, and E.H. Chester, Mass - balance model of pulmonary oxygen transport. IEEE Transactions on Biomedical Engineering, BME-19:pp. 205-213, 1972.

5. Yamamoto, W. and T. Hori, Phasic air movement model of respiratory regulation of carbon dioxide balance. Computers and Biomedical Research 3:pp. 699-717, 1971.

6. Pierce, A.K., D. Luterman, J. Loudermilk, G. Blomquist, and R.L. Johnson Jr., Exercise ventilation patterns in normal subjects and patients with airway obstruction. Journal of Applied Physiology 25: No. 3, pp. 249-254, 1968.

7. Milhorn, H.T., Jr., and D.R. Brown, Steady-state simulation of the human respiratory system. Computers and Biomedical Research 3:pp. 604-619, 1971.

8. Grodins, F.S., J. Buell, and A.J. Bart, Mathematical analysis and digital simulation of the respiratory control system. Journal of Applied Physiology 22: No. 3, pp. 260-276, 1967.

9. Milhorn, H.T., Jr. and P.E. Pulley, Jr., A theoretical study of pulmonary capillary gas exchange and venous admixture. Biophysical Journal 8:pp. 337-357, 1968.

10. Hilberman, M., R.W. Stacey, and R.M. Peters, A phase method of calculating respiratory mechanics using a digital computer. Journal of Applied Physiology 32: No. 4, pp. 535-541, 1972.

11. Hermansen, L. and J. Osnes, Blood and muscle pH after maximal exercise in man. Journal of Applied Physiology 32: No. 3 pp. 304-308, 1972.

12. Yamamoto, W.S., and W.F. Raub, Models of regulation of external respiration in mammals. Problems and promises. Computers and Biomedical Research 1:pp. 95-104, 1967.

NAL PAGE IS
POOR QUALITY

13. Albergoni, V., C. Cobelli, and G. Torresin, Interaction model between the circulatory and respiratory systems. IEEE Transactions on Biomedical Engineering, BME - 19: pp. 108-113, 1972.

14. Guyton, A.C., T.G. Coleman, and H.J. Granger, Circulation: Overall view. Annual Review of Physiology, Vol. 34, pp. 13-46, 1972.

15. Weissman, M.H., Respiratory-thermal modeling. Research Report-Biomedical Research Division, Environmental Physiology Branch, NASA-MSC, 1971.

16. Milhorn, H.T., Jr., The Application of Control Theory to Physiological Systems. Chapter 15. W.B. Saunders Company, Philadelphia, Pa., 1966.

17. Guyton, A.C., Textbook of Medical Physiology. Chapter 4, Chapter 39. W.B. Saunders Company, Philadelphia, Pa., 1966.

18. Mountcastle, V.B., Editor, Medical Physiology, 12th Edition, Vol.1, Chapter 40, C.V. Mosby Company, Saint Louis, Missouri, 1968.

19. Bradley, R.D., G.T. Spencer, and S.J.G. Semple, Rate of change of CSF P_{CO_2} and HCO_3^- in acid-base disturbances in man. Symposium on Cerebrospinal Fluid and the Regulation of Ventilation. Editors, Brooks, C. McC., F.F. Kao, and B.B. Loyd. F.A. David Company, Philadelphia, Pa., 1965.

ASD
APOLLO SYSTEMS DEPARTMENT
GENERAL ELECTRIC
HOUSTON, TEXAS

TECHNICAL INFORMATION RELEASE

TIR 741-MED-3030

FROM	TO
R. C. Croston, Ph.D.	J. A. Rummel, Ph.D.

DATE	WORK ORDER REF:	WORK STATEMENT PARA:	REFERENCE:
5/22/73	MA-252T	NAS9-12932	

SUBJECT

Respiratory Control System Simulation Study Report

Attached is a study report which was submitted to G.E. by Dr. R. R. Gallagher in partial fulfillment of his subcontract.

R. C. Croston
R. C. Croston, Ph.D.

Attachment
/db

CONCURRENCES

Counterpart:

Medical Projects Unit Manager Dr. C. Fulcher

Engrg. & Advanced Programs Subsection Mgr. W. J. Beittel 5/24/73

DISTRIBUTION GE/AGS: Central Product File

ASD 4028

STUDY REPORT

GENERAL ELECTRIC COMPANY
CONTRACT NUMBER
036-E31001-M5906

RESPIRATORY CONTROL SYSTEM SIMULATION

by

R. R. GALLAGHER, Ph.D.
DEPARTMENT OF ELECTRICAL ENGINEERING
KANSAS STATE UNIVERSITY
MANHATTAN, KANSAS

RESPIRATORY CONTROL SYSTEM SIMULATION

SUMMARIZATION OF THE MAJOR FEATURES OF MILHORN'S RESPIRATORY SYSTEM MODELS

TABLE OF CONTENTS

		Page
I.	INTRODUCTION	1
II.	MODEL VARIATIONS AND SIGNIFICANT FEATURES	2
	A. Milhorn's Basic Compartmental Respiratory Model	2
	B. A Model Illustrating Static, Dynamic, Mechanical, and Cyclic Phenomena	7
	C. A Model Emphasizing Venous Admixture	9
	D. A Model Maximizing Steady-State Information	11
	E. A Model Evaluating Transient Ventilatory Responses	17
	F. A Model Evaluating CSF Subsystem Involvement in Ventilation	21
III.	CONCLUSIONS	25
IV.	BIBLIOGRAPHY	29

I. INTRODUCTION

A group of respiratory system models which is of interest from the viewpoint of evaluation for their application within the goals of the NASA project is that of Milhorn and models related to Milhorn's research. In a previous Study Report a modified version of Grodins' model was investigated illustrating its response to particular parameter variations and various work load conditions. Most of Milhorn's models, although developed under different experimental conditions and for varying motivations, contain features that are similar to Grodins' work. For this reason it seems appropriate to discuss the major features of Milhorn's models and perhaps suggest special modifications for Grodins' model which might utilize these features. Therefore, the major thrust of the following material will be to summarize the theory and assumptions of Milhorn's models keeping in mind the conditions for which they are applicable and to describe potential applications of Milhorn's work to improve the existing Grodins' program.

II. MODEL VARIATIONS AND SIGNIFICANT FEATURES

Within the listed references (1-6) Milhorn et al. have published several model variations each of which was developed for a particular experimental arrangement or environmental condition. Instead of correlating the results of the referenced research and confusing the various system terminologies it will be more instructive to independently deal with each research effort. This approach will be more justifiable as the constraints and experimental developments are enumerated. In addition, the models will be discussed in a chronological manner.

A. Milhorn's Basic Compartmental Respiratory Model

Many of the assumptions and mathematical formulations of the compartmental model of the respiratory system that appears in Milhorn's text (1) are also used in his more recent work. Here it was assumed that the chemical factors that control alveolar ventilation are CO_2 and O_2 with the effects of the H+ stimulus related to P_{CO_2} by a linear relationship.

The basic assumptions can be summarized as follows (1):

1. The circulatory system containing no mixing phenomena but with regionally associated time constants interconnects the lung, brain, and body compartments.
2. Dissociation curves for O_2 and CO_2 are equal for arterial and venous blood.
3. Brain blood flow is dependent upon cerebral-arterial P_{CO_2} and P_{O_2} relationships.

4. Arterial P_{O_2} is linearly related to alveolar P_{O_2}.
5. Venous P_{O_2} is equal to tissue P_{O_2}.
6. Arterial P_{CO_2} is equal to alveolar P_{CO_2}.
7. Venous P_{CO_2} is equal to tissue P_{CO_2}.
8. Linear relationship between P_{CO_2} and P_{O_2} which controls minute alveolar ventilation.
9. Respiratory quotient equals unity.
10. Metabolism and cardiac output are constant.
11. System simulates acid-base balance disturbances.
12. H+ concentration is a function of P_{CO_2}.
13. Carotid and aortic bodies are sensitive to O_2.

The model comprizes a controlled system and a controlling system. External disturbances in either the form of CO_2 excess, O_2 deficiency, or both are considered inputs into the controlled system. The regulation aspects of the system are accomplished via ventilatory and circulatory parameters. $P_{a_{CO_2}}$, $P_{a_{O_2}}$, and H+ are monitored outputs of the controlled segments of the system. These variables are weighted giving a value for alveolar ventilation ($\mathring{V}_A$). $\mathring{V}_A$ is then considered a second input to the controlled system along with the environmental disturbances, thus completing the negative feedback formulation.

Input-output block diagrams are utilized in the development of the equations which quantitatively describe the system. There is one such diagram for each of the following components.

1. Ventilatory controller
2. Lung compartment

3. Brain compartment
4. Body compartment
5. Venous mixing
6. Cerebral circulation
7. Comparator for cardiac output, cerebral blood flow, and body tissue blood flow
8. Transportation lags in circulatory system
9. Overall compartmental model.

The expressions for the time rate of change of CO_2 and O_2 volumes in the brain, body, and lung compartments are developed. These six equations contain twenty-eight variables. Using the previously listed assumptions, mathematical relationships are derived such that eight variables are used in eight differential equations describing the normal human respiratory control system. The eight variables are

1. $\dot{Q}_B$ - cerebral blood flow (liters/min)
2. $\dot{V}_A$ - minute alveolar ventilation (liters/min)
3. $C_{B_{CO_2}}$ - brain tissue CO_2 concentration (vol fraction)
4. $C_{T_{CO_2}}$ - body tissue CO_2 concentration (vol fraction)
5. $C_{A_{CO_2}}$ - alveolar CO_2 concentration (vol fraction)
6. $C_{B_{O_2}}$ - brain tissue O_2 concentration (vol fraction)
7. $C_{T_{O_2}}$ - body tissue O_2 concentration (vol fraction)
8. $C_{A_{O_2}}$ - alveolar O_2 concentration (vol fraction).

Six of these eight equations describe the time rate of change in the variables $C_{B_{CO_2}}$, $C_{T_{CO_2}}$, $C_{A_{CO_2}}$, $C_{B_{O_2}}$, $C_{T_{O_2}}$, and $C_{A_{O_2}}$.

Another equation is called the cerebral circulatory controller equation and describes the time rate of change in brain blood flow. The final equation, the ventilatory controller equation, describes the alveolar ventilation in terms of various weightings on the controlling functions of the medullary respiratory center, carotid and aortic bodies, and the mechanical portion of the lungs. In effect, this latter equation, described as

$$\mathring{V}_A = a(C_{B_{CO_2}})^{\frac{1}{k_2}} - b + d\,(m - k_5\, P_B C_{A\beta_{O_2}})^n \geq 0 \qquad (1)$$

provides the simulation with the necessary feedback mechanism.

As was observed with Grodins' simulation the ventilation controller equation is a very sensitive feature of the entire system. Ventilation is controlled by a different set of variables in Milhorn's model than in Grodins' model. However, the major difference evolves from the fact that Milhorn's model simulates the ventilation as a sum of the effects of P_{CO_2}, H+, and P_{O_2} with the final programmed equation having the effects of the H+ concentration embedded in the empirical constants of the equation. To evaluate and compare the physiological responses of Grodins' simulation for a ventilatory equation like Milhorn's equation and Grodins' equation one must be restricted to the resting state and normal sea level conditions. Increase in ventilation due to exercise would be determined only by the alteration in metabolic rates and would not involve any neurological control as does the exercise controller equation of the present Grodins' model.

Sufficient experimental data was not available at the time; therefore, a description of the cerebral blood flow in Milhorn's model was based upon several assumptions. The first assumption is that a three-fold increase in oxygen concentration in air doesn't alter the cerebral blood flow. A decrease in oxygen concentration to 10% increases the cerebral blood flow by 35%. For a further decrease to 5% O_2 was assumed to double the normal cerebral blood flow. An empirical relationship describing the effects of P_{CO_2} upon cerebral blood flow (developed by Kety and Schmidt (7)) was utilized. Combining the effects of CO_2, O_2, and normal cerebral blood flow, the equation is written with the empirical constants as

$$\mathring{Q}_B = k_o\left[\left(\sum_{i=1}^{5} k_i \left(C_{A_{\phi_{CO_2}}}\right)^i\right) + k_6 \left(k_7 - \frac{1}{k_8} C_{A_{\phi_{O_2}}}\right)^S\right] + \mathring{Q}_{B_N} . \qquad (2)$$

Considerable emphasis was placed upon the steady-state analysis of Milhorn's model. The only transient analyses performed with model were on- and off- transient responses for alveolar ventilation as the system was subjected to instantaneous changes in the levels of CO_2 and O_2 concentrations at the inputs to the lung compartment. Probably the most beneficial result of the forementioned research was the realization that much more experimental and simulation research was needed to fully describe the respiratory control system and realize a simulation's potentials. This includes the investigation of cerebrospinal fluid influence, variations in cardiac output and circulation time delays, and the relationships between alveolar and end- alveolar capillary P_{O_2} and P_{CO_2}.

B. A Model Illustrating Static, Dynamic, Mechanical, and Cyclic Phenomena

In a progress report concerning a conceptual view of a digital computer model of the human respiratory system (2) Milhorn discusses both the static and dynamic features of the model and builds upon the previous work. Within the static component the controlled system equations describe the alveolar tension of CO_2 and O_2. Both tensions are described as functions of their respective inspired gas tensions, production and consumption rates of CO_2 and O_2 respectively, the respiratory quotient, and the barometric and water vapor pressure. The two controller equations considered were those of Gray,

$$\mathring{V}_A = aP_{A_{CO_2}} - b + c\,(d - P_{A_{O_2}})^{n} \geq 0, \tag{3}$$

and Lloyd and Cunningham,

$$\mathring{V} = D\,(P_{A_{CO_2}} - B)\left[1 + A\,/\,(P_{A_{O_2}} - C)\right]; \quad P_{A_{CO_2}} \geq 40 \text{ mmHg}. \tag{4}$$

As described by Milhorn,

$$\mathring{V}_A = \mathring{V} - fV_D \tag{5}$$

where fV_D corresponds to minute dead space. All parameters described in this paragraph can be altered and appropriate responses observed.

The dynamics of this model centered around a restructuring of the ventilatory controller equation. Initially, experimental evidence indicated that ventilation response could be simulated by weighting the influence of the H+ at 55% and the influence of CO_2 at 45%. This weighting scheme was further refined by experiments from Lambertsen's laboratory

which associated special weightings of the H+ contribution from the peripheral sensors, a central receptor in the brain, and a central receptor in the cerebrospinal fluid. The equation illustrating this weighting is

$$\dot{V} = 0.12\ \dot{V}(C_{PS_{H+}}) + 0.44\ \dot{V}(C_{B_{H+}}) + 0.44\ \dot{V}(C_{CSF_{H+}}). \qquad (6)$$

The contribution from the O_2 sensing mechanism evolved from Equation 4.

Exercise alters the gaseous exchange mechanism in the lungs. The effective area of the pulmonary membrane is increased by the change in blood flow. Milhorn has investigated this area change by utilizing the equation,

$$A = A_o + \frac{1}{k_1 + k_2}\left(k_1 \frac{V_L}{V_{L_o}} + k_2 \frac{\dot{Q}_c}{\dot{Q}_{c_o}}\right), \qquad (7)$$

having the empirical constants, k_1 and k_2, V_L being the lung volume, $\dot{Q}_c$ the pulmonary blood flow, and the subscript O referring to normal values. No evaluation statements were made with regard to the simulation of Equation 7.

Milhorn suggests an analog flow diagram representing the mechanical dynamics of the system. No simulation results were available for evaluation of this model. Although the simulation was not detailed for the exercise phenomena a cyclic model was proposed in order to describe the possibility of the peripheral chemoreceptors being unidirectional rate sensitive. It was felt that the tie between the unidirectional rate sensitive detectors and the fluctuating arterial blood H+, CO_2, and O_2 concentrations could be better defined.

However, other sources do not emphasize these fluctuations; therefore, this refinement might not be appropriate with relationship to other system components. In any event, the cyclic pulmonary system is described by varying passageway resistances, anatomical and effective deadspaces, a-v shunts for the blood, and the feature of venous admixture.

In this reference Milhorn also emphasizes the importance of the controller equation. The interrelationships between the cardiovascular and respiratory systems were experimentally investigated with the goal being to expand the range of Lloyd and Cunningham's controller equation range for $P_{A_{CO_2}}$. The experimental apparatus of Holloman, et al. (8) was utilized to establish an empirical model for $P_{A_{CO_2}} < 40$ mm Hg. Further results for $P_{A_{CO_2}} < 40$ mm Hg was to be presented at a later date.

C. A Model Emphasizing Venous Admixture

Milhorn and Pulley (3) have published a theoretical study which is believed to be of value in the evaluation of diseased states of the respiratory system, i.e. emphysema, pulmonary congestion, or any condition that would affect the pulmonary membrane's functions. One feature of this model is its description of the capillary shunts and the corresponding description of the blood gas tensions (venous admixture case) at the mixing point of the end alveolar capillary blood and the arterial blood (through the bypass).

ORIGINAL PAGE IS
OF POOR QUALITY

This study was not intended to be a complete simulation of the respiratory system, but instead, a component was developed which would be incorporated in a more complete computer simulation. The development of the pulmonary gas exchange equations evolved from a description of the rate of flow of gas across the surface area of n parallel cylinders each representing a capillary segment. Here, the total number of capillaries is defined as

$$n = (\mathring{Q} - \mathring{Q}_s)/f \tag{8}$$

where $\mathring{Q}$ = cardiac output (lit/min)

$\mathring{Q}_s$ = pulmonary shunt flow (lit/min)

and f = blood flow through a single capillary (lit/min). Further development yielded an expression for capillary gas exchange as a function of gas tensions. Capillary gradients were then developed dependent upon surface area, membrane thickness, cardiac output, or all possible combinations of these variables.

As stated previously, one of the salient features of this simulation was that of the venous admixture phenomenon. Under normal venous and alveolar gas tensions it was shown that approximately 1.3 per cent of the total cardiac output was shunted past the capillary system. From this fact the simulation of the admixture phenomenon can be detailed.

Although the simulation is adaptable to the study of inert gases, i.e. N_2 and He_2, the immediate concern is related to extractable features associated with O_2 and CO_2. Interrelationships between CO_2 and O_2, the Haldane and Bohr

effects, complicate the development. Considering the compartmentalization of Grodins' model and the mathematical development associated with the capillary gas exchange mechanism of the model discussed here it is doubtful that any of this model's features can be directly applied to Grodins' system. The features of this model would be of value if a refinement of Grodins' model included a more detailed description of the gas exchange mechanism associated with the lung compartment. Another aspect of the model by Milhorn and Pulley (3) is that it illustrates no simple adaptation to the study of exercise and its control of ventilation. The most important advantage in the use of this model would be the component of the simulation associated with the admixture phenomenon as the fractional gaseous concentrations of the environment were altered.

D. A Model Maximizing Steady-State Information

In the steady-state simulation of the human respiratory system by Milhorn and Brown (4) emphasis is directed toward justifying that ventilation be described by a function of the receptor sites' stimuli as CO_2 and O_2 levels are altered. This is extremely important if faithful reproduction of transient responses are to be obtained. Since receptor site locations, numbers of sites, and the general nature of the responses at these sites are ill-defined this research emphasizes the steady-state respiratory system and attempts to more fully utilize the large quantities of information from the steady-state.

The system is divided into a controlled system component and a controlling system component. As described in some of Milhorn's previous work (1) the controlled system has alveolar ventilation, $\dot{V}_A$, as an input calculated from the controlled system with alveolar O_2 tension and alveolar CO_2 tension as outputs. These two outputs are treated as inputs to the controlling system, thus completing the feedback system.

This particular model by Milhorn is more compatible with Grodins' model than the one previously described (1) in that there are system descriptions that might be readily adaptable to alterations in Grodins' model. Alveolar O_2 and CO_2 tensions are described by two equations which contain variables which are closely associated with those of Grodins' program. These equations are repeated here, described in terms of inspired O_2, O_2 consumption, alveolar ventilation, respiratory quotient, water vapor pressure, and barometric pressure.

$$P_{AO_2} = P_{IO_2} - \frac{\dot{V}_{O_2}}{\dot{V}_A}\left[P_B - P_{H_2O} + P_{IO_2}(1-R)\right] \tag{9}$$

$$P_{ACO_2} = P_{ICO_2} + \frac{\dot{V}_{CO_2}}{\dot{V}_A}\left[P_B - P_{H_2O} + P_{ICO_2}\left(\frac{1}{R} - 1\right)\right] \tag{10}$$

Plots of these equations are given for various values of P_{IO_2} and P_{ICO_2} with $2.5 \leq \dot{V}_A \leq 100$ liters/min and constant O_2 consumption. When P_{IO_2} is varied P_{AO_2} is low for all values of P_{IO_2} if $\dot{V}_A$ is low. As $\dot{V}_A$ is increased a steady-state value of P_{AO_2} is assumed which approximates P_{IO_2}

for $\dot{V}_A > 60$ liters/min. The opposite relationships are established between $\dot{V}_A$, P_{ICO_2}, and $P_{A_{CO_2}}$.

When Equations 9 and 10 are plotted for various levels of O_2 consumption ($\dot{V}_{O_2}$) with $2.5 \leq \dot{V}_A \leq 100$ liters/min, $P_{A_{O_2}}$ and $P_{A_{CO_2}}$ vary in the following manner. As expected, for all levels of O_2 consumption, if $\dot{V}_A$ is low $P_{A_{O_2}}$ is low and $P_{A_{CO_2}}$ is high. As $\dot{V}_A$ is increased beyond approximately 60 liters/min a steady-state value for $P_{A_{O_2}}$ (140 mm Hg) is assumed irregardless of the level of O_2 consumption. Likewise, as $\dot{V}_A$ is increased the value of $P_{A_{CO_2}}$ decreases rapidly and assumes steady-state values below 10 mm Hg for $\dot{V}_A > 60$ liters/min.

The graphical dependence of $P_{A_{O_2}}$ and $P_{A_{CO_2}}$ upon the barometric pressure, P_B, is shown for steady-state values of $\dot{V}_A$, $2.5 \leq \dot{V}_A \leq 100$ liters/min. $P_{A_{O_2}}$ and $P_{A_{CO_2}}$ are described by a family of curves for variations in P_B ($300 \leq P_B \leq 1500$ mm Hg) which are similar to the family of curves for $\dot{V}_{O_2}$ variations. For these plots P_{IO_2} and P_{ICO_2} were held constant at 149.3 and 0.3 mm Hg, respectively.

The relationships for $P_{A_{O_2}}$ and $P_{A_{CO_2}}$ with $\dot{V}_A$ for different values of the respiratory quotient (R) are plotted. For low values of $\dot{V}_A$, $P_{A_{O_2}}$ is low and $P_{A_{CO_2}}$ is high independent of the specific value of R. However, as $\dot{V}_A$ is increased, $P_{A_{O_2}}$ is increased and approaches a steady-state value of 140 mm Hg for $\dot{V}_A \geq 40$ liters/min. In a similar manner, for all values of R, $P_{A_{CO_2}}$ is decreased as $\dot{V}_A$ increases.

Although perhaps difficult to justify quantitatively, the above results for $P_{A_{O_2}}$ and $P_{A_{CO_2}}$ versus $\mathring{V}_A$ as the different variables in Equations 9 and 10 are independently altered are physiologically justifiable in a qualitative sense.

The major thrust of Milhorn and Brown's work with the controlling component of the model is in the comparison of Gray's classical equation and Lloyd and Cunningham's equation (4). Gray's controller equation is very similar to Equation 1. With the empirical constants evaluated it is written as

$$\mathring{V}_A = 1.8P_{A_{CO_2}} - 67.5 + 4.24(10)^{-6}\,(104 - P_{A_{O_2}})^{4.9} \geq 0 \qquad (11)$$

Equation 11 is developed using assumptions that are not justifiable. The fact that CO_2 and O_2 effects are not just additive as illustrated in Equation 11 has been shown. Also, experimental data was not available for the entire range of ventilation even though the equation was developed to simulate the entire range of $\mathring{V}_A$.

Describing CO_2 and O_2 effects upon ventilation as multiplicative as well as additive is one of the major contributions of Lloyd and Cunningham's work. Experimental data shows that the relationship between ventilation and $P_{A_{CO_2}}$ can be described by a straight line with a slope dependent upon $P_{A_{O_2}}$. This slope was then described as a hyperbolic function of $P_{A_{O_2}}$. Thus the interdependence of these variables are more involved than in an additive arrangement. The equation that evolved with values for the empirical constants is given by

$$\mathring{V} = 2(P_{A_{CO_2}} - 37.24)\ (1 + 13.6/(P_{A_{O_2}} - 25)) \geq 0 \qquad (12)$$

for $P_{A_{CO_2}} \geq 37.24$.

The relationship between $\mathring{V}$ and $\mathring{V}_A$ is developed as follows.

$$\mathring{V}_A = \mathring{V} - f\ V_D \qquad (13)$$

where V_D = dead space

and $f = \mathring{V}/V_T$ = respiratory frequency.

Dead space is calculated from an empirical relationship.

$$V_D = 0.0785V_T + 0.1107 \qquad (14)$$

where $V_T = 0.134\ \mathring{V}^{0.7}$ = tidal volume.

In addition to the equation that describes the relationship between alveolar ventilation and minute volume other important qualities which distinguish Lloyd and Cunningham's equation from Gray's equation are listed here.

1. As mentioned previously, CO_2 and O_2 effects are both multiplicative and additive.
2. It is not extended beyond known experimental data (valid only for $P_{A_{CO_2}} \geq 37.24$ mm Hg).
3. Multiplicative effects produce a more significant response under the conditions of low O_2 - high CO_2 levels.

Several three-dimensional plots are presented by Milhorn and Brown illustrating the comparison of Gray's controller equation and Lloyd and Cunningham's control equation. The following combinations of variables were considered.

Case A. P_{IO_2}, P_{ICO_2}, $\mathring{V}_A$

Case B. P_{IO_2}, P_{ICO_2}, V_T

Case C. P_{IO_2}, P_{ICO_2}, f

Case D. $P_{A_{O_2}}$, $P_{A_{CO_2}}$, $\mathring{V}_A$

Case E. $P_{A_{O_2}}$, $P_{A_{CO_2}}$, V_T

Case F. $P_{A_{O_2}}$, $P_{A_{CO_2}}$, f

A very brief explanation of each case is instructive.

Case A: Peak values for $\mathring{V}_A$ occurred for low P_{IO_2} and high P_{ICO_2} with Lloyd and Cunningham's equation giving the larger values. Lloyd and Cunningham's results were undefined when P_{ICO_2} and P_{IO_2} were both low.

Case B: Peak values for V_T occurred for low P_{IO_2} and high P_{ICO_2} with Lloyd and Cunningham's equation giving the larger values. Lloyd and Cunningham's results were undefined when P_{ICO_2} and P_{IO_2} were both low.

Case C: The highest frequency (breaths/min) occurred for low P_{IO_2} and high P_{ICO_2}. Lloyd and Cunningham's results were undefined when P_{IO_2} and P_{ICO_2} were both low.

Case D: Peak values for $\mathring{V}_A$ occurred for low $P_{A_{O_2}}$ and high $P_{A_{CO_2}}$ with Lloyd and Cunningham's equation giving the larger values. Lloyd and Cunningham's results illustrate an undefined region for $P_{A_{CO_2}} \leq$ 37.24 mm Hg.

Case E: Very similar results were obtained for V_T with both equations for $P_{A_{CO_2}} \geq 37.24$ mm Hg. Lloyd and Cunningham's equation did give larger values for V_T in the extreme cases corresponding to low $P_{A_{O_2}}$ and high $P_{A_{CO_2}}$.

Case F: Very similar results were obtained for f with both equations for $P_{A_{CO_2}} \geq 37.24$ mm Hg. Once again Lloyd and Cunningham's results were undefined for $P_{A_{CO_2}} \leq 37.24$ mm Hg.

A suggestion for implementation of Lloyd and Cunningham's equation into Grodins' model will be presented in a later section. Of course, this would have to be expanded to include the exercise phenomenon since this equation doesn't involve all of the physiological variables associated with exercise.

E. A Model Evaluating Transient Ventilatory Responses

Reynolds, et al.(5) developed an experimental technique for evaluating the transient ventilatory response to various mixtures of CO_2 in air. The recorded outputs for the system included respiratory frequency (f), tidal volume (V_T), alveolar oxygen tension ($P_{A_{O_2}}$), and alveolar carbon dioxide tension ($P_{A_{CO_2}}$). Minute ventilation in liters/min ($\mathring{V}$) was computed as a function of tidal volume and frequency.

Because of insufficient technology to adequately measure the cyclic phenemona associated with ventilatory transients

at the time of these experiments, the time constants associated with the respiratory variables were not well documented. Also the correlation between the strength of the stimuli and the magnitudes of the responses were uncharted. Therefore, the basic purpose of these experiments was to accurately record f, V_T, $P_{A_{O_2}}$, $P_{A_{CO_2}}$, and V for different step inputs of CO_2 - air mixtures in order to better define the transient response and justify the respiratory control system models in existence.

The experimental arrangement will not be completely discussed here. It should be mentioned that the experiments consisted of a 20-minute prestimulus period, a 25-minute stimulus period, and followed by an off-transient period of 20 minutes. The stimuli were 3, 5, 6, or 7% CO_2 - air mixtures.

A trigger circuit detected the flow signal. The gases were continuously sampled and analyzed by a Beckman LB-1 infrared CO_2 analyzer and a Thermox O_2 analyzer. The expiratory flow signals, O_2 tension, CO_2 tension, and the output of the trigger circuit were all recorded on magnetic tape. After the experiments the results were analyzed yielding the respiratory frequency, minute ventilation, and alveolar concentrations.

A summary of the results is directed toward the categories of tidal volume, respiratory frequency, minute ventilation, alveolar CO_2, alveolar O_2, transient half-times, and the subjective effects for the subjects.

1. Tidal volume: Rapid initial transient with a more rapid off-transient with all stimuli. No overshoot in either on- or off-transient.
2. Respiratory frequency: Slower on- and off-transient than with tidal volume. These data can be used in defining a better frequency evaluation in Grodins' model.
3. Minute ventilation: Smooth response for both on- and off-transient with no overshoots. Steady-state values are reached in a shorter period of time than that for the steady-state values of frequency. The opposite is true in comparison to the steady-state values of tidal volume.
4. Alveolar CO_2: Very rapid on-transients and off-transients with an overshoot occurring in the off-transient for all stimuli cases. This is in agreement with simulations using Grodins' program. Lower CO_2 levels also caused overshoots in the on-transient indicating that the stimuli were not of sufficient strength to ventilate the overload of CO_2.
5. Alveolar O_2: No overshoots were observed in relatively rapid on-transients. The half-times for the off-transients were longer than for the on-transients. There were overshoots in the off-transients for the higher concentrations of CO_2 input.

6. Transient half-times: On-transient half-times increased for f, $\dot{V}$, and V_T for increasing levels of CO_2. On-transient half-times for $P_{A_{O_2}}$ decreased as the CO_2 level was increased. On-transient half-times for $P_{A_{CO_2}}$ remained fairly constant for the various stimuli levels. In the off-transient V_T and V half-times decreased for increasing CO_2 levels. Off-transient P_{O_2} half-times increased for increasing CO_2 levels. Once again the P_{CO_2} half-times remained constant for increasing stimuli CO_2 levels. Generally speaking, the off-transients' half-times were shorter for each variable than the corresponding on-transients except for $P_{A_{O_2}}$. The respiratory frequency seemed to have the most sluggish response of all the variables.

   Average response plots of V_T, f, and $\dot{V}$ were given. The $\dot{V}$ versus time, t, plots for the various levels of CO_2 stimuli correspond to the results of similar simulations with Grodins' model although the exact inspired fractional concentrations of gases were not used.

7. Subjective effects: Subjective effects included dyspnea, warmth, dizziness, headache, and visual disturbances all with varying degrees of severity and at different levels

of stimuli. All subjects returned to a "normal" feeling after removal of the stimuli.

The above summaries of the responses of the variables to the CO_2 stimuli illustrate that much information can be gained from studying such transient responses. These types of relationships are particularly important when subjects are exposed to rapid changes in the gaseous mixtures of the air. Certainly this type of experimental evidence is needed to establish a more physiologically sound model.

F. A Model Evaluating CSF Subsystem Involvement in Ventilation

The H^+ concentration is a variable that is well established as a contributor to the control of ventilation. Grodins' model uses special weightings of the H^+ concentrations in the CSF compartment, the venous blood of the brain, and at the carotid bodies' site to control ventilation. With Grodins' model any combination of weightings for the $C_{CSF(H^+)}$ or $C_{a(H^+)}(t-\tau_{aB})$ can be utilized. Thus the research of Milhorn et al. (6) which attempts to establish an appropriate detecting site within the brain structure can be used to justify the weightings in Grodins' model. The primary purpose of this model was to establish a satisfactory transient response in ventilation which would apply if the CO_2 detection site was assumed to be on either side of the central receptors.

The controlled system aspect of the model was based upon the previous developments of Milhorn et al. (1) and Grodins

et al. (9) with the compartments being the brain, lungs, cerebrospinal fluid, tissue, and peripheral sensor (playing the role of the carotid bodies). The mathematical development is essentially the same as for Grodins' model except for the peripheral sensor. Since this is the most characteristic aspect of the model and the one which distinguishes the model from all others the equation which defines the CO_2 tension at the proposed sensor site is repeated here.

$$P_{CS_{CO_2}} = P_{B_{CO_2}} + (P_{CSF_{CO_2}} - P_{B_{CO_2}}) \exp\left[-X\sqrt{\frac{\mathring{Q}_{CS}\, S}{D/760}}\right] \qquad (15)$$

where

$P_{B_{CO_2}}$ = Deep brain tissue CO_2 tension,

$P_{CSF_{CO_2}}$ = Cerebrospinal fluid CO_2 tension,

$\mathring{Q}_{CS}$ = Average blood flow at sensor site,

S = CO_2 dissociation curve's slope,

D = Brain tissue CO_2 diffusion coefficient, and

X = Depth of sensor below medulla's surface.

With this model ventilation is controlled by peripheral sensor H^+ concentration ($C_{PS_{H^+}}$) and central sensor H^+ concentration ($C_{CS_{H^+}}$). In summary, $C_{CS_{H^+}}$ is given by

$$C_{CS_{H^+}} = \exp(-2.303\ pH_{CS}) \qquad (16)$$

where

$$pH_{CS} = 6.11 + \log\left(\frac{C_{CS_{CO_2}} - (\alpha_{CO_2}/760)P_{CS_{CO_2}}}{(\alpha_{CO_2}/760)\ P_{CS_{CO_2}}}\right) \qquad (17)$$

ORIGINAL PAGE IS
OF POOR QUALITY

with α_{CO_2} = Solubility of CO_2 in brain compartment
and $C_{CS_{CO_2}}$ = Concentration of CO_2 at sensor site. (6)

Pulmonary ventilation ($\mathring{V}$) is the sum of two signals. One signal involves the functional dependence upon $C_{CS_{H+}}$ and the other signal is a function of $C_{PS_{H+}}$. The weighting is distributed such that for a given weighting of the central sensors the peripheral sensors' signal has a weighting of 100% minus the central sensors' weighting. Tidal volume (V_T) is then generated from a functional relationship of $\mathring{V}$. In a like manner dead space volume (V_D) is generated from a linear relationship with V_T. Respiratory frequency (f) is the ratio $\mathring{V}/V_T$ which is then multiplied by V_D to yield minute dead space (fV_D). The difference between minute dead space and pulmonary ventilation is the alveolar ventilation ($\mathring{V}_A$). Alveolar ventilation is then used as an input to the controlled system.

The unique contribution of this research is associated with the determination of the sensor depth, X, which appears in Equation 15. A simulation was run for an inspired gaseous concentration of 7% CO_2 with varying values for X. The range of sensor depth tested was $0 \leq X \leq 1000\mu$ with the ventilation transient responding more rapidly for the sensor sites' greater depths. A value of 280μ was then used for further evaluation of the model. Utilizing a CO_2 tension gradient this depth corresponds to a position which is 77% of the distance between cerebrospinal fluid P_{CO_2} and deep brain tissue P_{CO_2}.

Responses for three different controller equations were evaluated. They were the linear controller equation of Milhorn (1),

$$\mathring{V}_A = a_1 P_{B_{CO_2}} - b_1 , \tag{18}$$

another controller equation developed by Grodins (9),

$$\mathring{V}_A = a_2 C_{CSF_{H+}} + b_2 C_{a_{H+}} - C_1 , \tag{19}$$

and the proposed controller equation of Milhorn et al. (6),

$$\mathring{V} \doteq wf_1 (C_{CS_{H+}}) + (1-W) f_2 (C_{PS_{H+}}). \tag{20}$$

Although no experimental data were shown the study indicates that the results of Equation 19 varied more from the normal expected response than the results of Equations 18 and 20. When these three controller equations were compared for perfusion of the medulla surface with a mock cerebrospinal fluid CO_2 tension of 71 mm Hg Equation 20 was indicated as giving the best representation of tidal volume (V_T) response. Several other reported research efforts by Milhorn et al. (6) supported the simulation results for the CSF perfusion studies, the fact that CSF ventilatory control shouldn't be based entirely upon CO_2 levels or H+ concentrations, and the fact that there is in all probability an optimum sensor depth.

C-3

III. CONCLUSIONS

A review of respiratory control system models developed by Milhorn and his associates has been presented. Chronologically speaking, the models that were discussed encompass those developments associated with the steady-state models published in the mid-1960's to the more recent investigation concerning a more detailed description of the CSF involvement with the control of respiration. The later developments also attempt to simulate transient responses as well as steady-state responses.

The model utilized in the evaluation of the CSF subsystem's function in the control of respiration most closely parallels the model developed by Grodins. (6,9). As was suggested in the Introduction one of the goals of this Study Report is to propose modifications for Grodins' model which stem from Milhorn's work. Most of the suggested modifications involve some aspect of the controller equation. Any of the suggested modifications will not involve the exercise simulation subroutines that presently exist in Grodins' modified program. The control of respiration and the system's variable responses that are related to exercise will need to be adjusted so that any new modifications are made compatible with existing exercise controller functions.

One form of a controller equation that would be relatively easy to incorporate into Grodins' model is the one suggested by Milhorn with the special weightings indicated by Lambertsen.

(2) This equation is defined as

$$\mathring{V} = 0.12\ \mathring{V}\ (C_{PS_{H+}}) + 0.44\ \mathring{V}\ (C_{B_{H+}}) + 0.44\ \mathring{V}\ (C_{CSF_{H+}}) \quad (21)$$

with all the variables defined in the same manner as with Grodins' model. The neurological exercise contribution could be added to this equation.

If Grodins' model was refined to simulate the actual gas exchange mechanism then the efforts of Milhorn and Pulley which describe the venous admixture phenomenon could be implemented. With the existing Grodins' model no quantitative benefit can be obtained from the venous admixture description.

If the ventilatory controller equation is considered to be a direct function of the O_2 and CO_2 arterial gas tensions instead of the H+ concentration detecting systems then the additive and multiplicative relationship

$$\mathring{V} = 2\ (P_{A_{CO_2}} - 37.24)\ (1 + 13.6/(P_{A_{O_2}} - 25)) \geq 0 \quad (22)$$

could be used. One must keep in mind that this equation is developed for $P_{A_{CO_2}} \geq 37.24$ mm Hg. With the present version of Grodins' program the alveolar CO_2 tension doesn't remain above 37.24 mm Hg when simulating variations in exercise under the environmental conditions of 5 Torr CO_2 at 260 mm Hg. Consequently, the limitations of this equation will need to be redefined. The variables involved here are easily accessible in Grodins program. Comparison of the system's responses using a form of this equation to the responses obtained using the weightings of compartmental H+ concentrations could be beneficial in establishing appropriate detector sites.

Also, the relationships which were developed in conjunction with Equation 22 between dead space, respiratory frequency, alveolar ventilation and minute ventilation (some of which are already used in Grodins' program) could be implemented. In particular, a more physiologically satisfying description of respiratory frequency could be obtained.

A more complex modification would involve the sensor site location for the CO_2 tension as described by Equation 15 and repeated here.

$$P_{CS_{CO_2}} = P_{B_{CO_2}} + (P_{CSF_{CO_2}} - P_{B_{CO_2}}) \exp\left[-x\sqrt{\frac{\dot{Q}_{CS}S}{D/760}}\right] \qquad (23)$$

Since the sensor depth (x) has been experimentally justified by Milhorn et al. (6) and all other terms are common to Grodins' program, the components of Grodins' controller equation which rely upon the H+ concentration of the venous blood of the brain and the CSF subsystem could be replaced by a form of Equation 23. This would be one component of the minute ventilation and would effectively combine the sensing mechanisms of the brain and CSF compartments. If it is more satisfying to have the controller equation be a weighted function of H+ concentrations the $P_{CS_{CO_2}}$ can be converted into a term corresponding to the H+ concentration at the effective sensor site. This relationship is also developed by Milhorn et al. (6)

As previously implied, any modification to Grodins' program evolving from Milhorn's research will need to be adjusted so that the exercise phenomenon can be simulated.

The latter two modifications that are suggested would be the most beneficial to pursue. They would add some detail and additional flexibility for adjusting responses which are missing in the present modified version of Grodins' model.

IV. BIBLIOGRAPHY

1. Milhorn, H.T., Jr., The Application of Control Theory to Physiological Systems. Chapter 15. W.B. Saunders Company, Philadelphia, Pa., 1966.

2. Milhorn, H.T., Jr., Conceptual idea of digital computer model of human respiratory system. Progress Report, NASA Contract No. NGR 25-002-015. 1968.

3. Milhorn, H.T., Jr. and P.E. Pulley, Jr., A theoretical study of pulmonary capillary gas exchange and venous admixture. Biophysical Journal, Vol. 8, No. 3, pp. 337-357, 1968.

4. Milhorn, H.T., Jr., and D.R. Brown, Steady-state simulations of the human respiratory system. Computers and Biomedical Research 3: pp. 604-619, 1971.

5. Reynolds, W.J., H.T. Milhorn, Jr., and G.H. Holloman, Jr., Transient ventilatory response to graded hypercapnia in man. Journal of Applied Physiology 33: No. 1, pp. 47-54, 1972.

6. Milhorn, H.T., Jr., W.J. Reynolds, and G.H. Holloman, Jr., Digital simulation of the ventilatory response to CO_2 inhalation and CSF perfusion. Computers and Biomedical Research 5: pp. 301-314, 1972.

7. Kety, S.S. and C.F. Schmidt, Nitrogen oxide method for quantitative determination of cerebral blood flow in man. Journal of Clinical Investigation 27: pp. 476, 1948.

8. Holloman, G.H. Jr., H.T. Milhorn, Jr., and T.G. Coleman, A sample data regulator for maintaining a constant alveolar CO_2. Journal of Applied Physiology 25: pp. 463, 1968.

9. Grodins, F.S., J. Buell, and A.J. Bart, Mathematical analysis and digital simulation of the respiratory control system. Journal of Applied Physiology 22: No. 3, pp. 260-276, 1967.

ORIGINAL PAGE IS
OF POOR QUALITY

6.3 Program Listing for the Modified Grodins' Respiratory Control System

Minor modifications are indicated in the right hand margins of subroutines RC13 and RC17. The addition to RC13 is to prevent the simulation from getting into a loop which was found to occur under certain conditions. The RC17 modification provides additional print routines as mentioned in the text.

General Electric Company TIR-741-MED- 4024

ORIGINAL PAGE IS
OF POOR QUALITY